# Engineering and Urology Society

## 37th Annual Meeting

Sunday May 5, 2024

San Antonio, TX

https://engineering-urology.org/

# *"Endourology Society Day"*

**Sunday, May 5th, 2024**
**7:00AM – 6:00PM EDT**
**Grand Hyatt San Antonio**
**Texas Ballroom A & B**
**San Antonio, TX**

## *7:30AM – 10:00AM*

**Engineering & Urology Society (EUS)**
***President: Jihad Kaouk, MD, Executive Director: Dan Stoianovici, PhD***
*https://engineering-urology.org/*

## *10:00AM – 11:00AM*

***President: Rafael Sanchez-Salas, MD***
*https://focaltherapy.org*

## *1:00PM – 5:30PM*

**Society of Urologic Robotic Surgeons (SURS) Meeting**
***President: Craig Rogers, MD***
*https://sursroboticsurgery.org/*

The Engineering and Urology Society holds its 37th Annual Meeting: “Opening a New Frontier in Contemporary Urology Practice: Accessibility, Accuracy, and Innovation” on Sunday, May 5th in San Antonio, Texas. The mission of the Engineering and Urology Society, a subsection of the Endourological Society, is to promote the development and application of new technology in urology through facilitating collaboration between engineers, physicists, and urologists.

We have organized a distinct program that highlights the latest advances in robotic urologic surgery platforms, intraoperative guidance using artificial intelligence (AI), and integrated biosensing systems to address unmet clinical needs in urologic cancer, infections, and stone disease. Our multidisciplinary speakers are comprised of leading urologic surgeons, engineers, and promising early stage investigators. They will speak to the development, validation, integration, and dissemination of these emerging technologies, as well as a call towards standardization in conducting research studies and reporting outcomes. Representative topics include initial reporting of a novel endoscopic robotic system; emerging AI applications in surgical education, kidney stone disease, prostate cancer, and bladder cancer; integrated biosensors for rapid infection diagnostics, and a smart toilet for precision health monitoring.

Two **poster sessions** in the afternoon provide researchers with the opportunity to present their work and update the attendees on the progress on the field and latest innovations. Overall, the review of the abstracts for the poster sessions was performed by a group of 31 international reviewers. We would like to thank the reviewers, listed at the end of this program book, for their essential contribution to the quality of the meeting and their constructive comments that they made for the research.

Based on the review scores, the Society **awards** two closely ranked top abstracts this year. These are listed at the end of this program book, together with the Top 10 abstracts, and Best Reviewer Awards. The authors of all awarded abstracts are invited to submit full length articles to the Journal of Endourology on the respective topics. We gratefully thank all reviewers for their hard work, objective scoring, and contribution to the success of the meeting. We thank Dr. George Nagamatsu the founder and first president of the society, and Dr. Jack Vitenson the first Society Treasurer for setting up the foundations based upon which we meet.

Please visit the website https://engineering-urology.org/ for a complete version of this program including the abstracts presented.

We welcome all urologists, engineers, scientists from industry and academia to join us for this cross-disciplinary experience.

Jihad Kaouk, M.D.
President, Engineering and Urology Society

Dan Stoianovici, Ph.D.
Executive Director, Engineering and Urology Society

The Focal Therapy Society (FTS) in partnership with the Endourological Society, aims to advance and position minimally invasive, image-targeted cancer treatment in a safe, effective, gland-preserving manner to extend and maintain quality of life. Our vision is to control or eradicate prostate or kidney cancer in a minimally invasive, image-targeted manner while optimizing the preservation of organ function. Focal therapy is gaining importance in medicine for several reasons:

- Precision Medicine: Focal therapy allows for targeted treatment of diseased tissue while preserving surrounding healthy tissue, minimizing side effects, and preserving organ function.
- Quality of Life: By preserving organ function, focal therapy can improve a patient's quality of life compared to more aggressive treatments like surgery or whole-gland treatments.
- Reduced Side Effects: Focal therapy typically results in fewer side effects compared to whole-gland treatments, such as urinary incontinence and erectile dysfunction in prostate cancer treatment.
- Patient Selection: Focal therapy is suitable for select patients with localized disease, providing a middle ground between active surveillance and radical treatments.
- Advancements in Technology: Advances in imaging and ablation technologies have improved the accuracy and effectiveness of focal therapy procedures, making them more viable treatment options.

Overall, focal therapy offers a promising treatment alternative reaching its tipping point, which refers to the moment when this approach to treating Prostate Cancer becomes widely accepted and adopted as a standard of care. Several factors will contribute to this tipping point and the Focal Therapy Society strives to address every aspect:

- Clinical Evidence: Accumulating clinical evidence demonstrating the effectiveness and safety of focal therapy compared to traditional treatments like surgery or radiation therapy.
- Advancements in Technology: Continued advancements in imaging, diagnostic tools, and ablative technologies that improve the accuracy and precision of focal therapy procedures.
- Patient Awareness and Demand: Increased awareness among patients about the benefits of focal therapy, leading to greater demand for this treatment option.
- Physician Training and Expertise: Expanded training and expertise among healthcare providers in performing focal therapy procedures, leading to greater confidence in recommending and performing these treatments.
- Guidelines and Recommendations: Inclusion of focal therapy as a recommended treatment option in clinical practice guidelines and consensus statements by professional medical societies.
- Healthcare System Acceptance: Acceptance and integration of focal therapy into healthcare systems, including reimbursement policies and infrastructure support.

The FTS supports and maintains an international registry open to all participating collaborators for the collection of real-world physician experience utilizing FT including outcomes and complications. The FTS will feature state-of-the-art presentations on FT topics of interest during the Endourological Societies' Specialty Day on Sunday, May 5th, 2024 in San Antonio. We have a rich and exciting agenda in 2024 with our next FTS annual meeting, the ***14th International Symposium on Focal Therapy and Imaging in Prostate and Kidney Cancer in conjunction with the Singapore Urological Association*** will be held in Singapore July 25th-26th, 2024. **The World Congress of Endourology 2024** will feature a dedicated Focal Therapy Session in Seoul, South Korea, August 12th-16th, 2024. On September 26th-28th we will hold the FTS-SURS combined Symposium with a unique approach combining Focal Therapy, Imaging, Artificial Intelligence, and Robotics, along with a special session with the FDA on these technologies. We welcome all stakeholders interested in these topics to join us and visit our website www.focaltherapy.org.

Rafael Sanchez-Salas, M.D.
President and Program Chair, Focal Therapy Society

Dear Colleagues and Friends,

On behalf of the Society of Urologic Robotic Surgeons, it is our pleasure to welcome you to the AUA SURS meeting this year, to be held in San Antonio, TX on Sunday, May 5, 2024 (1:00pm–5:30pm). The Society of Urologic Robotic Surgeons (SURS) strives to help surgeons and their teams advance robotic surgery techniques with a goal of promoting innovative treatments and improved outcomes.

The meeting will provide useful information for surgeons and teams at all levels of training and experience in robotic surgery. A diverse faculty will be featured, with both rising and established stars in robotic surgery giving video-based presentations and with expert robotic surgeons moderating and providing commentary. Sessions will include techniques using both Xi and SP robotic approaches and will discuss new and upcoming robotic technologies.

The Young Urologist/Rising Stars session includes video presentations from rising stars as well as presentations on approaches to robotic surgery training and a presentation on building a surgical practice, innovation, and balance. The GU robotic reconstruction session will cover upper and lower urinary tract reconstruction techniques. The prostate surgery session will feature presentations focusing on management of challenging scenarios as well as extraperitoneal and retzius sparing approaches. This session will also feature a presentation from the Focal Therapy Society on why to consider including focal therapy into your robotic surgery practice and how. The robotic kidney surgery session will tips for complex robotic partial nephrectomy, retroperitoneal approaches, tumor excision techniques, and managing complex situations. The robotic cystectomy session will cover cystectomy and diversion techniques and tips to improve efficiency and minimize complications. We look forward to a productive afternoon of learning at the AUA SURS meeting from a diverse faculty of robotic experts and rising stars demonstrating their techniques to improve outcomes in robotic urologic surgery. Thank you all for your dedication to advancing robotic surgery techniques and for your support.

Craig Rogers, MD
President and Program Chair, Society of Urologic Robotic Surgeons

# EXHIBITORS

**Boston Scientific**

Company Statement: Through collaboration and innovation, Boston Scientific is the preferred urology clinical and business partner that offers comprehensive breadth and depth of knowledge and products. We apply our experience to help you to proficiently treat your patients and navigate the complexities of healthcare. We present a robust portfolio of relevant innovations, as well as tailored training and solutions – designed and delivered with our unique collaborative approach.

**Cook Medical**

Company Statement: A patient-first philosophy and innovative spirit have helped Cook become a leader in urology. With a focus on stone management and biopsy, we pride ourselves on providing quality solutions without compromise. By uniting with healthcare professionals around the world, we're committed to advancing treatment and making a difference, together. At our core, we believe industry-physician collaboration is vital to providing better healthcare. Our Vista® Education and Training programs encourage sharing best practices and learning new techniques using Cook's latest product innovations.

**Focal One**

Company Statement: Focal One Robotic HIFU allows urologists to offer patients a non-invasive, outpatient procedure to target prostate tissue while preserving urinary continence and sexual function. The platform combines the latest imaging and HIFU technology to precisely contour and ablate the targeted lesion while avoiding critical structures. The fully robotic system auto-adjusts with 5 degrees of freedom while offering MRI-fusion planning and real-time imaging.

ExactVu is the world's first and only targeted biopsy system using 29MHz Micro-Ultrasound technology providing 300% improved resolution over traditional ultrasound. It offers real-time visualization and sampling of suspicious lesions in the prostate. The system allows urologists to perform transperineal or transrectal biopsies, with or without MRI fusion.

**Sonablate Corp.**

Company Statement: Sonablate Corp. is a world leader in non-invasive, focused ultrasound technologies, and it is committed to developing medical devices that support precise and innovative procedures for the treatment of a range of medical conditions. Sonablate Corp. currently designs and manufactures the Sonablate® HIFU device, which has 510(K) clearance in the U.S. for the ablation of prostate tissue. Sonablate also has NMPA clearance in China, CE Marking in the EU, and additional regulatory authorization in more than 50 additional countries.

## EDUCATIONAL GRANT ACKNOWLEDGEMENT

The Society of Urological Robotic Surgery (SURS) thanks the following company for providing an Independent Educational Grant for the Society of Urological Robotic Surgery (SURS) Meeting: **INTUITIVE**

## *Engineering & Urology Society Meeting*

**Program Chair: Jihad Kaouk**

| | | |
|---|---|---|
| 7:00AM | **Registration** | **Presenter / Moderator** |
| 7:30AM | **Welcome**: Opening a New Frontier in Contemporary Urological Practices | Jihad Kaouk |
| | **Session 1: Emerging Technologies in Urological Imaging and Surgical Precision** | |
| 7:35AM | Improving Target Prostate Biopsy Precision Using High-Definition Micro-Ultrasound | Adriana Pedraza |
| 7:44AM | Visualizing the Invisible: The Utility of PSMA-Radioguided Surgery | Giorgio Gandaglia |
| 7:53AM | Current Application of Augmented Reality with Real-Time Intraoperative Images Overlay | Francesco Porpiglia |
| 8:02AM | Clinical Utility of Customized, Precision 3D Printed Anatomic Models | Ahmed Ghazi |
| | **Session 2: Emerging Technologies in Surgical Robotics** | |
| 8:11AM | Contemporary Application of Single-Port Robotic Surgery: Regionalization of Surgical Access and Field to the Relevant | Anatomy Richard Link |
| 8:20AM | Redefining Endoscopic Surgery with Novel Transurethral Robotic Platform | Duke Herrell |
| 8:29AM | Contemporary Application of Multi-Modular Portable Robotic Platform | Sudhir Rawal |
| 8:38AM | Improved Navigation and Stone Clearance During Percutaneous Nephrolithotomy (PCNL) Using Electromagnetic-Guided Robotic Surgical Platform | Jaime Landman |
| | **Session 3: Emerging Technologies in Endourology** | |
| 8:47AM | New Technology for Retrograde Intrarenal Surgery: What We Have & What We Need | Jorge Gutierrez |
| 8:56AM | Advances in Endoscopic Treatment Options for Benign Prostatic Hyperplasia | Smita De |
| 9:05AM | A New Paradigm of Portable Ureteric Stent Insertion in the Emergency Room or Office-Based Endourological Procedures | Mantu Gupta |

| | | |
|---|---|---|
| | **Session 4: Artificial Intelligence & Telesurgery** | |
| 9:14AM | Telesurgery: The Next Frontier in Surgical Education and Healthcare Equity | Vipul Patel |
| 9:23AM | The Role of Artificial Intelligence in Urology | Koon Ho Rha |
| | **Best Abstract Awards** | |
| 9:35AM | Nanoparticle Coatings with Broad Spectrum Antibacterial and Antibiofilm Properties and Low Toxicity | Juan Sebastian Rodriguez-Alvarez |
| 9:45AM | Augmented Reality-Guided Transperineal Prostate Biopsy: Shifting the Paradigm | Lucille Cheng |
| | **Poster Sessions**<br>**Grand Hyatt San Antonio, Texas Ballroom D)** | |
| 1:00PM – 2:00PM | Session 1 | John Denstedt<br>Roxana Ramos |
| 2:30PM – 3:30PM | Session 2 | Ralph Clayman<br>Nicolas Soputro |

## *Focal Therapy Society Meeting*

**Program Chair: Rafael Sanchez-Salas**

**Objective**: To offer a comprehensive overview of the aspects currently under development in partial gland ablation for prostate cancer treatment

| | | **Presenter / Moderator** |
|---|---|---|
| 10:00AM | Welcome and Introduction | Thomas Polascik |
| | **Session 1: A Disruptive Innovation** | Courtney Phillips, Thomas Polascik Rafael Sanchez-Salas |
| 10:05AM | FALCON: A Quest for Consensus on Focal Therapy for Prostate Cancer | Lara Rodriguez Sanchez |
| 10:10AM | Debulking the Myths of Prostate Cancer Diagnosis Through Randomized Controlled Trials | Peter Chiu |
| 10:20AM | Epidemiology Applied to Focal Therapy in PCa. Where do we Stand? | Kae Jack Tay |
| 10:30AM | Concepts in Focal Therapy Margin Assessment: Treatment Planning and Implementation | Samir Taneja |
| 10:40AM | Panel Discussion | |
| | **Session 1: Striving for Improvement** | Kara Watts Ardeshir Rastinehad Herbert Lepor |
| 11:00AM | Genomic Classifiers: Can They Advise the Focal Therapist? | Sriram Deivasigamani |
| 11:10AM | Symbiosis of Treatments to Improve Outcomes on Focal Therapy | Timothy McClure |
| 11:20AM | Symbiosis of Treatments to Improve Outcomes on Focal Therapy | Armando Stabile |
| 11:30AM | Artificial Intelligence and Focal Therapy | Giovanni Cacciamani |
| 11:40AM | Panel Discussion | |

## *SOCIETY OF UROLOGIC ROBOTIC SURGEONS*

**Program Chair: Craig Rogers**

| | | Presenter / Moderator |
|---|---|---|
| 1:00PM | Welcome and SURS Update: | Craig Rogers |
| | **Session 1: Young Urologist / Rising Stars** | Ashok Hemal |
| 1:05 PM | Encore Feature of Rising Star Video from AUA Robotics Theater | Julett Han<br>Ahmed Ghazi |
| | Featured Fellow Video: David Strauss - Early Reconstruction for Anastomotic Leak | Lee Richstone |
| 1:30PM | Enhancements in Surgical Skills Training | Ahmed Ghazi |
| 1:40PM | Building Your Practice and Innovating While Balancing Wellness | Lee Richstone<br><br>Daniel Eun<br>Lee Zhao |
| | **Session 2: GU Robotic Reconstruction** | Jill Buckley |
| 1:50PM | **Lower Urinary Tract Reconstruction** | |
| 1:52PM | Fistula Management | Rene Sotelo |
| 2:05PM | Bladder Neck Reconstruction | Ziho Lee |
| | **Upper Urinary Tract Reconstruction** | |
| 2:20PM | Buccal Graft Update After 10 year Experience | Brian Chao |
| 2:33PM | Robotic Uretero-Enteric Stricture Revision | Ahmed Aly Hussein Aly<br>Kirsten Greene<br>Lee Richstone<br>James Peabody |
| | **Session 3: Robotic Prostate Surgery** | Aldonassimo Bocciardi |
| 2:47PM | Review of Challenging Scenarios | Vipul Patel |
| 3:01PM | Extraperitoneal Approaches (SP – Simple and Radical) | Jihad Kaouk |
| 3:14PM | Retzius Sparing Prostatectomy | Aldonassimo Bocciari |
| 3:30PM | Why Your Robotic Practice Should Include Focal Therapy and How | Rafael Sanchez-Salas<br><br>Jennifer Linehan<br>Tara Morgan<br>Michael Stifelman |
| | **Session 4: Robotic Kidney Surgery** | James Porter |
| 3:42PM | Complex Robotic Partial Nephrectomy Techniques: Hilar/Endophytic Tumor | Richard Link |
| 3:55PM | Tumor Excision – When and How to Enucleate | Craig Rogers |
| 4:08PM | Retroperitoneal Approaches | Simone Crivellaro |
| 4:21PM | Troubleshooting Complex Cases and Managing Complications | Ketan Badani |
| | **Session 5: Cystectomy / Diversion** | Mary Westerman<br>Timothy Wilson<br>Qiang Li |
| 4:37PM | Tips and Tricks to Expedite the Robotic Cystectomy Learning Curve | Roger Li |
| 4:50PM | Female Cystectomy: Minimizing Vaginal/Pelvic Floor Complications | Johar Raza |
| 5:05PM | Intracorporeal Diversion Techniques (SP) | Ryan Nelson |
| 5:15PM | Ureteral Anastomosis – Techniques to Minimize Complications | Bagdana Schmidt |

**POSTER SESSION 1**

1:00 PM – 2:00 PM

**Moderators**:
John Denstedt
Roxana Ramos

| No | Title | Presenting Author |
|---|---|---|
| 1 | ENHANCING PRECISION IN PROSTATE BIOPSY: INTRODUCING A LOW-FIELD MRI-GUIDED ROBOTIC SYSTEM | Akram Gholami |
| 2 | SINGLE-PORT ROBOTIC SURGERY FOR BUCCAL MUCOSAL GRAFT HARVEST AND URETEROPLASTY TO MANAGE LONG URETERAL STRICTURE | Alireza Aminsharifi |
| 3 | DEVELOPMENT AND VALIDATION OF A NEW ANALYTICAL MODEL FOR PREDICTING NEW BASELINE RENAL FUNCTION AFTER NEPHROURETERECTOMY FOR UPPER TRACT UROTHELIAL CARCINOMA | Raidizon Mercedes |
| 4 | NANOKNIFE ELECTROPORATION FOR TARGETED PROSTATE TISSUE ABLATION IN MEN WITH LOCALIZED INTERMEDIATE-RISK PROSTATE CANCER: PRELIMINARY RESULTS FROM THE PRESERVE TRIAL | Arvin K George |
| 5 | **TOP 10 ABSTRACT** DEVELOPMENT OF A NOVEL LUBRICITY EVALUATION MODEL FOR URETERAL ACCESS SHEATHS | Brandon Camp |
| 6 | **TOP 10 ABSTRACT** WHERE IS MY NEEDLE? USE OF A NEEDLE TIP INDICATOR FOR PERCUTANEOUS RENAL ACCESS IN ROBOTIC-ASSISTED PCNL | Saif Sayed |
| 7 | COMPARING THE EFFECTS OF PERFUSION DECELLULARIZATION PROTOCOLS ON BLADDER ACELLULAR MATRIX (BAM) PROTEIN CONTENT, STRUCTURE, AND MECHANICS | Cecelia Eggleston |
| 8 | SIMULATED FLUOROSCOPY IN A PHYSICAL SIMULATOR FOR TRAINING IN PLACEMENT OF ADJUSTABLE CONTINENCE THERAPY DEVICES | Lawrence Yeung |
| 9 | INTEGRATION AND VERIFICATION OF VISUALIZED PROSTATE BIOPSY SYSTEM | Alejo Ballester |
| 10 | EFFICACY OF DVIU VERSUS BALLOON DILATION TO TREAT RECURRENT URETHRAL STRICTURE FOLLOWING FAILED URETHROPLASTY | David Gilbert |
| 11 | HIGH INTENSITY FOCUSED ULTRASOUND (HIFU) BASED TISSUE ELASTICITY MAPPING FOR PLANNING PROSTATE ABLATION | Minho Song |
| 12 | **TOP 10 ABSTRACT** THE MEASUREMENT OF INTRARENAL PRESSURE IN URETEROSCOPY WITH LASER LITHOTRIPSY: A PROSPECTIVE TRIAL | Jamie Finegan |
| 13 | EXPLORING THE FEASIBILITY OF GPT-4 AS A DATA EXTRACTION TOOL FOR RENAL SURGERY OPERATIVE NOTES | Jessica Y Hsueh |

| | | |
|---|---|---|
| 14 | INVESTIGATING THE CLINICAL REASONING ABILITIES OF GPT-4: A POSTOPERATIVE COMPLICATION ANALYSIS FROM RENAL SURGERIES | Jessica Y Hsueh |
| 15 | STRONG AND ELASTIC: COMPARISON OF TENSILE PROPERTIES BETWEEN THE VAGINA, BLADDER, AND URETHRA | Jooyoung David Song |
| 16 | COMPARISON OF TENACIO PUMP AND MS PUMP EFFICIENCY USING SURFACE ELECTROMYOGRAPHY (sEMG) | Justin Lee |
| 17 | EARLY RESULTS OF URETHRAL BULKING WITH POLYACRYLAMIDE HYDROGEL IN MALE STRESS URINARY INCONTINENCE: A MULTI-INSTITUTIONAL RETROSPECTIVE COHORT | Luke Griffiths |
| 18 | BURST WAVE LITHOTRIPSY FOR OBSTRUCTING URETEROLITHS IN PET CATS | Eva Furrow |
| 19 | **TOP 10 ABSTRACT** THE EFFECT OF PROSTATE SIZE AND NUMBER OF CORES AT SYSTEMATIC PROSTATE BIOPSY | Misop Han |
| 20 | AUTOMATIC KIDNEY STONE SEGMENTATION IN CT SCANS USING DEEP-LEARNING NEURAL NETWORK | Murillo F Bouzon |
| 21 | POTENTIAL CLINICAL APPLICATION OF PATIENT-SPECIFIC 3D PRINTED MODEL FOR SURGICAL PLANNING PRIOR TO HIGH-INTENSITY FOCUSED ULTRASOUND (HIFU) | Nicolas A Soputro |
| 22 | IMPROVING SURGICAL PRECISION OF SINGLE PORT TRANSVESICAL PARTIAL PROSTATECTOMY WITH PATIENT-SPECIFIC 3D PRINTED MODEL | Nicolas A Soputro |
| 23 | ADVANCING PELVIC RECONSTRUCTIVE SURGERY: VAGINAL ACCESS RETROPERITONEAL SACROCOLPOPEXY WITH HYSTERECTOMY USING SINGLE-PORT (SP) ROBOTIC DA VINCI SYSTEM | Omer Anis |
| 24 | A MACHINE LEARNING ARCHITECTURE FOR SEGMENTATION AND FEATURE EXTRACTION OF LAPAROSCOPIC TOOLS TO IDENTIFY SURGERY STEPS | Rafael Zacarias Palierini |
| 25 | APPLICATIONS OF A REMOTELY OPERATED SUCTION AND IRRIGATION SYSTEM FOR ROBOT-ASSISTED SURGERY IN UROLOGY | Roxana Ramos-Carpinteyro |
| 26 | INITIAL ANALYSIS OF A NOVEL WIRELESS MOTORIZED SINGLE-USE FLEXIBLE URETEROSCOPE | Runhan Ren |
| 27 | TOTALLY TRANSPERINEAL ULTRASOUND MRI FUSION-GUIDED TRANSPERINEAL PROSTATE BIOPSY IN PATIENTS WITH NO RECTUM | Sarah Azari |
| 28 | FOCAL THERAPY ELIGIBILITY: AN EVALUATION OF INITIAL AND CONTINUED CANDIDACY FOR FOCAL THERAPY IN A GRADE GROUP 2 ACTIVE SURVEILLANCE COHORT | J Bradley Mason |

| | | |
|---|---|---|
| 29 | NOVEL DUAL BALLOON CATHETER TO REDUCE CATHETER-RELATED COMPLICATIONS: RESULTS OF A PROSPECTIVE, SINGLE-CENTER, RANDOMIZED CONTROLLED TRIAL | Onuralp Ergun |
| 30 | CIRCUMFERENTIAL TRANSMISSION OF SHOCKWAVE ENERGY TO THE ERECT PENIS | Irwin Goldstein |
| 31 | **TOP 10 ABSTRACT**<br>A NOVEL LLM-MEDIATED DATA EXTRACTION TOOL: A COMPARATIVE STUDY IN PATIENTS WHO UNDERWENT RADICAL PROSTATECTOMY | William S Azar |
| 32 | **TOP 10 ABSTRACT**<br>IMPACT OF INTEGRATED, REAL-TIME DIGITAL MEASUREMENT ON SURGEON DECISION MAKING IN URETEROSCOPIC STONE SURGERY | Alexander Krueger |
| 33 | A BENCHTOP KIDNEY MODEL FOR MEASURING TRANSIENT INTRARENAL PRESSURE DURING SIMULATED URETEROSCOPY | Alycia Abbott |
| 34 | **TOP 10 ABSTRACT**<br>PROSPECTIVE EVALUATION OF EFFICACY, SAFETY, CUMULATIVE LASER ENERGY, AND STONE-FREE RATES IN THE POST-MARKET THULIUM FIBER LASER (SOLTIVETM SUPERPULSED LASER SYSTEM) REGISTRY: INSIGHTS FROM TEAM OF WORLDWIDE ENDOUROLOGICAL RESEARCHERS (T.O.W.E.R.) RESEARCH CONSORTIUM | Ben H Chew |

**POSTER SESSION 2**

2:30 PM – 3:30 PM

**Moderators**:
Ralph Clayman
Nicolas Soputro

| No | Title | Presenting Author |
|---|---|---|
| 35 | TRI-LAYER URETERAL STENTS, WITH ANTI-ENCRUSTATION SURFACE, OFFER IMPROVED COMFORT: RESULTS FROM AN INTERNATIONAL STENT REGISTRY | Ben H Chew |
| 36 | THE USE OF 3-D PRINTING IN THE PLANNING OF COMPLEX ROBOTIC UROLOGIC SURGERY | Ryan L Buettner |
| 37 | IMPLEMENTATION OF A NOVEL ELECTROMAGNETIC DEVICE IN PROSTATE CANCER DIAGNOSTIC PATHWAY: COMPARISON WITH MULTIPARAMETRIC MRI AND DIGITAL RECTAL EXAMINATION | Carlo Bellorofonte |
| 38 | EVALUATING EFFICACY OF PERCUTANEOUS PROCEDURES PLANNED VIA AUGMENTED REALITY | Lucille G Cheng |
| 39 | FUNDAMENTALS, APPLICATIONS, AND LIMITATIONS OF AUGMENTED REALITY IN UROLOGICAL SURGERY: A PRACTICAL PRIMER FOR THE PRACTICING PHYSICIAN | Lucille G Cheng |
| 40 | **BEST ABSTRACT AWARD** AUGMENTED REALITY-GUIDED TRANSPERINEAL PROSTATE BIOPSY: SHIFTING THE PARADIGM | Lucile G Cheng |
| 41 | PROTOTYPE PASSIVE DRIVER AND MAGNETIC RESONANCE ELASTOGRAPHY TO IDENTIFY PROSTATE TISSUE PROPERTIES | Cody J Johnson |
| 42 | IS SHORTER BETTER? ASSOCIATION BETWEEN PAIN INTENSITY, URETERAL STENT INDWELLING TIME, AND PATIENT FACTORS FROM AN INTERNATIONAL PROSPECTIVE REGISTRY | Connor M Forbes |
| 43 | 3D SLICER: DETERMINATION OF ACCURATE UROLITHIASIS VOLUMES | Jacob C Tsai |
| 44 | EXPERIMENTAL MODEL OF POSITIONING DEVICE FOR MALE UROGENITAL TRACT BIOPSY IN MINIMALLY INVASIVE AUTOPSY | Júlia Alarcon Pinto |
| 45 | USING MATHEMATICAL MODELING TO INVESTIGATE THE IMPACT OF SUCTION DURING URETEROSCOPY ON RISK OF LASER-INDUCED THERMAL DAMAGE | Jessica Williams |
| 46 | **BEST ABSTRACT AWARD** NANOPARTICLE COATINGS WITH BROAD SPECTRUM ANTIBACTERIAL AND ANTIBIOFILM PROPERTIES AND LOW TOXICITY | Juan Sebastian Rodriguez-Alvarez |
| 47 | HOW TO GET A BETTER PERCUTANEOUS ACCESS: A CAUSAL MODEL FOR ROBOTIC-ASSISTED PCNL | Lauren Friend |
| 48 | QUANTITATIVE PIXEL INTENSITY ANALYSIS FOR CHARACTERIZING HYPOSPADIAS ANATOMY: ENTROPY AND RANGE ASSESSMENT IN FAVORABLE VERSUS UNFAVORABLE CASES | Meghana Noonavath |

| | | |
|---|---|---|
| 49 | MAPPING THE PREDICTIVE LANDSCAPE OF PREOPERATIVE CT WITH DEEP LEARNING ACROSS RENAL TUMOR OUTCOMES | Nicholas E Heller |
| 50 | AUTOMATICALLY CURATING REDCap DATABASES USING OPEN-SOURCE LARGE LANGUAGE MODELS: A PILOT STUDY WITH KIDNEY TUMOR PATHOLOGY REPORTS | Nicholas E Heller |
| 51 | CORRELATION OF PENILE GRAYSCALE PHARMACO-ULTRASONOGRAPHY WITH ERECTILE TISSUE COMPOSITION IN MEN WITH ERECTILE DYSFUNCTION | Noel N Kim |
| 52 | DEISGN AND PERFORMANCE EVALUATION OF A TRANSRECTAL HISTOTRIPSY DEVICE FOR PROSTATE ABLATION | Pavel B Rosnitskiy |
| 53 | SINGLE-USE DIRECT IN-SCOPE SUCTION (DISS™) FLEXIBLE URETEROSCOPE IN SUCTIONING OF DISINTEGRATED RENAL STONES | B Geavlete |
| 54 | COMBINED DIRECT IN-SCOPE SUCTION (DISS™) FLEXIBLE URETEROSCOPE WITH BENDABLE ACCESS SHEATH FOR COMPLETE STONE REMOVAL | B Geavlete |
| 55 | NEW TECHNOLOGIES IN FLEXIBLE URETEROSCOPY—WHAT IS THE LIMIT NOW OF THE ONE SESSION STONE REMOVAL? | B Geavlete |
| 56 | FLEXIBLE URETEROSCOPY LITHOTRIPSY IN STAGHORN CALCULI: BENDABLE VERSUS TRADITIONAL ACCESS SHEATH | B Geavlete |
| 57 | BENDABLE SUCTION URETERAL ACCESS SHEATH: A COMPARISON WITH STANDARD URETERAL ACCESS SHEATH IN RENAL STONE URETEROSCOPIC TREATMENT | B Geavlete |
| 58 | IRRIGATION FLUID BACK-FLOW IN NEW BENDABLE URETERAL ACCESS SHEATH USED WITHOUT SUCTION DURING FLEXIBLE URETEROSCOPIC APPROACH OF RENAL STONES | B Geavlete |
| 59 | **TOP 10 ABSTRACT** SAFETY AND EFFICACY OF ELECTROMOTIVE DRUG ADMINISTRATION IN THE RENAL PELVIS: FIRST IN-VIVO PORCINE REPORT | Seyedamirvala Saadat |
| 60 | PROSTATE CANCER DETECTION VIA TRANSURETHRAL INTRODUCTION OF PRE-CONDITIONED ANT COLONIES | David Smith |
| 61 | *IN VITRO* SIMULATION OF CAVITATION BEHAVIORS IN BURST WAVE LITHOTRIPSY (BWL) | Wayne Kreider |

**ABSTRACT #1**

## ENHANCING PRECISION IN PROSTATE BIOPSY: INTRODUCING A LOW-FIELD MRI-GUIDED ROBOTIC SYSTEM

Akram Gholami[1], Neel Sancheti[1], Sreeja Vangapelli[1], Paul Brathwaite[1], Nariman Nasab[1], Aleksandar Nacev[1]
[1] Research and Development Department, Promaxo Inc., Oakland, California, USA

**Introduction:** Magnetic Resonance Imaging (MRI) delivers comprehensive imaging of the prostate when compared to ultrasound. As a result, MRI-guided biopsies offer more precise targeting of prostatic lesions during prostate biopsies, which is critical to accurate diagnosis, management, and outcome for prostate cancer. However, the cost and feasibility of using high-field MRI scanners make accessibility to this more accurate form of diagnosis limited, which has grown an interest in the use of low-field MRI scanners for image-guided prostate biopsies. Additionally, the introduction of a robot, specifically engineered to work within the spatial and environmental constraints of the low-field MRI, can improve biopsy accuracy further by reducing chances of human error during the procedure.

**Methods:** In this project, we developed an MRI-guided prostate biopsy robot (Figure 1) compatible with the single-sided, low-field Promaxo MRI system (Promaxo Inc., Oakland, California, United States). The biopsy robot consists of 5 degrees of freedom (DOF), employs MRI-safe materials, has a compact design to fit in low-field MRI scanners, and is actuated with pneumatic stepper motors (PneuStep motor, John Hopkins University). The biopsy robot uses a spherical parallel mechanism to insert the biopsy gun from various angles. Needle insertion at different depths is achieved via a translation screw after angulation. The robotic system has infinite possible solutions for reaching a target point, which enables obstacle avoidance in the system.

**Results:** The system's performance will be evaluated in two stages. First, on a benchtop experiment independent of imaging, and later, in an MRI-guided experiment. In this abstract, we are presenting the first stage evaluation results using a multi-modality prostate phantom model that stimulates the human prostate and the surrounding structure (Yezitronix Group Inc. Automation & Control Industries Inc.). The benchtop experiment focused on piercing the phantom on a vertical line, 5.34 mm apart at equal depth. The needle placement accuracy is verified by comparing the vertical distance between air tracks in Computed Tomography (CT) scan images of the phantom to . The experiment results show an absolute error on the vertical line, and in depth.

**Conclusion:** We built a robotic prostate biopsy system and evaluated the biopsy robot's precision on the benchtop. In conclusion, the overall concept, design, and implementation showed feasibility in preliminary experiments, which helps to reduce the chances of human errors in procedures and enhances patient outcomes. In the future, comprehensive studies will be done in image-guided targeting tests with the Promaxo MRI system.


**Figure 1:** MRI-Guided prostate biopsy robot

**ABSTRACT # 2**

## SINGLE-PORT ROBOTIC SURGERY FOR BUCCAL MUCOSAL GRAFT HARVEST AND URETEROPLASTY TO MANAGE LONG URETERAL STRICTURE

Alireza Aminsharifi, Joseph Smith, Max Yudovich, Austin Bramwell, Ali Ziada
Department of Urology, PennState College of Medicine, Hershey Medical Center, Hershey, PA

**Introduction:** To evaluate the feasibility and describe the technique of using the single-port (SP®) robotic system for performing robotic transoral (i.e. buccal mucosal graft (BMG) harvest) and transperitoneal (i.e. BMG ureteroplasty) surgeries for management of long ureteral stricture.

**Methods:** Between September 2023 and February 2024, two patients with proximal ureteral strictures underwent BMG ureteroplasty. The SP® robotic system was utilized for harvesting BMG from oral cavity and for ureteral reconstruction. Case 1involved a 14-year-old male adolescent with a 4cm- length right proximal ureteral stricture starting about 1 cm proximal to the ureteropelvic junction. It was diagnosed in the context of recurrent pyelonephritis. Case 2 was a 60-year-old male with 5cm proximal left ureteral stricture starting at the level of L4 down to the lower border of L5. It happened after multiple sessions of laser lithotripsy for a proximal ureteral stone. In both patients, obstructive uropathy was managed with percutaneous nephrostomy (PCN) and the anatomy was characterized with ureteroscopy, retrograde and antegrade studies. Surgery was conducted in 3 steps in lateral decubitus position. a) Accessing the peritoneal cavity via a 4cm incision over the midclavicular line at the umbilical level, followed by docking of the SP® robot and ureter dissection, identification of the site of stricture and measurement of its length (Figure A). b) Transoral robotic surgery: The dependent cheek (contralateral to the diseased ureter) was used for harvesting the BMG. After adequate exposure of the inner cheek, the parotid duct as well as the upper and lower borders of the dissection was marked (Figure B). After docking of the robot outside the oral cavity, the BMG was harvested (Figures C, D). Hemostasis was done by bipolar energy and the defect was left opened. C) Onlay-augmented BMG ureteroplasty entailed robot re-docking, incising of the stricture and BMG anastomosis to the ureteral plate over a double-J stent and coverage of the repair with perinephric fat (Figures E, F).

**Results:** Foley catheter was removed 48- hours after surgery and the PCN was capped. The site of BMG-harvest healed completely in 10-14 days after surgery. Ureteroscopy was done 6 weeks after surgery and the double J stent was removed. Ureteroscopic evaluation showed patency of the site of stricture with complete epithelialization of the BMG. Antegrade and retrograde studies showed free drainage of the contrast. PCN was removed subsequently, and the patients remained symptom-free in short-term follow up (3 months for case 1 and 3 weeks for case 2).

**Conclusion:** Using a single-port robotic system offers the advantages of transoral and transabdominal surgery for BMG harvest and ureteroplasty with minimally invasive methods. After exploration and measurement of the diseased segment, the surgeon can use the SP®- robot to harvest the BMG in decubitus position, a task that would have been cumbersome with traditional open technique. Long-term outcomes of this technique need further investigations.

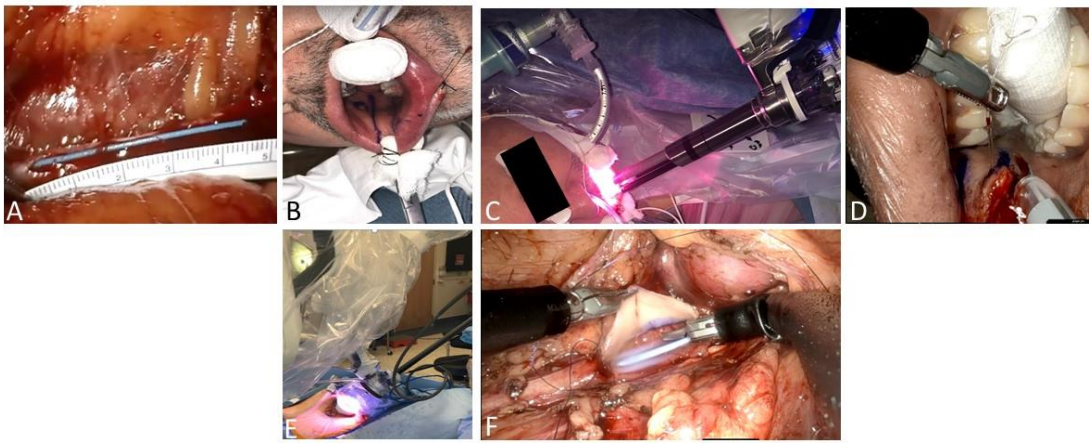

**ABSTRACT # 3**

## DEVELOPMENT AND VALIDATION OF A NEW ANALYTICAL MODEL FOR PREDICTING NEW BASELINE RENAL FUNCTION AFTER NEPHROURETERECTOMY FOR UPPER TRACT UROTHELIAL CARCINOMA

Raidizon Mercedes[1], W Chen[2,3], J Petucci[2,3], A Katoch[2,3], V Honavar[3,4], A Aminsharifi[1]
[1] Department of Urology, PennState College of Medicine, Hershey Medical Center, Hershey, PA
[2] Institute for Computational and Data Sciences, [3]Clinical and Translational Sciences Institute, [4]Center for Artificial Intelligence Foundations and Scientific Applications, University Park, PA

**Introduction:** In preoperative planning for radical nephrectomy (RN), validated models predict new baseline renal function (eGFR) in patients with renal cell carcinoma (RCC) [1]. This study evaluates the performance of RCC models in predicting new base line eGFR in patients undergoing nephroureterectomy (NU) for upper tract urothelial carcinoma (UTUC). We then developed and validated a new predictive model for these patients.

**Methods:** Data on 3,404 patients with UTUC managed with NU (2006-2023) were queried. Inclusion required both pre- and 3-12 months postoperative eGFR data. To predict postoperative eGFR, the RCC equation by Palacios et al. [PMID: 33356481] was initially used and compared with actual results. The area under the ROC (AUROC) curve was calculated to evaluate the predictive performance of RCC model when applied to UTUC patients, defining two classes based on an eGFR threshold of ≥45 ml/minute/$m^2$.
Two additional models (linear regression and logistic regression) were trained to predict postoperative eGFR after NU. Generalized model performance was assessed using 5-fold cross-validation and compared to the baseline RCC model.

**Results:** When applied to UTUC patients, the RCC model demonstrated lower predictive accuracy (47.03%, ($R^2$: 0.28, Pearson correlation: 0.79)). Notably, it exhibited a predictive bias of 13.62, indicating a tendency to overestimate postoperative renal function (Table 1).
In contrast, the linear regression model showed an improvement over the RCC model, $R^2$ =0.62, explaining a greater variance in postoperative eGFR. The model's bias was significantly reduced to -1.40, leading to more precise predictions. The logistic regression model outperformed both models in terms of accuracy (82.58%) in identifying patients with eGFR < 45 ml/min/1.73 $m^2$ and the highest AUROC of 0.89, signifying excellent capability in distinguishing eGFR threshold of ≥45 ml/minute/$m^2$ (Table 1).

**Conclusion:** Our study showed that predicting baseline eGFR after nephrectomy with the RCC model requires improvement before use in UTUC patients. Patient demographics and tumor biology variations may explain this observation. We developed and internally validated new models with satisfactory predictive performance. External validation is needed before widespread clinical use.

**Table 1**: Performance metrics for the trained linear and logistic regression models and the reference RCC model in predicting new base line eGFR in patients undergoing nephroureterectomy for UTUC. Values in parentheses for the models trained in this study indicate the standard deviation from the mean of the performance metrics across the 5-Fold cross-validation.

| Metric | RCC Model | Linear Regression | Logistic Regression |
|---|---|---|---|
| $R^2$ | 0.28 | 0.62 (0.03) | |
| Pearson Correlation* | 0.79 | 0.79 (0.02) | |
| Bias | 13.62 | -1.40 (0.99) | |
| Accuracy (%) | 47.03 | 67.04 (1.27) | 82.58 (0.02) |
| AUROC (eGFR threshold of ≥45 ml/minute/$m^2$) | 0.72 | 0.81 (0.02) | 0.89 (0.02) |

*Pearson correlation coefficient between prediction and observed/target values
AUROC: Area under the ROC

**ABSTRACT # 4**

## NANOKNIFE ELECTROPORATION FOR TARGETED PROSTATE TISSUE ABLATION IN MEN WITH LOCALIZED INTERMEDIATE-RISK PROSTATE CANCER: PRELIMINARY RESULTS FROM THE PRESERVE TRIAL

Arvin K. George[1], Ranko Miocinovic[2], Amit R. Patel[2], Derek J. Lomas[3], Andres F. Correa[4], David Y. T. Chen[4], Ardeshir R. Rastinehad[5], Edward M. Uchio[6], Abhinav Sidana[7], Brian T. Helfand[8], Jeffrey C. Gahan[9], Alice Yu[10], Srinivas Vourganti[11], Al Baha Barqawi[12], Wayne G. Brisbane[13], James S. Wysock[14], Thomas J. Polascik[15], Timothy D. McClure[16], Jonathan A. Coleman[17]

[1] VA Ann Arbor Health System; [2] Duly Health and Care; [3] Mayo Clinic; [4] Fox Chase Cancer Center; [5] Northwell Health System; [6] University of California, Irvine; [7] University of Cincinnati Cancer Center; [8] Northshore University Healthsystem; [9] University of Texas Southwestern Medical Center; [10] Moffitt Cancer Center; [11] Rush University Medical Center; [12] University of Colorado Anschutz Medical Campus; [13] University of Florida; [14] NYU Grossman School of Medicine; [15] Duke University Medical Center; [16] Weill Cornell Medicine; [17] Memorial Sloan Kettering Cancer Center

**Introduction:** Irreversible electroporation (IRE) is a therapeutic modality for the focal ablation of prostate cancer (PCa) using high voltage electrical pulses to alter the permeability of the cell membrane, resulting in cell death. PRESERVE (NCT04972097) aims to evaluate the tolerability and effectiveness of the NanoKnife System to ablate prostate tissue in a large, multi-center US trial through the Society of Urologic Oncology Clinical Trials Consortium.

**Methods:** This prospective, single-arm pivotal trial includes subjects who met the following criteria: clinical stage ≤T2c, PSA ≤15 ng/mL, and Grade Group (GG) 2 or 3. Subjects received IRE and are followed to a primary effectiveness endpoint of negative in-field biopsy at 12 months. MRI is performed at 3 and 12 months. Intermediate endpoints include assessment of graded toxicities and PSA.

**Results:** Among 128 subjects enrolled at 17 centers, 121 received treatment with NanoKnife. Mean age was 66.6 years. A majority (87.7%) had stage T1c with a distribution of GG 2 (80.2%) and GG 3 (19.8%). Tumor location included apex (n=48), base (n=17) and midgland (n=51); 56.9% were posterior and 43.1% were anterior. Mean procedure duration (first needle placed to last needle removed) was 54.1 minutes (IQR 38.0-63.5) and median number of treatment probes was 4 (IQR 4-5).

PSA response demonstrated a median reduction from baseline of 60.3%, 67.2% and 67.6% at 1, 3 and 6 months, respectively. 87 subjects (71.9%) experienced any adverse event, the majority (88.5%) were Grade ≤2 and transient. The most common events related to NanoKnife included hematuria (31.4%), urinary urgency (11.6%), urinary retention (10.7%), dysuria (9.9%), hematospermia (9.9%) and erectile dysfunction (9.9%). SAEs were Grade 3 only and reported in 5 treated men (4.1%). Three were device-related including 1 patient who developed a rectourethral fistula repaired surgically.

**Conclusion:** Interim data from PRESERVE suggest IRE with NanoKnife can be safely applied in men with intermediate-risk PCa with low risk of peri-operative morbidity. Promising biochemical response outcomes will be confirmed with further assessment of imaging, oncologic, functional and safety outcomes.

**ABSTRACT # 5** **TOP 10 ABSTRACT**

# DEVELOPMENT OF A NOVEL LUBRICITY EVALUATION MODEL FOR URETERAL ACCESS SHEATHS

Brandon Camp[1], Andrei D. Cumpanas[1], Kevin Moreno-Ruiz[2], Zachary E. Tano[1], Bruce M. Gao[1], Jaime Landman[1], Ashlie Martini[2], Ralph V. Clayman[1]

[1] *Department of Urology, University of California, Irvine*

[2] *Department of Mechanical Engineering, University of California, Merced*

**Introduction:** The deployment force of a ureteral access sheath (UAS) directly influences both the size of UAS that can be inserted and the occurrence of ureteral injuries. In this regard, the role of UAS lubricity in facilitating the passage of UASs has yet to be elucidated. Accordingly, we sought to develop an *ex-vivo* model for evaluating the lubricity of 14Fr UASs on porcine ureteral tissue.

**Methods:** A custom-designed, 3D-printed ureteral holder was developed for fixation of ureteral segments (2.5 cm x 2.0 cm) throughout testing without producing undue tensile stress (**Figure 1**). The curved contour of the ureteral holder maintained a saline film at the urothelium-UAS interface throughout testing. Both distal and proximal ends of the ureteral segments were marked to ensure precision in simulating the direction of UAS deployment. Once locked in place, a tension load cell applied a constant normal force of 4 Newtons (N) (0.9 pounds), perpendicular to the urothelial surface. The tribometer (Rtec Instruments, San Jose, CA), a device capable of detecting changes in frictional forces in thousandths of a Newton, measured the friction force generated at the interface between the urothelium and the UAS. The UAS and urothelium were in contact for a total of 30 seconds, on a reciprocating length of 2.5 cm. The total testing time was divided into 3 intervals of 10 seconds each based on the direction of UAS deployment: cycle 1 (insertion), cycle 2 (retraction), cycle 3 (insertion). The coefficient of friction (COF) was determined as the ratio between the measured friction force and the applied normal force for each cycle. The COF is a relative metric that can only be interpreted based on the surface against which the catheter is tested. As such, ideally, all catheters under investigation need to be tested against the same ureter. To accomplish this, UAS testing order was randomized to preclude the risk of urothelial disruption impacting catheter-ureter interaction.

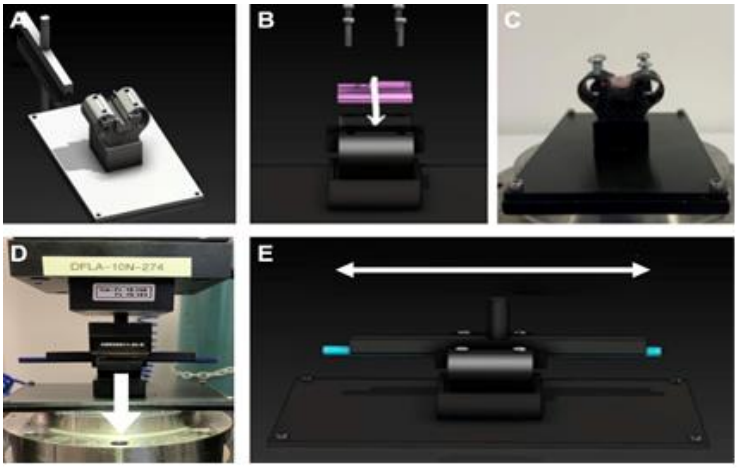


**Figure 1. Experimental set-up overview A.** 3D view of the novel ureteral holder. **B.** Adequate orientation of the proximal and distal ureteral ends **C.** Ureteral fixation using C-hinges **D.** Load cell applying the 4 N normal force **E.** Bidirectional UAS-ureteral interaction.

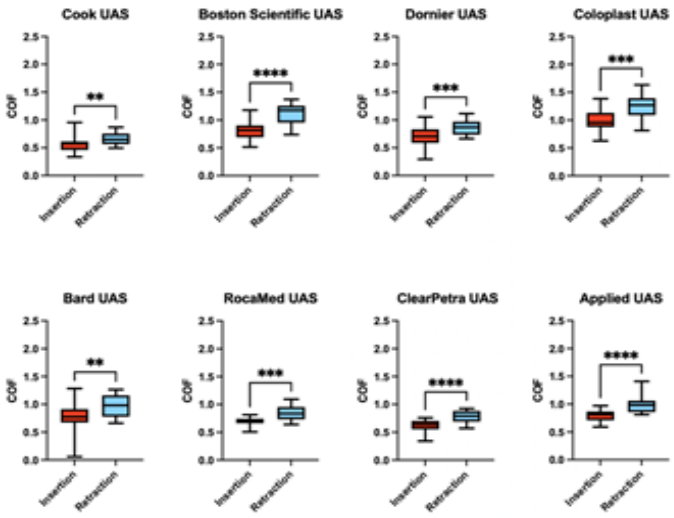


**Figure 2. Comparison of coefficient of friction values between the insertion and retraction cycles across different UASs.** Multiple unpaired sample t-tests with Welch corrections have been employed. *, **, ***, **** correspond to p values < 0.05, 0.01, 0.001 and 0.0001, respectively.

**Results:** Friction forces did not depict an increasing trend as multiple catheters were tested across the same ureter, indicating little degradation in the strip of ureter during testing. COF was higher during the retraction phase compared to the insertion phase for all UASs (**Figure 2**).

**Conclusion:** A novel reciprocating tribometer facilitates quantitative investigations into the mechanical interactions between a UAS and the ureter. Of note, among UASs studied, there was more friction recorded during retraction than insertion of the sheath.

**ABSTRACT # 6** **TOP 10 ABSTRACT**

# WHERE IS MY NEEDLE? USE OF A NEEDLE TIP INDICATOR FOR PERCUTANEOUS RENAL ACCESS IN ROBOTIC-ASSISTED PCNL

Saif Sayed PhD[1], Camilla Gomes MD[1,2], Brandon Cowan MD[1,2], Menglong Ye PhD[1], Elif Ayvali PhD[1], Hedyeh Rafii-Tari PhD[1]

[1] Johnson and Johnson, Inc, Redwood City, CA 94065

[2] Department of Surgery, University of California, San Francisco, CA 94143

**Introduction:** Accurate puncture of renal calices for percutaneous nephrolithotomy (PCNL) can be challenging, and influences both procedure success and complications such as injury to adjacent organs, violation of the pleural space, bleeding, or infection. We designed a feature indicating the projected needle position with a visual overlay on the endoscope view as part of the guided percutaneous access, which was implemented in the MONARCH™ Platform, Urology (Johnson & Johnson, Redwood City, CA). During percutaneous access, the needle tip is tracked by an electromagnetic field (EM) system. At the final phase of needle insertion, the algorithm interprets the needle tip's position in 3D space and projects this position onto a 2D image displayed as an overlay on the endoscope's feed (Figure 1). The objective of this study is to characterize the usability and accuracy of the needle tip indicator feature.

**Methods:** The algorithm was tested at 3 levels: 1. Spatial accuracy: how precisely a digital representation of needle tip aligns with the real-world location; 2. Latency: time lag between the initiation of a needle tip motion and the corresponding overlay update on scope view; and 3. Refresh rate: how many times the visual overlay is updated per second. We used a vision calibrated bench-top simulation of percutaneous access. To evaluate spatial accuracy, the needle was inserted at known 3D locations, and the 2D positions of needle tip alongside its projected indicator was recorded in the image. Calibration enabled transforming the 2D pixel difference between needle tip and its visual indicator to real-world distance in millimeter. A combination of 3 users, 5 scopes and 2 needles were used, and the needle was inserted at 4 different spatial locations for testing, with pre-determined confidence and reliability levels to meet success criteria. To test latency, a high-speed camera and software program measured the time lag between physical needle motion and the needle tip overlay update on the endoscope feed, and using different needles and hardware systems this was sufficiently repeated to ensure results were within 95% confidence interval of goal value.

**Results:** During the entire testing, spatial accuracy was maintained at a range of $\leq$2 mm with the physical location in anatomy space. The latency between the physical movement of the needle and the indicator's rendering on the UI was <450 msec. The refresh rate of the needle tip overlay was updated at a frequency of at least 12 Hz.

**Conclusion:** We characterized an algorithm's design which enables virtual overlay of needle tip during percutaneous access. We state that this demonstrates that the algorithm performance at a low latency and high spatial accuracy meets accepted threshold values, making this feature feasible as a guided user interface. This feature is intended to guide physicians for accurate percutaneous caliceal access during PCNL and increases autonomy by allowing urologists to intuitively learn to independently obtain percutaneous access. Clinical validation of this feature will be part of upcoming clinical studies of the MONARCH™ Platform, Urology.

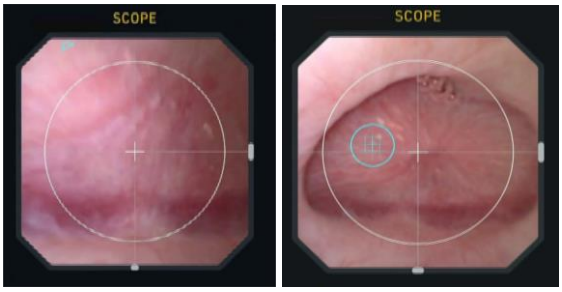


A B

**Figure 1.** MONARCH™ user interface with endoscopic view of a renal papilla. The live needle tip position during percutaneous access is overlayed as an arrow (A) signifying the relative needle location if it is approaching from outside of scope view, and transitions to a circle (B) if its projected position is in the scope's field of view.

**ABSTRACT # 7**

# COMPARING THE EFFECTS OF PERFUSION DECELLULARIZATION PROTOCOLS ON BLADDER ACELLULAR MATRIX (BAM) PROTEIN CONTENT, STRUCTURE, AND MECHANICS

Cecelia Eggleston[1], Felix Yiu[1], Jooyoung Song[1], Renea Sturm, MD[1]
[1] UCLA David Geffen School of Medicine Department of Urology

**Introduction:** Bladder acellular matrix (BAM) is a common biological scaffold for urologic tissue reconstruction and engineering. However, decellularization methods vary widely, and the unique properties of the bladder (e.g., thickness) of each organism can affect decellularization. This study compared two perfusion-based protocols, evaluating decellularization efficacy, protein yield, mechanics, and structural properties when applied to rabbit bladders.

**Methods:** Two candidate detergent protocols for tissue decellularization were selected based on literature review: Sodium Dodecyl Sulfate (SDS) and Detergent Enzymatic Treatment (DET). Tissue was obtained from adult New Zealand White male rabbits (n=3/cohort). Bladders were first distended at 4°C for 48 hours (h) with antibiotic solution. Decellularization then applied (1) 0.5% SDS for 28 h at room temperature (RT) OR (2) DET protocol using DI water (24 h, 4°C) then 4% Sodium Deoxycholate (4 h, RT). Both then applied DNase 2000 kU 1M NaCl (3h, RT). Each step used perfusion (0.3ml/min) and mechanical agitation (120 rpm). Decellularization efficacy, protein assays, and structure were assessed. Mechanical characterization used an Instron 345C-1 mechanical tester (0.5 N, 10 mm/min). SDS vs DET data was directly compared using two-tailed unpaired t-tests. Data is presented as mean ± standard error.

**Results:** Effective nuclei and DNA removal (>90%) was achieved by SDS and DET (Fig A, B, E). DET had greater preservation ($p \leq 0.0001$) of Elastin and Collagen compared to SDS. However, SDS had a significant increase ($p \leq 0.0001$) in GAG content versus DET (Fig C). Compared to native samples, there was a moderate overall loss in architecture, but tissue layers remained visible in both cohorts (Fig D). Additionally, there was no significant difference in tensile properties between SDS and DET (Fig F).

**Conclusion:** Perfusion-based decellularization with SDS or DET based protocols was efficient and effective. However, there were key difference in protein preservation that should be considered when utilizing these products. Further analysis of the effects of decellularization on core matrisome and matrisome associated protein yield using proteomics is planned.

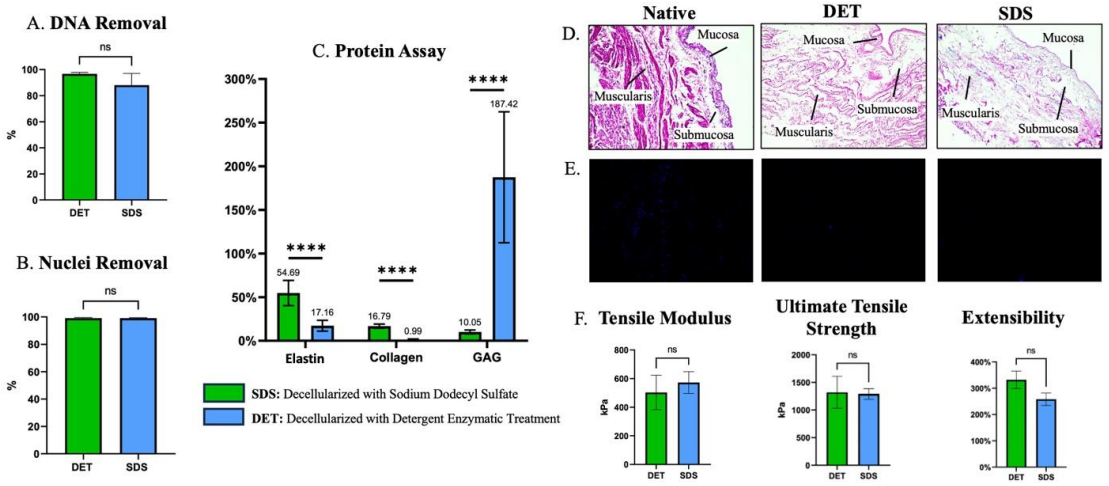


**Figure 1:** A. Percent DNA removal B. Percent nuclei removal C. Protein assays comparing bladders pre vs post-decellularization D. H&E histological structure E. DAPI nuclei immunofluorescence F. Mechanical Properties of decellularized bladder. ns $p < 0.05$, **** $p \leq 0.0001$

**ABSTRACT # 8**

## SIMULATED FLUOROSCOPY IN A PHYSICAL SIMULATOR FOR TRAINING IN PLACEMENT OF ADJUSTABLE CONTINENCE THERAPY DEVICES

Lawrence Yeung, MD[1], David Lizdas[1], Chong Zhao, PhD[1], Christopher Samouce, PhD[1], Andy Chen, Samsun Lampotang, PhD, FSSH, FAIMBE[1,2]
[1]University of Florida, Center for Safety, Simulation & Advanced Learning Technologies;
[2]University of Florida, Department of Urology

**Introduction:** Simulated fluoroscopy avoids exposure to ionizing radiation, facilitates logistics, reduces costs, and increases venues (e.g., workshops, exhibits, scientific meetings) where training can occur compared to using actual fluoroscopy in a simulator. We describe an application in a simulator that provides training in placement of surgical devices for the ProACT adjustable continence therapy procedure.

**Methods:** A transparent insert that slides into the simulator base contains the relevant anatomy: transparent resin pubic bones fastened to acrylic insert sidewalls, a genito-urinary diaphragm cast using dense transparent silicone placed between pubic bones, and a rectum, urethra, and bladder were molded with soft transparent silicone and placed in the insert. Transparent ballistics gel was poured to fill in the rest of the insert cavity. After the insert was placed in a base, a silicone penis with scrotal sac and urethra was attached to the top of the base. A brightness-adjustable LED ring light at the bottom of the base combined with a top-down camera registered over the insert and filtered to greyscale simulates a fluoroscopic view. A side camera provides sagittal views of trocar angulation and genitourinary diaphragm penetration. A back-end camera, simulating cystoscope retroflex, is used to observe indentation of the bladder by the trocar and coaptation of the bladder neck as the ProACT balloons are filled. A cystoscope camera, as sometimes used in this procedure, can be inserted into the urethra.

**Results:** Simulated fluoroscopic guidance along with internal anatomy views that are not usually visible clinically during ProACT implantation provide a wealth of information and feedback during training, without exposure to ionizing radiation. After the procedure, the insert can be removed, and balloon placement viewed for debriefing prior to insert replacement.

Two simulators were built. They have been used at multiple meetings and workshops to train in accurate placement of adjustable continence therapy devices.

**Conclusion:** This simulated fluoroscopy method can be applied for training in other fluoroscopy-guided procedures. Surgical educators looking to simulate complex interventions involving fluoroscopy for training purposes would be prime collaboration partners.

Figure 1: The built simulated physical anatomy relevant for ProACT procedure.


Figure 2: Four camera views: simulated fluoroscopy view, cystoscope view, side, and back views.

Acknowledgement: This project was funded by a grant from UroMedica.

**ABSTRACT # 9**

## INTEGRATION AND VERIFICATION OF VISUALIZED PROSTATE BIOPSY SYSTEM

Alejo Ballester, BS[1], Tomas Esteverena[1], Christopher Samouce, PhD[1], David Lizdas, BS[1], Chong Zhao, PhD[1], Sebastian Saramiento[1], Thomas Stringer, MD[2], Samsun Lampotang, PhD, FSSH, FAIMBE[1,2]
[1]University of Florida, Center for Safety, Simulation & Advanced Learning Technologies;
[2]University of Florida, Department of Urology

**Introduction:** The rate of prostate biopsy false negatives (PBxFN) is 21% - 47% in systematic prostate biopsy (sPBx)[1] and 16% - 30% in targeted prostate biopsy (tPBx).[2] The current practice leverages only the 2D information in the ultrasound screen and contains no information on the sPBx template locations. Our aim was to integrate and verify an intuitive guidance system for transrectal sidefire prostate biopsy[3] with actual prostate biopsy instrumentation.

**Methods:** A patient care system (PCS) prototype for visualized prostate biopsy (vPBx), utilizing electromagnetic (EM) tracking reversible retrofits for a transrectal ultrasound (TRUS) probe (BK 8818 Triplane), a biopsy device (Bard MC1825 MaxCore), and a urinary catheter (18 Fr dual balloon, Poesis Medical) placed inside the patient's prostate, was developed, and integrated to be used together with an ultrasound machine (BK Flex Focus 400). The software includes a replicated ultrasound screen from the ultrasound machine and a 3D perspective visualization of the prostate and tracked instrumentation. Both views feature cognitive aids to assist the user to accurately biopsy the template locations within 5 mm. Tracing and segmentation functionality allows the user to trace the prostate as viewed on the ultrasound for real-time prostate segmentation and reconstruction. The system was verified using prostate phantoms with 5 mm red spheres arranged in a double sextant template and registered to a virtual model. The red color distinguishes a hit from a miss. Systematic biopsies were performed on the prostate phantoms to evaluate the accuracy of the vPBx PCS.

**Results:** The vPBx system enabled an inexperienced user to sample the ground truth systematic biopsy template locations 12/12 times with a template deviation of 0.59 mm, a standard deviation 0.23 mm, and maximum core deviation of 1.11 mm.

**Conclusion:** A targeting and guidance system was developed and integrated with standard transrectal sidefire prostate biopsy instrumentation. The vPBx system has the potential to significantly reduce the prostate biopsy false negative rate for diagnosis of clinically significant prostate cancer (csPCa).

[1]Lampotang S. A translational roadmap to create the future of simulation in healthcare. In: Mahoney B, Minehart RD, Pian-Smith MC, eds. Comprehensive Healthcare Simulation: Anesthesiology. New York, NY: Springer Cham; 2020:325–336.
[2]Hanna N, et al. Multiparametric Magnetic Resonance Imaging-Ultrasound Fusion Biopsy Improves but Does Not Replace Standard Template Biopsy for the Detection of Prostate Cancer. J Urol. 2019 Nov;202(5):944-951. Epub 2019 Oct 9. PMID: 31144593.
[3]Lampotang S, Stringer T, Lizdas D. Visualized Prostate Biopsy: An Intuitive Three-Dimensional User Interface for Systematic and Targeted Biopsy. J Endourol. 2021 Aug;35(8):1198-1203. doi: 10.1089/end.2020.1013. Epub 2021 Feb 17. PMID: 33403896.

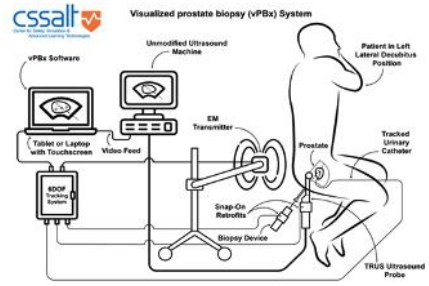


Figure 1: Schematic of the vPBx PCS setup.

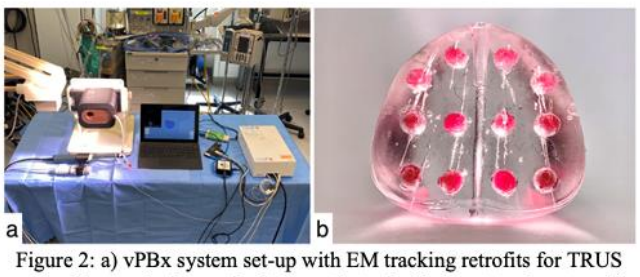


Figure 2: a) vPBx system set-up with EM tracking retrofits for TRUS probe, biopsy device, and urinary catheter inside prostate phantom. b) Needle traces show all twelve template cores of prostate phantom biopsied; all biopsy cores contained red gel.

Acknowledgement: This project was funded by the Bankhead-Coley Cancer Research Program through the Florida Department of Health.

**ABSTRACT # 10**

## EFFICACY OF DVIU VERSUS BALLOON DILATION TO TREAT RECURRENT URETHRAL STRICTURE FOLLOWING FAILED URETHROPLASTY

Gilbert, David BS[1,2]; Christ, Anastasia BA[1,2]; Gupta, Shubham MD[2]; Mishra, Kirtishri MD[1,2,3]
[1]Case Western Reserve University School of Medicine. [2]University Hospitals, Urology Institute, [3]MetroHealth Cleveland Medical Center

**Introduction:** Urethral strictures are a common condition with a prevalence of 229-627 per 100,000 males [PMC4708169]. They are regularly treated with interventions such as Direct Visual Internal Urethrotomy (DVIU) or Balloon Dilation (BD). However, reported success rates are highly variable with 35-96% for DVIU and 35-84% for BD [PMC4756988, PMC9181788, PMID29119701, PMC6995931]. While DVIU and BD are the most common interventions, urethroplasty can be used and has a success rate ranging from 18-100% depending on procedure type [PMC7857757]. If recurrent urethral stricture occurs following a failed urethroplasty, a salvaging endoscopic intervention may be performed. This study aims to describe the success rates of DVIU vs BD for recurrent urethral stricture following failed urethroplasty through a retrospective review. We are unaware of another study that directly compares success rates of DVIU vs BD as secondary interventions following urethroplasty.

**Methods:** The data used in this study were collected from TriNetX (TriNetX, Inc., Cambridge, MA, USA), a clinical research platform that collects and stores over 125 million patients' EHR data. Cohorts were constructed for both DVIU following urethroplasty and BD following urethroplasty. Given the small sample sizes, cohorts were not matched for comorbidities. Outcomes were defined as ≥1 instance of urethral stricture or stenosis, or retention of urine between 1 month and 3 years after DVIU or BD. Outcomes were assessed with Kaplan Meier, Hazard Ratios (HR) and log-rank tests to determine significance ($p<0.05$).

**Results:** DVIU (N=45) had a significantly higher probability (p=0.0353) of recurrent urethral stricture compared to BD (N=25), with respective 3-year incidence probabilities of 95.15% and 69.05% (Figure 1). DVIU had a median survival of 99 days while BD had a median survival of 355 days. DVIU had an increased hazard compared to BD with a HR of 1.901 (95% CI: 1.034, 3.497).

**Conclusion:** For patients experiencing recurrent urethral stricture post-urethroplasty, BD appears to have better three-year outcomes compared to DVIU. Additionally, the data suggest that in the short term BD may provide longer-lasting symptom relief before recurrence of urethral stricture. Future studies should prioritize larger sample sizes and consider a randomized control trial.

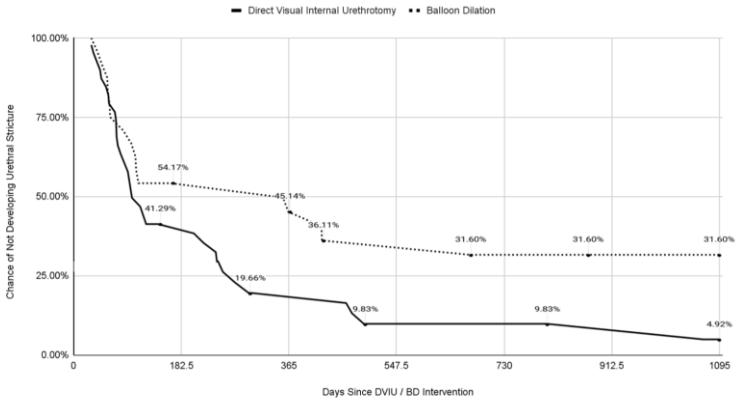


Figure 1: Three-year Kaplan Meier Demonstrating Probability of Developing ≥1 Instance of Urethral Stricture after Secondary Intervention Following Failed Urethroplasty

**ABSTRACT # 11**

## HIGH INTENSITY FOCUSED ULTRASOUND (HIFU) BASED TISSUE ELASTICITY MAPPING FOR PLANNING PROSTATE ABLATION

Minho Song[1,2,3], Oleg A. Sapozhnikov[2], Gerald Lee[4], Gabriel Regnault[4], Ivan M. Pelivanov[4], George R. Schade [5], Tatiana D. Khokhlova[2,3]

[1]Department of Mechanical Engineering, [2]Department of Gastroenterology, [3]Center for Industrial and Medical Ultrasound, Applied Physics Lab[4]Department of Bioengineering, [5]Department of Urology, University of Washington, Seattle, Washington, USA

**Introduction:** Accurately determining the margins of prostate cancer (PCa) during planning of endorectal high intensity focused ultrasound (HIFU) based ablation under B-mode ultrasound (US) imaging is challenging (even with MR-Fusion technology). Shear wave elastography (SWE) is a mature imaging tool for localization of PCa with high sensitivity and specificity, but is limited by push capabilities for larger depths and a lack of "built-in" arrangements in clinical focal therapy systems. Using the endorectal HIFU transducers for pushing, and the integrated US imaging probe for tracking the resulting tissue displacement circumvents these limitations. We aimed to develop a HIFU-SWE method of mapping tissue elasticity and validate it in tissue-mimicking phantoms with the long-term goal of using it to precisely localize prostate cancer during transrectal HIFU based focal therapy.

**Methods:** A 1.5 MHz HIFU transducer (focal length 60 mm) with in-line US probe produced a 1 ms long localized push at its focus through acoustic radiation force in 5 cm cuboid tissue-mimicking phantoms. An US probe driven by Verasonics V1 system was used to track the resulting speckle displacement along the HIFU axis over a 50 ms time window. The phantoms were fabricated from 6% polyvinyl alcohol (PVA) with 3% $Al_2O_3$ powder with different elastic moduli by changing the number of freeze-thaw cycles within 1-3. The elastic moduli of the phantoms were calibrated by optical coherence elastography (OCE) and SWE imaging and were 5, 23 and 50 kPa. Finite differences numerical modelling was used to predict shear wave propagation over the observation time.

**Results:** The shear wave propagation pattern following the push by the elliptically shaped HIFU focal area included "classic" side-propagating shear waves, and those propagating along the HIFU axis. These "longitudinal" shear waves formed due to diffraction of the "classic" shear waves and propagated faster by a constant factor related to the shape of the HIFU focal area (Fig.1B). Tracking of the "longitudinal" shear wave propagation along the HIFU axis via speckle tracking was feasible, and yielded the values of 5 kPa, 25 kPa, and 47 kPa for the three phantoms.

**Conclusion:** HIFU push enabled SWE measurement of elastic modulus along the HIFU axis with high accuracy. Future studies will implement this technique onto a transrectal HIFU array to perform SWE measurement throughout the potential treatment region of interest to map the elastic modulus in tissue and localize PCa immediately prior to treatment.

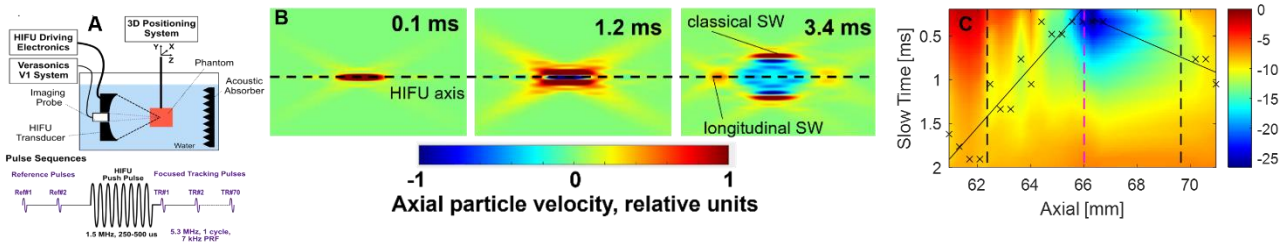


Fig.1. A) Schematic of the HIFU SWE measurement and pulsing sequence. B) Numerically simulated shear wave propagation when excited by a 1 ms long HIFU pulse. C) Shear wave displacement along the HIFU axis measured in the softest phantom.

**ABSTRACT # 12** **TOP 10 ABSTRACT**

# THE MEASUREMENT OF INTRARENAL PRESSURE IN URETEROSCOPY WITH LASER LITHOTRIPSY: A PROSPECTIVE TRIAL

Jamie Finegan, Jonathan Katz, Jonathan Berger, Seth Bechis, Manoj Monga, Roger Sur
University of California, San Diego

**Introduction**: Intrarenal pressure (IRP) during Ureteroscopy with laser lithotripsy (URS) is believed to be a major adjustable risk factor for post-operative sepsis. Pyelovenous backflow is known to occur at greater than 30mmHg. Despite this, measuring intrarenal pressures during kidney stone surgery is not currently standard of care. The objective of our study was to show that continuous IRP measurement with a pressure guidewire during URS is safe and feasible alongside a Boston Scientific Navigator HD ureteral access sheath (UAS).

**Methods**: We performed an analysis of a single institutional prospective data collection of patients with renal and/or ureteral stones who underwent flexible URS. We collected demographic data as well as intraoperative data including UAS size and IRP (continuously measured using the COMET II Pressure Guidewire, Boston Scientific Marlborough, MA). The Comet II pressure guidewire was introduced to the renal pelvis fluoroscopically through a dual lumen catheter, and correct placement was confirmed visually by a ureteroscope. We calculated the mean, median, and maximum IRP for each patient. Data was collected at baseline (just before access sheath placement) and continued until the removal of the access sheath at the end of treatment. Finally, we tracked intraoperative complications and infectious complications.

**Results**: A total of 55 patients were analyzed with a median age of 58 and 42% male. We found an average case time of 64.4 minutes, and an average stone size of 13.2 millimeters. UAS sizes included 11/13Fr (n=31), 12/14Fr (n=19), 13/15Fr (n=3), and no access sheath (n=2). We found that our baseline IRP had a median of 23mmHg across all patients. The average increase in pressure after inserting the access sheath was lower for the 12/14 sheath compared to the 11/13 sheath [Graph 1]. At baseline the average pressure of the 12/14 sheath was lower than the 11/13 sheath; and at treatment the average pressure of the 12/14 sheath was lower than the 11/13 sheath. There were no adverse events or intraoperative complications; however, two patients were excluded due to the Comet II pressure guidewire breaking in their urinary system (single fragment removed with a basket). There were three episodes of postoperative urinary tract infections (5.7%).

**Conclusion**: We found that intraoperative monitoring of IRP is safe and feasible, with the Comet II guidewire providing a mechanism to monitor the impact of alterations on IRP. Larger access sheaths conferred lower IRP. Our goal moving forward is to continue to collect data to describe any potential relationships between IRP and patient outcomes.

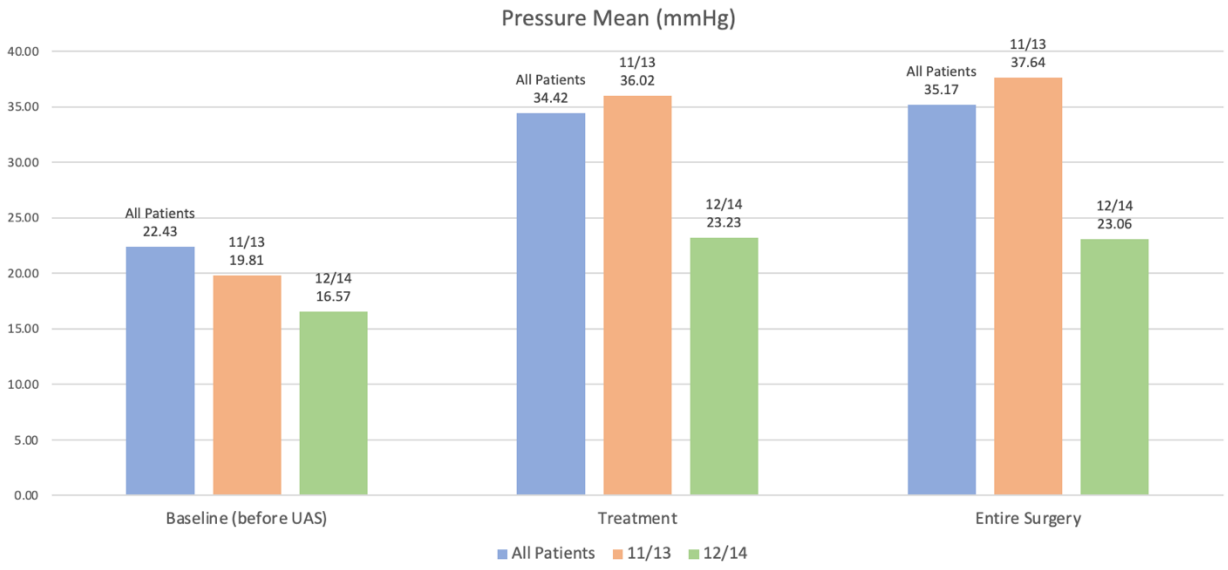


Graph: Intrarenal pressures of patients who underwent URS with a UAS

**Source of Funding**: Boston Scientific

**ABSTRACT # 13**

## EXPLORING THE FEASIBILITY OF GPT-4 AS A DATA EXTRACTION TOOL FOR RENAL SURGERY OPERATIVE NOTES

Jessica Y. Hsueh[1], Daniel Nethala[1], Shiva Singh[2], Jason A. Hyman[1], David G. Gelikman[2], W. Marston Linehan[1], Mark W. Ball[1]

[1] Urologic Oncology Branch, National Cancer Institute, National Institutes of Health
[2] Radiology and Imaging Services, Clinical Center, National Institutes of Health
[3] Molecular Imaging Branch, National Cancer Institute, National Institutes of Health

**Introduction:** Artificial intelligence (AI) has become more accessible to the public with large language models (LLMs) like ChatGPT. In healthcare, the potential for AI to assist with daily tasks and improve scientific communication is immeasurable. Few studies have looked at AI as a tool for data extraction, which requires immense time and effort while being prone to human error. Our study sought to evaluate a practical application of the LLM GPT-4 in extracting operative data for renal cancer patients.

**Methods:** Deidentified operative notes were compiled in a secure database. GPT-4 was queried to extract information on laterality, surgery, approach, estimated blood loss (EBL), and ischemia time. The extracted information was then compared to a preexisting human-curated database. Discrepancies were manually reviewed. The number of matched and correct data points was used to calculate match and accuracy rates for GPT-4 and human-curated extraction.

**Results:** 1498 patients from January 2003 to January 2023 underwent renal surgery at our institution. The match rate was high for laterality (94.6%), surgery (92.5%) and approach (89.4%) but lower for EBL (77.1%) and ischemia time (25.6%). GPT-4 was more accurate in extracting information for laterality (96.6% GPT-4 accuracy rate vs. 96% human-curated rate) and EBL (90.3% accuracy rate vs. 85.5% human-curated rate). There was a 99.3% human-curated accuracy rate (vs. 93% GPT-4 rate) for surgery and a 97.9% human-curated accuracy rate (vs. 90.8% GPT-4 rate) for approach. Notably, ischemia time had a human-curated accuracy rate of 95.6% compared to a 30.7% GPT-4 rate.

| | GPT-4 | Human-Curated |
|---|---|---|
| Laterality (n = 1480) - no. (%) | | |
| Accuracy Rate | **1429 (96.6%)** | 1420 (96%) |
| Match Rate | 1400 (94.6%) | |
| Surgery (n = 1498) - no. (%) | | |
| Accuracy Rate | 1392 (93%) | 1487 (99.3%) |
| Match Rate | 1386 (92.5%) | |
| Approach (n = 1492) - no. (%) | | |
| Accuracy Rate | 1355 (90.8%) | 1460 (97.9%) |
| Match Rate | 1334 (89.4%) | |
| EBL (n = 1498) - no. (%) | | |
| Accuracy Rate | **1353 (90.3%)** | 1281 (85.5%) |
| Match Rate | 1155 (77.1%) | |
| Ischemia Time (n = 567) - no. (%) | | |
| Accuracy Rate | 174 (30.7%) | 542 (95.6%) |
| Match Rate | 145 (25.6%) | |

Table 1: Summary of match rates, GPT-4 accuracy rates, and human-curated accuracy rates for laterality, surgery, approach, EBL, and ischemia time. Bold is used to denote where GPT-4 had a higher accuracy rate than human-curated extraction.

**Conclusion:** Match and accuracy rates were higher for nominal categorical variables. GPT-4 data extraction was particularly error prone for variables with heterogenous documentation styles. The role of a standard operative template to aid data extraction will be explored in the future. GPT-4 can be used as a powerful efficient data extraction tool with human feedback and oversight to efficiently compile large-scale databases and reduce time and effort required for this task.

**ABSTRACT # 14**

## INVESTIGATING THE CLINICAL REASONING ABILITIES OF GPT-4: A POSTOPERATIVE COMPLICATION ANALYSIS FROM RENAL SURGERIES

Jessica Y. Hsueh[1], Daniel Nethala[1], Shiva Singh[2], Jason A. Hyman[1], W. Marston Linehan[1], Mark W. Ball[1]
[1] Urologic Oncology Branch, National Cancer Institute, National Institutes of Health
[2] Radiology and Imaging Services, Clinical Center, National Institutes of Health

**Introduction:** Large language models (LLMs), a subset of artificial intelligence, can understand and generate human speech through natural language processing, with immense potential to support human tasks. Many have questioned the role of LLMs in science and medicine, which require strong critical thinking and analysis skills. The objective of our study was to evaluate the LLM GPT-4's clinical reasoning abilities by analyzing postoperative complications from renal surgery discharge summaries.

**Methods:** Prompts were engineered in GPT-4 to extract from deidentified discharge summaries whether there were any postoperative complications and what the complication was. GPT-4 was asked to interpret each complication's Clavien-Dindo classification and institutional-specific category (genitourinary, respiratory, etc.). GPT-4's database was compared to a human-curated database. Discrepancies were manually reviewed to determine the number of same data points and calculate match and accuracy rates.

**Results:** 944 renal surgeries were conducted from August 2005 to March 2022. There was a 79.6% match rate between GPT-4 and human-curated data in detecting postoperative complications. Accuracy rates were 86.7% for GPT-4 and 92.9% for human-curated. A subgroup of 139 patients had a complication detected by both GPT-4 and human with available Clavien-Dindo and category information. There was a 37.4% overall match rate for Clavien-Dindo classification and a 55.4% match rate for category.

**Conclusion:** GPT-4 was able to detect with high accuracy if there were any postoperative complications, showing its strength in data extraction and reasoning for simple tasks. It struggled more with the complex task of further analyzing complications, especially with Clavien-Dindo, a classification system that requires more critical thinking and interpretation. With manual oversight, GPT-4 can aid clinicians in analyzing postoperative complications to improve patient outcomes.

Table 1: Summary of detection of postoperative complications for human-curated and GPT-4. Accuracy and overall match rates are bolded.

| | GPT-4 (n = 944) no. (%) | Human-Curated (n = 944) no. (%) |
|---|---|---|
| Complication | 216 (22.9%) | 279 (29.6%) |
| # matched cases | 151 | |
| No Complication | 728 (77.1%) | 665 (70.4%) |
| # matched cases | 600 | |
| Overall Match Rate | **751 (79.6%)** | |
| Accuracy Rate | **818 (86.7%)** | **877 (92.9%)** |

Table 2: Summary of postoperative complications based on Clavien-Dindo and category for human-curated data and GPT-4 data. Overall match rates are calculated and bolded.

| | GPT-4 (n = 139) no. (%) | Human-Curated (n = 139) no. (%) |
|---|---|---|
| Clavien-Dindo | | |
| Grade 1 | 37 (26.6%) | 2 (1.4%) |
| Grade 2 | 54 (38.8%) | 76 (54.7%) |
| Grade 3a | 35 (25.2%) | 28 (20.1%) |
| # matched cases | 7 | |
| Grade 3b | 0 (0%) | 13 (9.4%) |
| # matched cases | 0 | |
| Grade 4a | 12 (8.6%) | 20 (14.4%) |
| # matched cases | 9 | |
| Grade 4b | 0 (0%) | 0 (0%) |
| Grade 5 | 1 (0.7%) | 0 (0%) |
| Overall Match Rate | **52 (37.4%)** | |
| Category | | |
| Gastrointestinal | 10 (7.2%) | 10 (7.2%) |
| Genitourinary- Bleeding | 42 (30.2%) | 45 (32.4%) |
| Genitourinary- Other | 30 (21.6%) | 7 (5.0%) |
| Genitourinary- Urine Leak | 45 (32.4%) | 55 (39.6%) |
| Infectious | 5 (3.6%) | 9 (6.5%) |
| Neurologic | 1 (0.7%) | 1 (0.7%) |
| Renal | 2 (1.4%) | 2 (1.4%) |
| Respiratory | 4 (2.9%) | 10 (7.2%) |
| Overall Match Rate | **77 (55.4%)** | |

**ABSTRACT # 15**

## STRONG AND ELASTIC: COMPARISON OF TENSILE PROPERTIES BETWEEN THE VAGINA, BLADDER, AND URETHRA

Jooyoung David Song[1], Felix Yiu[1], Yadi Huo[1], George Aninwene II[1], Gladys Ng[1], Renea Sturm[1]
[1] Department of Urology, David Geffen School of Medicine, University of California Los Angeles.

**Introduction:** Vaginal replacement or repair of tissue is limited, with many conditions using either bowel, skin, or peritoneum as potential autologous donor graft sources. Porcine small intestinal submucosa (SIS) has been evaluated in urogynecologic reconstruction and regenerative medicine, but its role as a tissue engineering scaffold remains limited [PMID31432871]. An aspect of decellularized matrices that has been inconsistently reported is their mechanics, despite functional and wound healing effects of substrate elasticity [PMID35442107]. The study aim was to comparatively evaluate the elastic modulus, ultimate tensile strength, and extensibility of vaginal, bladder, urethral tissue, and SIS.

**Methods:** Native proximal (PV) and distal (DV) vaginal and supra-trigonal bladder samples were obtained from healthy adult New Zealand white rabbits. Vaginal, bladder, urethral, and SIS (Biodesign 1-layer, Cook) longitudinal (2x1cm) samples were extended (2 mm/min) with the Instron 34SC-1 at room temperature until visible rupture, assessing tensile modulus (TM), ultimate tensile strength (UTS), and percent extensibility (EXT). Unpaired two-tailed t-tests compared PV versus DV, and vagina versus bladder, urethral, or SIS cohorts, respectively. Data was reported as mean ± standard error.

**Results:** TM, UTS, and EXT of the PV (n=6) were 334.05 kPa ± 44.78, 458.28 kPa ± 41.94, and 208.97% ± 26.76, respectively. The TM, UTS, and EXT of the DV (n=7) were 501.39 kPa ± 66.60, 577.30 kPa ± 71.77, and 147.51% ± 9.61 respectively. There was no significant difference between PV and DV tissue TM ($p>.05$) or UTS ($p>.05$), but PV EXT was significantly higher than DV EXT ($p<.05$). Vaginal TM and UTS were significantly higher than bladder TM ($p<.01$) and UTS ($p<.001$) and urethral TM ($p<.0001$) and UTS ($p<.0001$). Vaginal EM and UTS were significantly lower than SIS EM ($p<.0001$) and UTS ($p<.0001$). Vaginal EXT was significantly higher than SIS EXT ($p<.0001$).

**Conclusion:** Vaginal tissue exhibited significantly more strength (UTS) and resistance to deformation (TM) than bladder or urethral tissue. In addition, SIS had an approximately 5-fold higher UTS, with less than half the stretchability (EXT) of vaginal tissues, consistent with a stiffer substrate. Tensile data is critical to inform bioinspired scaffold development, with this study providing target mechanics based on a commonly applied animal model in urogynecologic translational research.

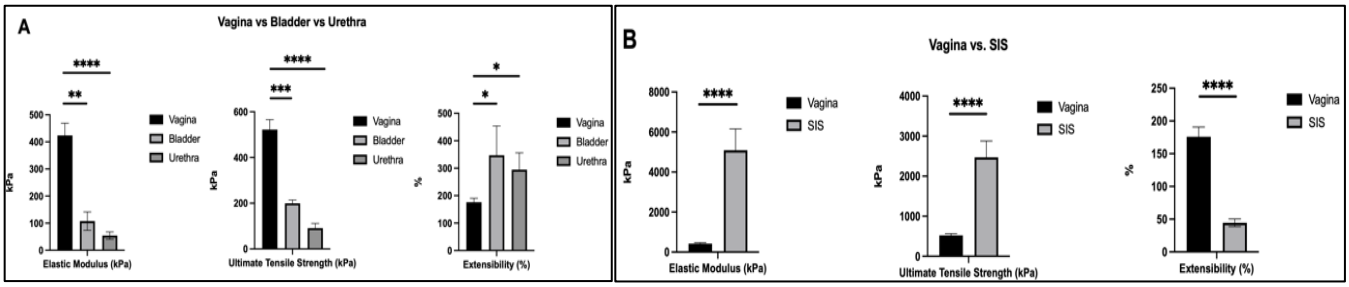


**Figure:** A. Tensile properties of vagina, bladder, and urethra. B. Tensile properties of vagina and SIS. *, **, ***, and **** denote $p<0.05$, $p<0.01$, $p<0.001$, and $p<0.0001$ respectively.

**ABSTRACT # 16**

# COMPARISON OF TENACIO PUMP AND MS PUMP EFFICIENCY USING SURFACE ELECTROMYOGRAPHY (sEMG)

Justin Lee MD, Daniel Schoenfeld MD, Gregory Joice MD[1]
[1] Columbia University Irving Medical Center, New York, NY 10032

**Introduction:** Inflatable penile implant (IPP) pumps can be difficult to inflate especially in older men. This study compares the efficiency of the TENACIO and Momentary Squeeze (MS) Pumps in filling IPP cylinders.

**Methods:** Two pumps (Boston Scientific's MS and TENACIO Pumps) were utilized in an *ex-vivo*, head-to-head trial. Pumps were supplied by Boston Scientific Corportation. Three separate tasks were performed on identical AMS 700™ IPPs with: 1] Fill from empty to max (max defined as 3 consecutive pumps where pump is not fully compressed), 2] 10 full pump squeezes (allowing for complete refill of pump bulb between pumps), and 3] Fill from 10ml to 40ml. sEMG (Delsys Trigno®) data was collected from the thenar, flexor carpi radialis (FCR), and extensor carpi radialis (ECR) muscle groups. The sEMG was normalized to the participant's own max voluntary contraction (MVC) for each muscle group (**Figure 1**). Cumulative muscular workload (CMW) was calculated as time integral of the MVC. Average muscular work per second (AWS) was calculated by dividing CMV by time to completion. T-tests were used to compare differences in time, CMW, and AWS.

**Results:** 10 participants performed each task. Time to completion was significantly faster in the TENACIO group compared to the MS group across all 3 tasks (27% faster, p = 0.002; 35% faster, p=0.001; 70% faster, p=0.001, respectively). There was no statistically significant difference in CMW for any task for all muscle groups. However, the AWS for TENACIO was significantly higher for all tasks in all 3 muscle groups (thenar, FCR, ECR) (**Figure 2**). The TENACIO Pump was up to 71% more efficient (FCR, Task 3 (10 full squeezes) compared to the MS Pump.

**Conclusion:** The TENACIO Pump is significantly faster at filling and pumps with significantly greater efficiency compared to the MS Pump in an *ex-vivo*, head-to-head trial of three independent tasks utilizing sEMG data. Future studies are needed to understand efficacy in-vivo and patient satisfaction with this pump.

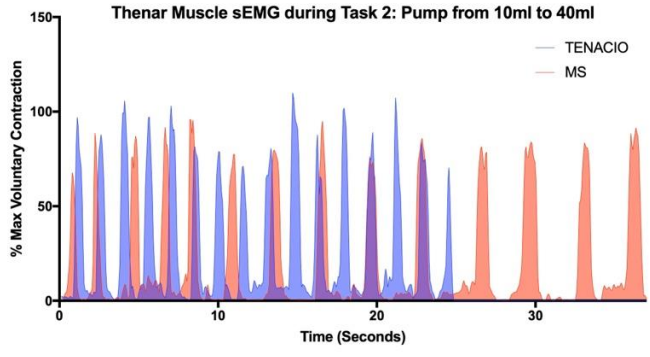


**Figure 1**: Thenar muscle group sEMG activity for one participant during Task 2: Pump from 10ml to 40ml with TENACIO (blue) and MS (red) pumps represented in %MVC.

**Figure 2**: Mean average muscular workload per second

| | TENACIO | MS | p value |
|---|---|---|---|
| **Thenar** | | | |
| **Task 1** | 29.84 | 20.03 | 0.004 |
| **Task 2** | 24.73 | 14.82 | 0.003 |
| **Task 3** | 24.95 | 15.91 | 0.001 |
| **FCR** | | | |
| **Task 1** | 26.80 | 21.23 | 0.037 |
| **Task 2** | 25.33 | 17.28 | 0.007 |
| **Task 3** | 26.22 | 15.28 | 0.020 |
| **ED** | | | |
| **Task 1** | 24.12 | 17.50 | 0.014 |
| **Task 2** | 25.64 | 16.53 | 0.003 |
| **Task 3** | 20.04 | 14.53 | 0.002 |

**ABSTRACT # 17**

## EARLY RESULTS OF URETHRAL BULKING WITH POLYACRYLAMIDE HYDROGEL IN MALE STRESS URINARY INCONTINENCE: A MULTI-INSTITUTIONAL RETROSPECTIVE COHORT

Luke Griffiths [1], Allie Tabakin [1], Maya Srinath [1], Wai Lee [1], and Donna Deng[2]
[1]Smith Institute for Urology, Northwell Health, Manhasset, NY
[2]Department of Urology, Kaiser Permanente, Oakland, CA

**Introduction:** Stress urinary incontinence (SUI) in men is estimated to affect up to 17% of men and can be associated with iatrogenic causes, such as radical prostatectomy (RP), radiation therapy (RT), and outlet procedures for benign prostatic hyperplasia. The use of urethral bulking agents in both men and women have historically lacked durability and could be associated with tissue inflammation, abscess, or erosion. With the advent of urethral bulking with polyacrylamide hydrogel (PAHG) to treat SUI in women, there have been findings of prolonged efficacy, while its effect in men has not been reported. Our objective is to present our experience with PAHG in men as part of a multi-institutional retrospective analysis.

**Methods:** Our cohort included men treated with PAHG for SUI from 2021 to 2023 at two academic institutions, with all procedures performed by 2 urologists. Patients were excluded if they were lost to follow-up or had incomplete data postoperatively. The primary endpoint was improvement from baseline in pads per day (PPD). improvement, and complications reported.

**Results:** A total of 34 patients underwent PAHG. Of these, 24 patients met inclusion criteria. The median number of PAHG procedures performed on each patient was 2. The majority of patients (95.8%) had iatrogenic SUI from RP, while 5 (20.1%) patients had a history of RT. Overall, 5 (21.7%) patients experienced a 50% improvement in PPD from baseline. Patients reported post-PAHG a mean improvement of 22.6% (± 29.2) with 43.3% (± 41.6) satisfaction rate. The median follow-up interval 6.2 (± 6.7) months. The UDI-6 composite score after PAHG improved from baseline 6.9 (± 2.1) to post procedural 2.1 (± 1.3) (Table 1). No post-operative complications were reported.

**Conclusion:** PAHG offers a less invasive alternative treatment for SUI in men that could potentially provide greater durability over traditional bulking agents with minimal tissue fibrosis and inflammation. Our preliminary findings demonstrate early efficacy, but longer follow-up is needed to reach further conclusions. Moreover, further analysis of larger cohorts could shed light on ideal patient selection for optimal results.

**Table 1.** *Baseline demographics and procedure outcomes*

| Total patients | 24 | *p-value* |
|---|---|---|
| Age | 68.5 ± 6.7 | |
| BMI | 27 ± 3.0 | |
| Follow up (months) | 6.2 ± 6.7 | |
| Prior history of | | |
| BPH surgery | 1 (4.2%) | |
| Prostate cancer | 23 (95.8%) | |
| Prostatectomy | 23 (95.8%) | |
| Radiation | 5 (20.8%) | |
| % improved | 22.6 ± 29.2 | |
| % Satisfaction | 43.3 ± 41.6 | |
| pre PPD | 2.3 ± 1.2 | |
| post PPD | 2.1 ± 1.3 | .252 |
| Pre UDI6 total | 6.9 ± 2.1 | |
| Post UDI6 total | 5.6 ± 2.5 | .105 |
| Post operative complications | 0 | |

BMI = Body mass index; BPH = Benign prostate hyperplasia; PPD = Pads per day; UDI6 = Urinary Distress Inventory
All nominal values are presented in n (%)
All continuous variables are presented in mean ± standard deviation

**ABSTRACT # 18**

## BURST WAVE LITHOTRIPSY FOR OBSTRUCTING URETEROLITHS IN PET CATS

Eva Furrow[1], Adam Hunt[1], Jody P. Lulich[1], Marissa Torre[1], Adam D. Maxwell[2,3], Kaizer Contreras[3], Ga Won Kim[3], Michael R. Bailey[2,3] Michael S. Borofsky[4]

[1]Department of Veterinary Clinical Sciences, University of Minnesota, St. Paul, MN
[2]Department of Urology, University of Washington School of Medicine
[3]Center for Industrial and Medical Ultrasound, Applied Physics Laboratory, University of Washington
[4]Department of Urology, University of Minnesota, Minneapolis, MN

**Introduction:** Obstructing ureteroliths are common in cats, and mortality is 6-18% with surgery. Burst wave lithotripsy (BWL) is a non-invasive, ultrasound-guided, handheld focused ultrasound technology that successfully and safely disintegrates ureteroliths in humans. We report results of the first treatments in cats.

**Methods:** Cats with obstructing ureteroliths were enrolled. The BWL therapy transducer was coupled with a micro-convex imaging transducer. Cats were anesthetized, and stones were treated for up to 60 minutes at 0.8-1 MHz. Biochemical and abdominal imaging data were evaluated at immediate (1-3 day) and short term (2-4 week) follow up. A second treatment was performed if indicated. Adverse events were recorded and characterized by severity and relationship to BWL. Technical success was defined as resolution of obstruction, urolith passage, or apparent fragmentation.

**Results**: Five cats were treated with BWL, including one with bilateral obstructions and four with unilateral obstructions. In total, 6 ureters and 11 ureteroliths were treated. Four cats required a second treatment due to persistent (3) or worsening (1) obstruction; the latter was classified as a major adverse event possibly related to BWL. Technical success was achieved for 8 of 11 ureteroliths. Four had a reduction in serum creatinine (median decrease of 29%, range 6-46%). One cat had persistent obstruction and no clinical improvement.

**Conclusions:** BWL shows promise as a minimally invasive therapy for ureteroliths in cats. In cats with multiple ureteroliths, multiple treatments or a longer treatment might be necessary. Additional data are needed to determine how BWL outcomes compare to current treatment modalities.

Acknowledgement: Work supported by NIDDK P01 DK043881, NIDDK K01 DK104854, ORIP K01 OD019912, UL1TR002494, UW Comotion F2022-8524-Bailey, the EveryCat Health Foundation, and the Focused Ultrasound Foundation.

**ABSTRACT # 19** **TOP 10 ABSTRACT**

# THE EFFECT OF PROSTATE SIZE AND NUMBER OF CORES AT SYSTEMATIC PROSTATE BIOPSY

Michael E. Rezaee[1], Misop Han[1], Katarzyna J. Macura[3], Bruce Trock[1], Amin Herati[1], Christian Pavlovich[1], Dan Stoianovici[1,2]
[1]Brady Urological Institute [2]Robotics Laboratory, [3]Department of Radiology, Johns Hopkins University

**Introduction:** Systematic biopsy (SB) can detect clinically significant prostate cancer (csPCa) that is not detected by fusion MRI-targeted biopsy (TB) alone, due to false negatives on multiparametric magnetic resonance imaging (mpMRI) [PCM35507051] and needle targeting errors [PMC3876458]. Some urologists considered reducing the number of SB cores when used in conjunction with TB [PMC35027690] or eliminating SB all together in mpMRI negative patients [PMC31326219]. Conversely, nearly 60% of urologists who perform biopsies reported the same or increased use of SB without MRI [AUA2022]. It is unclear how to best incorporate SB in the mpMRI era. The purpose of this study [PMC38184758] is to estimate the effect of prostate volume and number of SB cores on sampling csPCa ( > 0.5cm$^3$ [PCM7506797]) with a biopsy simulation [EUS2018 Abs.43] using clinical data.

**Methods:** SB plans with an increasing number of cores were simulated on prostate images from 42 consecutive patients enrolled in a transrectal ultrasound robot-assisted [EUS2017 Abs.34] biopsy clinical trial [EUS2023 Abs.11]. Patients aged 45 to 75 underwent pre-biopsy mpMRI interpreted according to PI-RADS v2.1. An example with a 15-core SB plan optimized for one of the patients is shown in Figure 1. In short, the goal of the optimization method is to fill the prostate as much as possible with capsules [EUS2022 Abs.36]. The degree with which the capsules fill the gland is used to quantify the csPCa detection probability (csCDP). Figure 1 also shows that mpMRI depicted regions of interest (ROI) were sampled at SB. The aims of the simulation were to evaluate the joint influence of the number of SB cores and prostate volume on 1) csCDP and 2) percentage of ROIs successfully sampled by SB alone using linear mixed statistical models.

**Results:** Median prostate volume (interquartile range [IQR]) was 47.2 cm$^3$ (35.6-65.6) , ROI was 0.6 cm3 (0.4 - 0.8) for ROI volume, and PI-RADS v2.1 score was 4.0 (3-5). csCDP increased with the increasing number of simulated SB cores and decreased substantially with larger prostate volume. For example, in small prostates (<40 cm$^3$), over 80% of csPCa can be detected with 15 SB cores, whereas in large ones (>80 cm$^3$), 15 cores may only detect 30%. Similarly, the percentage of mpMRI ROIs sampled by SB increased with the increasing number of SB cores and decreasing prostate size. For example, 18-core SB alone may sample 80% of ROIs in < 60 cm$^3$ glands, but only 50% in larger prostates [PMC38184758].

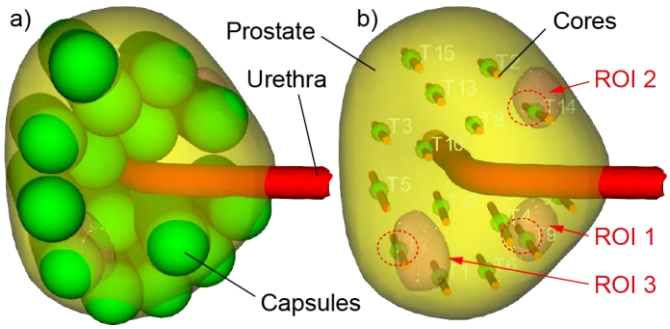


Figure 1: SB plan example: Prostate volume 41cm$^3$, three ROIs, 15-core personalized SB plan: a) Prostate filled with Capsules resulting in 59% csCDP; b) The same SB plan showing biopsy cores and how all 3 ROIs were sampled by SB: ROI1 sampled by core T9 over 8.5mm, ROI2 by T14 over 5.05mm, and ROI3 by T7 over 1.95mm.

**Conclusions:** In smaller prostates, SB can achieve adequate cancer detection even without pre-biopsy mpMRI, fusion, and TB. In larger prostates, SB alone is likely to result in inappropriate sampling and under-detection of csPCa.

**Disclosure**: Under a license agreement between Eigen Health Services and the Johns Hopkins University, author DS, and the University are entitled to royalty distributions related to technology described in this article. This arrangement has been reviewed and approved by the Johns Hopkins University in accordance with its conflict-of-interest policies.

**Acknowledgment**: Research reported in this publication is supported by the National Cancer Institute of the National Institutes of Health under award number R01CA247959, PI Stoianovici.

**ABSTRACT # 20**

## AUTOMATIC KIDNEY STONE SEGMENTATION IN CT SCANS USING DEEP-LEARNING NEURAL NETWORK

Murillo F. Bouzon[1], Weverson da Silva Pereira[1], Rafael Zacarias Palierini[1], Oscar E. H. Fugita[2], Paulo Sergio Silva Rodrigues[1]

[1] Centro Universitário FEIB [2] Hospital Universitário USP

**Introduction:** The gold standard radiological exam for kidney stone diagnosis is the non-contrast computed tomography (NCCT) due to its high sensitivity and specificity. During the analysis of the CT scans, the radiologist must not only detect the stones but also gather other information such as the number of stones, location, size and density, skin-stone distance, and infundibulum-pelvic angle, for example. To help the diagnosis, automatic segmentation of stones in CT exams is a valuable tool that may help locate the stones and estimate their sizes faster. Deep-learning neural networks, such as the U-Net architecture, demonstrated promising results in medical image segmentation. However, these deep-learning algorithms need large datasets of images manually labeled for training the learning model. To solve this problem, we developed a novel dataset of manually annotated images to train a deep-learning neural network model for kidney stone segmentation on CT scans.

**Methods:** The U-Net architecture was used for urinary stone segmentation due to the consistent results obtained in the literature related to medical image segmentation. To create the dataset, we manually annotated 838 CT scans, marking the stone regions for each scan. Then, we trained a U-Net for urinary stone segmentation using the annotated CT images and evaluated its performance.

**Results:** The model segmented the stone regions correctly in most cases. Our best model obtained a Dice value of **95.1%** and a Jaccard value of **91.9%**. To generalize the error on unseen data, we performed a 5-fold test validation, and the model obtained a mean Dice value of **92.1 ± 2.11%** and amean Jaccard value of **86.43 ± 1.81%**.

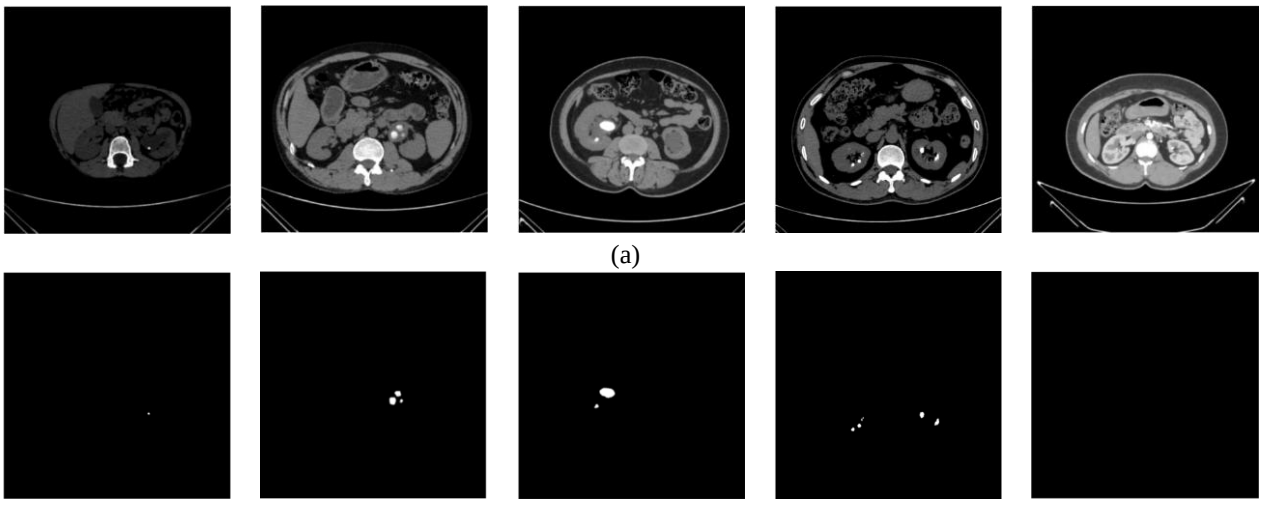

(a)

(b)

Figure: (a) – Original exam image. (b) – Segmentation results.

**Conclusion:** Our results indicate that using an annotated dataset for training deep learning models for kidney stones segmentation is a promising technique. It can lead to the development of novel automatic diagnosis systems that may be helpful to the diagnosis, localization, and stone size estimation. In the future, this approach could be a valuable tool for developing an automated surgery path planning system based on the characteristics extracted from the segmentation of the stone.

**ABSTRACT # 21**

# POTENTIAL CLINICAL APPLICATION OF PATIENT-SPECIFIC 3D PRINTED MODEL FOR SURGICAL PLANNING PRIOR TO HIGH-INTENSITY FOCUSED ULTRASOUND (HIFU)

Nicolas A Soputro[1], Jaya S Chavali[1], Jason Scovell[1], Roxana Ramos-Carpinteyro[1], Adriana M Pedraza[1], Carter D Mikesell[1], Ruben Olivares[1], Jihad Kaouk[1]

[1] Department of Urology, Glickman Urological & Kidney Institute, Cleveland Clinic

**Introduction:** Given the favorable cancer-specific survival outcomes in localized prostate cancer and the morbidity associated with whole-gland treatments on functional outcomes, recent years have seen the increasing adoption of focal treatments, including focal ablative therapy and partial prostatectomy. High-Intensity Focused Ultrasound (HIFU) represents one example of focal therapy, which focuses on the targeted treatment of an index lesion using thermal energy delivered through a transrectal probe. Appreciating the balance between the oncological outcomes and maximal functional preservation, this study sought to demonstrate the potential utility of a patient-specific 3D printed model for preoperative planning to improve precision and facilitate training for HIFU.

**Methods:** Our patient was a 58-year-old man with Gleason 3+4 prostate cancer. His preoperative multiparametric Magnetic Resonance Imaging (mpMRI) identified a single PIRADS 4 lesion in the left mid/base peripheral zone measuring 1.1cm without evidence of extraprostatic extension. The mpMRI images were used to create the 3D digital reconstruction that was subsequently utilized to generate the patient-specific Hydrogel-based 3D-printed model with distinctive hyperechoic lesion that can be visualized on ultrasound (Lazarus 3D, Albany, OR). The procedures were performed using the Focal One® Robotic Focal HIFU instrument (Focal One, Austin, TX).

**Results:** The procedure was performed under general anesthesia with the patient positioned on the left lateral decubitus position. The HIFU probe was inserted through the anal verge and advanced proximally to delineate the margins of the prostate and to map the areas for ablation. The ablation was successfully performed on 15g of prostate tissues without any complications and the patient was discharged home on the same day. With a similar position adopted for the 3D-printed model, the HIFU probe was slowly advanced through the rectal opening to characterize the prostate and the index lesion. The location and size of the lesion bear close resemblance to the preoperative MRI and intraoperative ultrasound images. A total of two cycles of ablation was trialed on the model with a maximum probe temperature set at 15.5°C (or 59.9°F). The model was then dissected to confirm the successful effects of the ablation as represented by the hollowed appearance of the targeted area compared to the untreated area.

**Conclusion:** Herein, we highlighted the feasibility of applying all steps of focal ablative therapy on a patient-specific 3D-printed model with demonstrable ablative effects confirmed on the subsequent dissection of the model. The trial can be expanded to evaluate the accuracy of the model involving a larger cohort of patients, as well as to assess its clinical utility for remote/virtual surgical training and rehearsal for the expanding repertoire of focal therapy approaches.

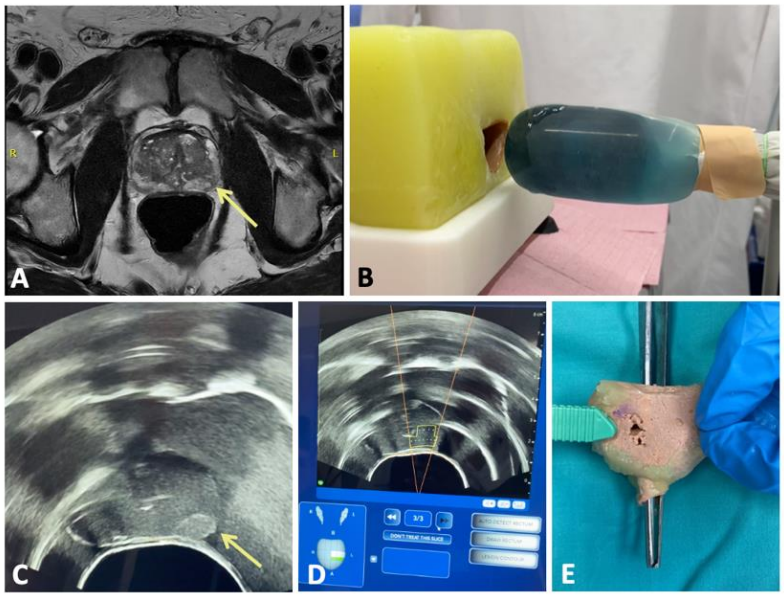


**Figure 1. (A)** Preoperative mpMRI images with the 1.1cm left mid/base peripheral zone lesion; **(B)** the insertion of the Focal One® probe into the patient-specific 3D printed Hydrogel-based model; **(C)** sonographic appearance of the model prostate with the lesion also visualized; **(D)** the ablative treatment applied to the 3D model with the treated area contoured in blue; **(E)** the dissection following ablative treatment of the 3D model showcasing the hollowed appearance of the targeted area compared to the smooth appearance of the non-treated area.

**ABSTRACT # 22**

## IMPROVING SURGICAL PRECISION OF SINGLE PORT TRANSVESICAL PARTIAL PROSTATECTOMY WITH PATIENT-SPECIFIC 3D PRINTED MODEL

Nicolas A Soputro[1], Roxana Ramos-Carpinteyro[1], Adriana M Pedraza[1], Jaya S Chavali[1], Jason Scovell[1], Carter D Mikesell[1], Jihad Kaouk[1]

[1] Department of Urology, Glickman Urological & Kidney Institute, Cleveland Clinic

**Introduction:** Single Port Transvesical Robotic Partial Prostatectomy (SP TV-RAPP) represents a novel surgical alternative for the management of organ-confined, clinically significant prostate cancer. The technique relies on the targeted surgical excision of the index lesion, warranting surgical precision to ensure the best oncological and functional outcomes. This study sought to evaluate the clinical utility of surgical rehearsals using patient-specific 3D-printed anatomical models to further advance the perioperative outcomes associated with this organ-sparing surgery for prostate cancer.

**Methods:** Since its introduction in 2021, SP TV-RAPP has been performed on 22 patients. The eligibility for the procedure and the surgical technique have been described previously. Of note, patients were positioned in supine lithotomy and the direct percutaneous access into the bladder was facilitated by a purpose-built SP Access Kit that was inserted through a single 3.5cm suprapubic incision. Once the robot was docked, all dissection steps and vesicourethral anastomosis (VUA) were completed from within the bladder. An intraoperative frozen section was routinely obtained from the surgical bed prior to VUA to ascertain the surgical margin. As part of our standard of care for SP TV-RAPP, we have included the addition of a patient-specific 3D model since November 2023. Using multiparametric Magnetic Resonance Imaging (mpMRI) and 3D reconstruction, the individual 3D models were generated using proprietary silicone-based material (Lazarus 3D, Albany, OR). All surgical rehearsals were performed immediately before the actual procedure by the same experienced robotic surgeon (JK).

**Results:** All SP TV-RAPP were completed successfully without the need for additional port, conversion, or intraoperative complication. Surgical rehearsal using the patient-specific 3D printed models was performed in five patients. The average age of the group was 69.7±28.4 years with all patients diagnosed with Gleason 3+4 prostate cancers on preoperative biopsy. All patients had a preoperative mpMRI with an average prostate volume of 42.9±14.6 mL and an average lesion diameter of 1.48±0.63 cm. In two patients, the index lesion was located anteriorly while in the remaining patients, the lesions were located in the posterior peripheral zones. While the excision times were faster during the surgical rehearsal (13.6±3.32 vs. 35±18.6 minutes), the specimen volumes obtained during the rehearsal and *in-vivo* remained similar (25.2±17.9 vs. 26.8±15.2 mL). In two cases, surgical rehearsal provided a better appreciation of the anatomy, including the extent of the disease and the shape of the prostate relative to the bladder neck. Nevertheless, a negative surgical margin was achieved in all cases.

**Conclusion:** Herein, we have demonstrated the feasibility of developing an innovative patient-specific pre-surgical simulation program for SP TV-RAPP. The customized 3D printed models were value-accretive in tailoring our surgical approach to promote better oncological outcomes and functional preservation. Further comparative studies are required to evaluate the potential of the 3D models for training and enhancing surgical performance within the domains of focal surgical treatments for prostate cancer.

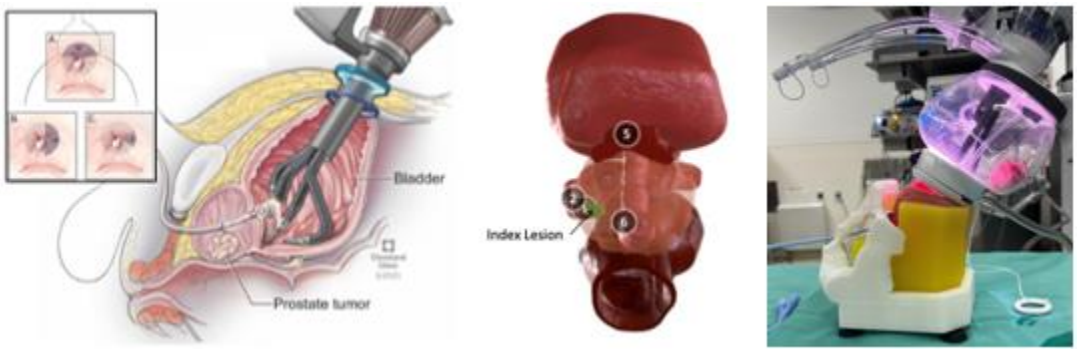


**Figure 1. (Left)** Intraoperative approach for SP TV-RAPP; **(Middle)** Digital twin 3D reconstruction based on the patient's mpMRI images; **(Right)** Surgical rehearsal of SP TV-RAPP using the patient-specific 3D printed model.

**ABSTRACT # 23**

# ADVANCING PELVIC RECONSTRUCTIVE SURGERY: VAGINAL ACCESS RETROPERITONEAL SACROCOLPOPEXY WITH HYSTERECTOMY USING SINGLE-PORT (SP) ROBOTIC DA VINCI SYSTEM

Omer Anis, MD[1], Nicolas Soputro, MD[1], Roxana Ramos, MD[1], Jaya Sai S Chavali MD[1], Taylor Trump MD[1], Jihad Kaouk, MD[1], Ly Hoang Roberts, MD[1]

[1]Glickman Urological and Kidney Institute, Cleveland Clinic, Cleveland, OH, USA

**Background.** Sacrocolpopexy is a standard surgical procedure for apical prolapse with various approaches including open or laparoscopic robotic-assisted, transabdominal or transvaginal. However, these techniques require intraperitoneal access risking injury to organs, create noticeable abdominal scars, or increase postoperative constipation and pain. We introduce a novel extraperitoneal transvaginal dissection technique for sacrocolpopexy using a purpose-built Da Vinci Single-Port (SP) robotic system (Intuitive Surgical Inc, Sunnyvale, CA), aiming to enhance patient outcomes and utilize natural orifice transluminal endoscopic surgery.

**Methods.** Single female cadaver was placed in dorsal lithotomy position with Trendelenburg. Vaginal incision was made at the posterior fornix for retroperitoneal access, followed by transvaginal placement of a purposebuilt SP Access Kit. The SP robot was directed caudo-cranially utilizing a floating dock technique, and retroperitoneal dissection was achieved from the rectovaginal pouch to the sacral promontory. Total vaginal hysterectomy, bilateral salpingoophrectomy (TVH, BSO) was performed. Mesh fixation to the anterior longitudinal ligament and vaginal mucosa using a pulley system was done for prolapse reduction.

**Results.** Initial findings indicate the feasibility and safety of completing an extraperitoneal transvaginal dissection using the SP system. There was no evidence of gross peritoneal violation or injury to the rectum, bowels, blood vessels, or ureter at the end of the procedure. TVH, BSO was feasible. Mesh placement via novel pulley system demonstrated robust apical support confirmed on vaginal examination.

**Conclusion.** Extraperitoneal dissection for robotic sacrocolpopexy using a single-port robotic Da Vinci system is an advancement in pelvic reconstructive surgery. Benefits include enhanced surgical precision, complete preservation of the peritoneum and intraperitoneal organs, improved visualization of the pre-sacral area, and mitigation of the risk for intraperitoneal organ injury especially in hostile abdomens. The SP robot's narrow profile, flexible endoscope, and double-jointed instruments allow transvaginal retroperitoneal access to improve surgical outcomes. Limitations include the need for a learning curve working in a confined space and restricted angles of access. Further work on mesh placement is ongoing. Continued refinement and rigorous evaluation are imperative to optimize surgical outcomes.

Figure 1. Cadaver in dorsal lithotomy with Trendelenburg. SP docked transvaginally utilizing the purposebuilt access kit.

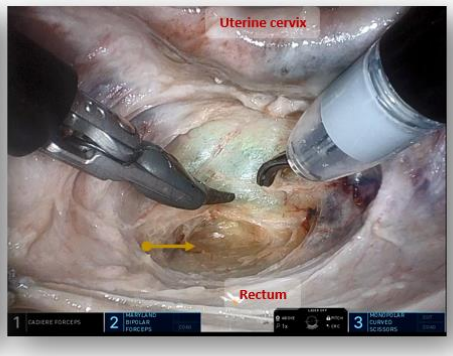


Figure 2. Retroperitoneal access via dissection into rectovaginal pouch (yellow arrow), posterior to cervix.


Figure 3. Extraperitoneal dissection from rectovaginal pouch to sacral promontory (SP), avoiding rectum and bowels medially and ureter and vessels laterally.

**ABSTRACT # 24**

# A MACHINE LEARNING ARCHITECTURE FOR SEGMENTATION AND FEATURE EXTRACTION OF LAPAROSCOPIC TOOLS TO IDENTIFY SURGERY STEPS

Rafael Zacarias Palierini[1], Matheus Silva Henrique[1], Murillo Freitas Bouzon[1], Oscar Eduardo Hidetoshi Fugita[2], Paulo Sergio Silva Rodrigues[1]
[1]Centro Universitário FEI [2] Hospital Universitário da Universidade de São Paulo

**Introduction:** Laparoscopy is a minimally invasive surgical technique that can be used in the diagnosis and treatment of many urological diseases. It replaced the open approach for most surgeries, due to many advantages such as faster surgical recovery, shorter hospital stays, less pain and better aesthetic results. However, laparoscopy demands a steep learning curve. In laparoscopy, a video camera captures images of the internal organs and the surgical instruments, generating visual data that can be used in automatic medical assistance tools. Deep learning in medical decisions is a valuable tool for medical image detection and recognition. For laparoscopic surgeries, the surgery step identification could be used to develop automated surgery robots and surgical training simulators. Previous publications used deep learning in surgery for surgical steps classification. However, these publications did not evaluate the surgical instruments position and orientation on the video images. This project presents a deep learning architecture that combines the segmentation of surgical instruments and their feature extraction to identify the surgical steps of laparoscopic surgeries.

**Methods:** An architecture based on Mask R-CNN, Segment Anything and Long Short-Term Memory (LSTM) is presented. The Mask R-CNN was used to identify the instruments present on the frame as well as the bounding boxes of each one. The Segment Anything was used to segment the instruments inside the bounding boxes. The Geometric cues were extracted from the segmentation using a skeleton algorithm. These features were concatenated in a vector format to represent the content of the frame and the vectors were fed forwarded to a LSTM neural network that can learn the context from a sequence and make a binary vector classification of the surgery step based on the frame vectors.

**Results:** The Cholec80 dataset was used to train and validate the architecture, that achieved a minimum and maximum instruments classification accuracy of 86.06% and 94.25%, respectively. On the surgery step recognition, the architecture was unable to identify the last surgery step and achieved a minimum and maximum accuracy of 77% and 95%.

**Conclusion:** Our results indicate that it is possible to achieve good results by extracting relevant features without forwarding the whole frame to the model, reducing the complexity of the network. The proposed architecture was not able to correctly classify the last step of the surgery and more research is needed on feature extraction field to improve the quality of the vectors forwarded to the neural network.

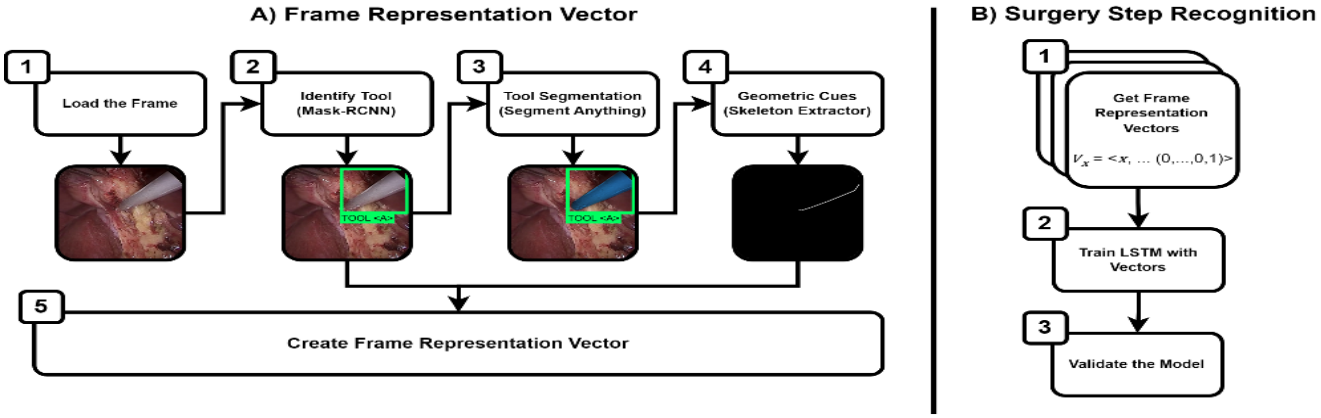


Figure: (a) – Frame representation vector methodology. (b) – Surgery step recognition methodology.

**ABSTRACT # 25**

## APPLICATIONS OF A REMOTELY OPERATED SUCTION AND IRRIGATION SYSTEM FOR ROBOT-ASSISTED SURGERY IN UROLOGY

Roxana Ramos-Carpinteyro[1], Jaya S. Chavali[1], Nicolas Soputro[1], Adriana M. Pedraza[1], Carter Mikesell[1], Jihad Kaouk[1]
[1] Urology Department, Cleveland Clinic, Cleveland, OH

**Introduction:** As part of the surgical armamentarium, rigid suction devices have played a pivotal role in open, laparoscopic, and multi-port (MP) robotic surgeries, facilitating optimal visualization and aiding in the estimation of blood loss. However, when the novel robotic techniques with the single-port (SP) system further regionalized surgery, an appropriately sized suction device became imperative. We aim to describe the applications, tips and tricks of the remotely operated suction and irrigation (ROSI) system (Vascular Technology, Inc., Nashua, NH) in urological robot-assisted surgery (RAS).

**Methods:** The ROSI system is composed of a control unit, a 24-inch flexible suction/irrigation probe (diameter of 5 mm), and a foot switch (which can be controlled by the robotic surgeon or a bedside assistant). For easier handling and to prevent obstruction with manipulation, the tip of the device is prepared with a suture. The probe can go through any 5-8 mm assistant port; in the case of MP cases, another instrument can pass through the same port simultaneously.

Once inside the patient, the ROSI probe can be directly placed in the area of interest by the robotic surgeon. It can also be left alone in the continuous suction mode if blood pooling is present. The probe can remain inside the patient the whole case. The main application of ROSI during urological RAS is suction of blood and other bodily fluids, such as urine and semen, especially during transvesical approaches. Other applications include irrigation for hemostasis revision and blunt retraction.

**Results:** In our experience with >1000 SP RAS cases performed by three surgeons from 2018 to 2023, we found that ROSI provides autonomy to the console surgeon and proper functioning regardless of the level of training of the bedside assistant. Furthermore, we found that ROSI is comparably useful in MP RAS (Figure).

Occasional technical difficulties arise with ROSI and it is important to know how to solve them. For example, if too much of the probe is inside the surgical field, it will stoop and the surgeon will have a hard time handling it, therefore it should be gently retracted by the bedside assistant so that it regains a straight position. Another positional issue happens when the probe is let go, moves anteriorly, and obstructs visibility. The console surgeon can fix this by zooming out and re-positioning the probe with the lateral instruments. Finally, when clogging happens the probe should be pulled out, purged with a straight 5 mm instrument, and cleaned.

**Conclusion:** The ROSI system was designed for easier and autonomous manipulation in confined surgical areas seen with SP RAS, but its utility has expanded to standard MP RAS as an additional tool for delicate suction and retraction.

ROSI used with da Vinci SP, daVinci Xi and HUGO™ robotic systems.

**ABSTRACT # 26**

# INITIAL ANALYSIS OF A NOVEL WIRELESS MOTORIZED SINGLE-USE FLEXIBLE URETEROSCOPE

Authors: Runhan Ren[1], Victor KF Wong[1], Connor M Forbes[1], Mitchell R Humphreys[2], Brett A Johnson[3], Joseph C Liao[4], Thomas Chi[5], Ben H Chew[1]

[1]University of British Columbia, [2]Mayo Clinic Arizona, [3]UT Southwestern Medical Center, [4]Stanford University, [5]University of California San Francisco

**Introduction:** The use and availability of single-use flexible ureteroscopes are increasing since they improve on traditional reusable scopes in terms of initial cost, sterilization, maintenance, and repair costs. While advances in optics have been made, most single-use ureteroscopes still require a wired plugin connection to processing towers, despite advances in wireless technology. We evaluated the specifications of a novel wireless, motorized, single-use flexible ureteroscope (UroViu Corp, Los Altos CA).

**Methods:** A prototype of the ureteroscope was examined and assessed against expectations of advancement in technology and requirements of users.

**Results:** This ureteroscope consists of a reusable processor core with image capture, motor, battery, and Wi-Fi transmitter housed within a disposable pistol grip handle (Figure 1). The optical system consists of a camera with a 120-degree field of view and a 2 – 50 mm depth of field that illuminates the area of interest using LEDs. The cannula has an outer diameter of 7-8 Fr with a 67 cm long channel for irrigation. It includes a separate instrument channel of 3.6 Fr. The disposable handle has a lever for upward and downward deflection of 270 degrees. 135-degree of axial rotation is achieved through motorized control, which allow the physician's hand to remain in a neutral, ergonomic position. This ureteroscope transmits wirelessly to a portable relay station, containing a 13-inch screen and latency of 150 ms.


Figure 1. The UroViu single-use ureteroscope and portable relay station.

**Conclusion:** This novel, ergonomic, wireless, and portable single-use flexible ureteroscope system meets basic requirements for ureteroscopic procedures. Further *in vitro* and *in vivo* assessments will determine benefits and limitations of this novel technology.

**ABSTRACT # 27**

## TOTALLY TRANSPERINEAL ULTRASOUND MRI FUSION-GUIDED TRANSPERINEAL PROSTATE BIOPSY IN PATIENTS WITH NO RECTUM

Sarah Azari[1], Sahil H Parikh[2], Zoë Blake[2], Christopher Koller[2], William Azar[2], Charles Hesswani[2], Kyle Shuppe[2], Alexander P. Kenigsberg[2], Daniel R. Nemirovsky[2], Neil Mendhiratta[2], Daniel Nethala[2], Maria Merino[2], Howard L. Parnes[2], Sandeep Gurram[2], Barris Turkbey[2], Bradford J. Wood[2], Sheng Xu[2], Peter A. Pinto[2]

[1]Department of Urology, George Washington University School of Medicine & Health Sciences, Washington DC

[2] National Cancer Institute, National Institutes of Health, Bethesda, MD

**Introduction:** Standard prostate biopsy, transrectal or transperineal, requires a transrectal ultrasound. Prostate biopsy in patients with no rectum continues to challenge urologists. Alternatives include in gantry MRI or CT guided biopsy, which is cumbersome and only allows for targeted biopsy, not systematic. We developed a platform for comprehensive office-based biopsy using transperineal ultrasound. We evaluated the feasibility of an exclusively transperineal approach to MRI-guided fusion prostate biopsy in patients with no rectum and suspicion of prostate cancer (PCa)

**Methods:** From 2018 to 2023, 10 patients at our institution underwent 11 transperineal ultrasound probe-guided MRI fusion biopsies. A curved array ultrasound transducer was used. A novel software platform was developed to allow transperineal ultrasound fusion in real time with prostate MRI utilizing electromagnetic tracking (Figure 1). Biopsy included MRI-targeted and systematic 12 cores taken in a Barzell technique. Demographics, MRI results, and pathology results were collected prospectively. Descriptive statistics were performed.

**Results:** In total, 18 lesions were targeted from 11 biopsy sessions from 10 patients. The median age was 72 years, median prostate volume was 72cc, and median PSA was 7.7ng/mL. The median PSA density was 0.11ng/mL$^2$. The median number of lesions on MRI was 1.5. There were 5 PI-RADS 5 lesions, 7 PI-RADS 4 lesions, 3 PI-RADS 3 lesions, and 3 PI-RADS 2 lesions. The cancer detection rate was 73%. The cancer detection rate for clinically significant PCa (≥Grade Group 2) was 64%. 3 patients had in gantry MRI or CT guided prostate biopsy prior, all 3 of which had atypical or benign pathology on MRI/CT guided biopsy and PCa diagnosed on subsequent transperineal ultrasound biopsy. In 3 of the 8 biopsies where cancer was detected, the targeted cores had a higher grade than the systematic cores. Prostate tissue was identified in 93% of cores. There were no postoperative infections or other adverse events.

**Conclusion:** Totally transperineal ultrasound MRI fusion guided prostate biopsy is a safe and effective approach for patients in whom transrectal ultrasound is not possible. The cancer detection rate is similar to transrectal ultrasound biopsy. We are continuing to develop this platform for widespread use.

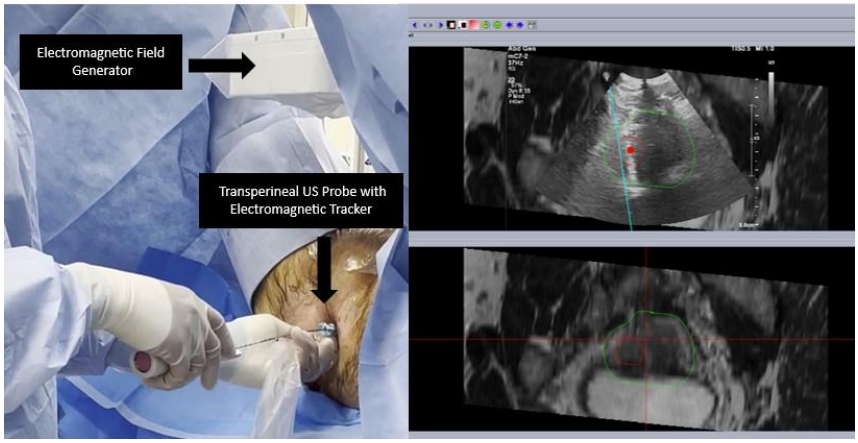


Figure1: Totally Transperineal (TTP) MRI/US fusion biopsy technique (Left) and Software interface demonstrating transperineal ultrasound fusion to MRI (Right)

**ABSTRACT # 28**

## FOCAL THERAPY ELIGIBILITY: AN EVALUATION OF INITIAL AND CONTINUED CANDIDACY FOR FOCAL THERAPY IN A GRADE GROUP 2 ACTIVE SURVEILLANCE COHORT

J. Bradley Mason[1], Sarah Azari[2], Alexander P. Kenigsberg[3], Christopher Koller[3], Sahil Parikh[3], William Azar[3], Kyle Schuppe[3], Charles Hesswani[3], Zoë Blake[3], Neil Mendhiratta[3], Daniel R. Nemirovsky[3], Daniel Nethala[3], Maria Merino[3], Bradford J. Wood[3], Peter L. Choyke[3], Howard L. Parnes[3], Sandeep Gurram[3], Baris Turkbey[3], Peter A. Pinto[3]

[1]Department of Urology, The MedStar Health-Georgetown University Hospital, Washington DC [2]Department of Urology, George Washington University School of Medicine & Health Sciences, Washington DC [3] National Cancer Institute, National Institutes of Health, Bethesda, MD

**Introduction:** The advent of multiparametric magnetic resonance imaging (mpMRI) has helped to localize clinically significant prostate cancer (csPCA). Focal Therapy (FT) has emerged in the mpMRI era, which can treat MRI-visible lesions while avoiding side effects of whole-gland treatment. However, FT remains an investigational treatment option for PCa patients with intermediate-risk disease. Little is known about how many patients on active surveillance (AS) with Gleason grade group (GG) 2 disease retain eligibility for FT over time, or risk factors for loss of eligibility. The objective of this study is to evaluate initial and long-term FT eligibility (FTE) of patients with GG2 disease.

**Methods:** A prospectively maintained cohort was retrospectively queried for patients initiated on AS between 2009 and 2020 with GG2 PCa. Patients with biopsy-concordant GG2, unilateral, MRI-visible PIRADS 2-5 lesions amenable to hemiablation were considered FT candidates. Those with PSA>20 ng/mL, >4 MRI lesions, bilateral (BL) MRI-visible/biopsy-concordant lesions, or contralateral GG≥2 PCa or MRI-invisible lesions were excluded. Patients were considered to progress if they developed BL GG≥2 disease or unilateral GG≥3 PCa. Patients without GG progression-maintained FTE and those with GG progression maintained FTE if they had unilateral biopsy-concordant/MRI-visible GG≤3, no contralateral GG≥2 disease, and PSA<20 ng/mL. Univariate and multivariate analyses were conducted to compare patients who maintained and lost FTE.

**Results:** 252 PCa patients were identified as eligible for FT with an average follow-up of 3.4 years, 83 of whom (33%) had GG2 disease and were FT candidates. 29/83 (35%) lost FT eligibility, 19/83 (23%*)* with progression to high-risk disease, 6/83 (7.2%) due to development of BL GG≥2 disease, and 4/83 (4.8%) with development of MRI-invisible csPCA. Univariate analysis demonstrated that those who lost FTE had smaller prostates than those who maintained it (44.9 mL vs. 56.2mL, respectively, p=0.018). PSA density was similar between the groups. No significant differences were noted in initial imaging and pathologic parameters. No factors significantly associated with loss of FTE were identified on logistic regression.

**Conclusions:** 33% of the patients on AS had GG2 disease and were initially eligible for FT. 65% of patients with GG2 disease were still eligible for FT after a median follow up of 3.4 years, over one third of these patients lose FTE. This data regarding the loss of a FT therapeutic window could prove useful in counseling GG2 patients considering AS, FT, or radical treatment.

**ABSTRACT # 29**

## NOVEL DUAL BALLOON CATHETER TO REDUCE CATHETER-RELATED COMPLICATIONS: RESULTS OF A PROSPECTIVE, SINGLE-CENTER, RANDOMIZED CONTROLLED TRIAL

Onuralp Ergun M.D., Sijo Parekattil M.D., Ahmet Gudeloglu M.D., Richard Mendelson PhD., Sophia Rodriguez MA, Marcos Colon MA, Alana Anthony MA

**Introduction and Objective:** The Foley catheter was introduced in the late 1930s and has been one of the most utilized devices in the medical setting. Complications associated with Foley catheter use have been reported previously and contribute to increased healthcare costs. A novel dual balloon catheter named Duette™ (Poiesis Medical LLC, USA) has recently emerged, aiming to reduce these complications. This study aims to compare the short-term complication rates of these two catheters (Duette vs Foley as the control group).

**Methods:** We conducted a prospective randomized controlled trial. After receiving institutional review board approval, we enrolled 63 patients who underwent REZUM procedure for benign prostatic hyperplasia (BPH) and got catheterized postoperatively between May 2022 and January 2023. Patients who consented to the study were randomly assigned to either the standard foley catheter (n=31) or the novel Duette catheter (n=32). The catheters stayed in for approximately a week. Catheter-related adverse events were assessed post-operatively with a patient-centered questionnaire. Baseline characteristics like pre-op prostate size, post-voiding residual volume (PVR), and international prostate symptom scores (IPSS) were also evaluated.

**Results:** Baseline characteristics (age, prostate size, catheter size, length of dwell) between the Duette and Foley catheter were comparable. The incidence of bladder spasms was markedly lower in patients using the Duette catheter. Statistically, the reduction in bladder spasms with the Duette was significant (p=0.037), with 84% of Duette patients experiencing none or only occasional mild spasms, compared to 67% in the Foley group. The other measured outcomes—such as the necessity for re-catheterization, incidences of urine leakage, hematuria, infections requiring antibiotics, suprapubic tenderness, and catheter occlusion—did not differ significantly between the two groups. Notably, the rate of premature catheter removal was equivalent, with two patients from each group having their catheters removed earlier than planned.

**Conclusions:** This study demonstrates that the novel dual balloon catheter is a safe and feasible alternative to the standard Foley, with the main advantage being fewer and milder bladder spasms without increasing other risks associated with catheter use. The results reveal a promising adverse event profile, which could suggest a reduction in healthcare costs. Further trials involving more patients and more disciplines are warranted to confirm these findings.

**ABSTRACT # 30**

# CIRCUMFERENTIAL TRANSMISSION OF SHOCKWAVE ENERGY TO THE ERECT PENIS

Irwin Goldstein[1], Sue W. Goldstein[1], Erich Theuer[2], Nikolaus Hopfenzitz[3], John Warlick[4]
[1] San Diego Sexual Medicine, [2]Medical Simulation Engineering, [3]MTS Medical, [4]Softwave TRT

**Introduction:** Low intensity shockwave therapy (LiSWT) improves erectile function in men with ED by inducing mechanotransduction-associated regenerative mechanisms. The applicator is usually applied to the right and left lateral aspects of the flaccid penis. In our facility, to improve the efficacy of mechanotransduction-associated regenerative mechanisms, treatment strategies have evolved to increase shockwave energy absorption. Since intracavernosal pressure and penile volume are determinants of absorption of shockwave energy in tissue we started applying LiSWT to the dorsal and then ventral surfaces during erection. Furthermore, we found that shockwave energy passing through the erect penis is reflected back when using a curved air reflector placed contralaterally to the applicator. We herein introduce a device conceptualized to provide circumferential transmission of shockwave energy to the entire erect penis, theorized to further improve energy absorption to the erectile tissue.

**Methods:** The new device would consist of a tube, similar to a vacuum erection device, with a warm, water-filled sleeve inside (Figure 1). After pharmacologic erection is achieved, the penis would be coated with ultrasound gel and inserted into the tube. Pressure in the sleeve would be increased by adding enough water to ensure full contact of its surface with the penis. The LiSWT OP155 applicator (Softwave TRT, Urogold MTS) would then be applied directly to the glans penis so that the shockwave energy was aimed longitudinally toward the shaft, providing shockwave energy simultaneously to the entire penis. Computer modeling of LiSWT energy propagation with this conceptualized device of shockwave applied to the glans penis was performed using FEM modeling with program systems ANSYS, MATLAB and PZFLEX/ONSCALE and compared to models of LiSWT applied to the contralateral surface area of the penis: i) flaccid, ii) erect and (iii) erect with curved air reflector.

**Results:** Utilizing the concept of circumferential transmission of shockwave energy to the entire erect penis at one time, computer modeling is shown in the axial direction (Figure 2) and in the longitudinal direction (Figure 3). Shockwave energy is transmitted initially through the water inside the sleeve surrounding the penile shaft, and subsequently passes from the outside of the penis to the inside equally along the entire erect penile shaft without loss of energy through the penis.

**Conclusion:** We show a computer model of a novel strategy for penile LiSWT to maximize mechanotransduction and energy absorption for men with ED.

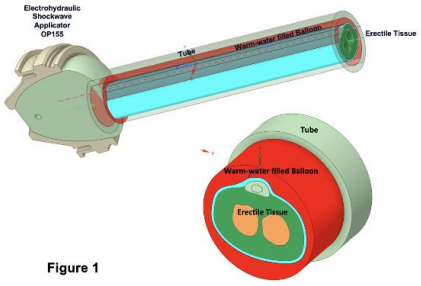

Figure 1

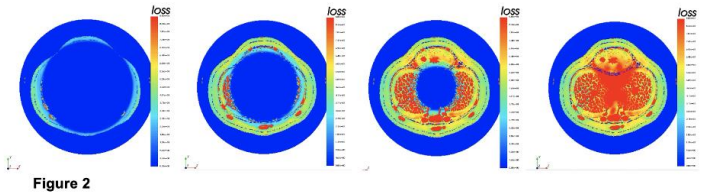

Figure 2

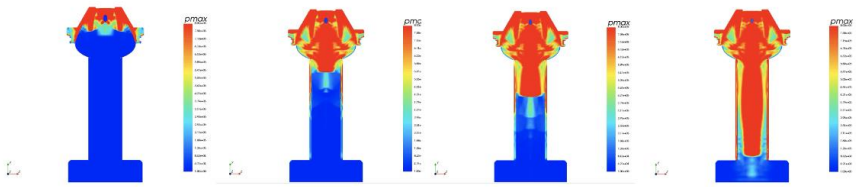

Figure 3

Figure 1. New device. Figure 2. Axial view of computer modeling of energy absorption.
Figure 3. Longitudal view of computer modeling of energy absorption.

**ABSTRACT # 31** **TOP 10 ABSTRACT**

# A NOVEL LLM-MEDIATED DATA EXTRACTION TOOL: A COMPARATIVE STUDY IN PATIENTS WHO UNDERWENT RADICAL PROSTATECTOMY

William S. Azar[1], Dylan M. Junkin[2], Nicholas Williams[2], Sahil H. Parikh[1], Charles Hesswani[1], Kyle C. Schuppe[1], Christopher R. Koller[1], Daniel Nethala[1], Neil Mendhiratta[1], Alexander P. Kenigsberg[1], Sandeep Gurram[1], Peter A. Pinto[1]

[1] Urologic Oncology Branch, National Cancer Institute, National Institutes of Health, MD, USA

[2] Palantir Technologies, CO, USA

**Introduction:** The integration of large language models (LLMs) into healthcare is set to transform data management and medical research. In this study on patients who underwent radical prostatectomy (RP), we describe and assess the extraction accuracy of our LLM-powered data tool, the National Institutes of Health (NIH) Integrated Data Analysis Platform (NIDAP) Text Extraction Program (NTEP), a Federal Risk and Authorization Management Program (FedRAMP)-authorized AI application.

**Methods:** A total of 369 patients enrolled in a clinical trial (NCT02594202) who underwent RP at the NIH and whose pathology reports were read by expert genitourinary pathologists were included in this study. We manually curated a ground truth dataset containing 4,797 datapoints for 13 variables abstracted from RP pathology reports: 6 were binary variables, 3 were categorical, 2 were discrete, and 2 were continuous. We then conducted a comparative analysis between the ground-truth dataset and a dataset created using NTEP, an artificial intelligence application pioneered by the Urologic Oncology Branch at the NIH that allows researchers to develop custom-built LLM prompts aimed at extracting data directly from electronic health record (EHR) documents using GPT-4. Prompt engineering was conducted by a researcher experienced with the use of NTEP. The NTEP-generated dataset was then subject to minor processing and formatting to allow for statistical comparison between extraction methods. The comparison was assessed using Cohen's Kappa (κ) coefficient for binary and categorical variables and mean squared error (MSE) with Pearson's correlation coefficient for continuous and discrete variables.

**Results:** For binary variables surgical margin status, lymph node involvement and seminal vesical invasion, the LLM demonstrated a κ-score of 1, indicating a 100% match to the ground truth dataset. For extraprostatic extension, lympho-vascular invasion, and perineural invasion, the LLM's κ-score was 0.99. Overall, 2,210/2,214 (99.8%) of binary datapoints were correctly identified by the LLM. Of note, proportions of positives to negatives for binary variables ranged between 5% and 76%, ensuring data heterogeneity. For categorical variables, the LLM demonstrated a κ-score of 1 when extracting case number and pathologist name and a κ-score of 0.99 when extracting the Gleason sum, correctly identifying 1,102/1,104 (98.2%) categorical instances. For discrete variables, the LLM demonstrated a 100% match with the manually curated dataset for number of positive lymph nodes, but it miscalculated the total number of lymph nodes dissected for one patient, resulting in a MSE of 0.0027 and a Pearson's coefficient of 0.99. For continuous variables, the LLM demonstrated a 100% match with the ground-truth dataset for prostate dimensions but failed to identify the prostate weight in 1 patient (0.27% of the dataset), otherwise demonstrating a MSE of 0 and a Pearson's coefficient of 1 for prostate weight.

**Conclusion:** This study illustrates how data extraction using LLM directly from EHR can potentially replace manual extraction. We describe the effectiveness of our tool, NTEP, in accurately extracting binary, numerical and categorical variables directly from EHR RP pathology reports using LLM and robust prompt engineering. Future studies should include larger cohorts and multiple dataset curators to further validate our platform's scalability and efficiency against traditional manual extraction.

**ABSTRACT # 32** **TOP 10 ABSTRACT**

# IMPACT OF INTEGRATED, REAL-TIME DIGITAL MEASUREMENT ON SURGEON DECISION MAKING IN URETEROSCOPIC STONE SURGERY

Alexander Krueger, B.S.[1], Drew Marie Smith[2], Andrew T. Parzych, B.S.[2], Robert Qi, MD[2], Aaron M. Potretzke, MD[2], Dan Stoianovici, PhD[3], David Holmes III, Ph.D.[4,5], Mark Lifson, Ph.D.[6], Kevin Koo, M.D., M.P.H.[2]

[1]Mayo Clinic Alix School of Medicine Rochester; [2]Mayo Clinic Department of Urology; [3]Johns Hopkins University, Baltimore, MD[4]Physiology & Biomedical Engineering; [5]Biomedical Imaging Resource; [6]Center for Digital Health;

**Introduction:** Accurate estimation of stone fragment size during ureteroscopic lithotripsy facilitates decisions to extract fragments or leave them behind for spontaneous passage. A novel software capable of accurately measuring these fragments in real-time during ureteroscopy has been developed, but the impact on surgeons' decision-making is not known. The aim of this study is to assess the clinical use of this software and its impact on intraoperative decision-making.

**Methods:** Adult patients undergoing elective flexible ureteroscopy and laser lithotripsy for renal stones were prospectively enrolled. Surgeons could request digital measurement of stones or fragments at any time during the procedure. All measurements were reported to the surgeon in real-time. Surgeons were surveyed after each case about the reasons for taking measurements and how the measurements impacted their intraoperative decisions. 30-day clinical complications were recorded.

**Results:** Among a total of 51 patients undergoing ureteroscopy, surgeons took an average of 2.1 (range 1-6) intraoperative measurements per case. The software was deployed successfully in all cases. Surgeons reported that the primary purpose of taking intraoperative measurements was to determine whether post-lithotripsy fragments were extractable (26, 51.0%) or sufficiently small to leave behind (5, 9.8%). However, surgeons also took measurements prior to lithotripsy to confirm extractability (23, 45.1%), or to assess overall stone size (4, 9%). Following stone measurements, surgeons changed intraoperative plans in 17 (33%) cases and instead continued lithotripsy (8, 15.7%), extracted fragments (7,13%), or left fragments behind for passage (2, 3.9%) (figure). Surgeons rated the ability to take intraoperative measurements as "very helpful" (66%) or "somewhat helpful" (34%). In no cases (0%) were measurements "not helpful." The time burden of taking affected procedural efficiency in only 4% of cases. There was 1 sepsis complication among the cases (2%).

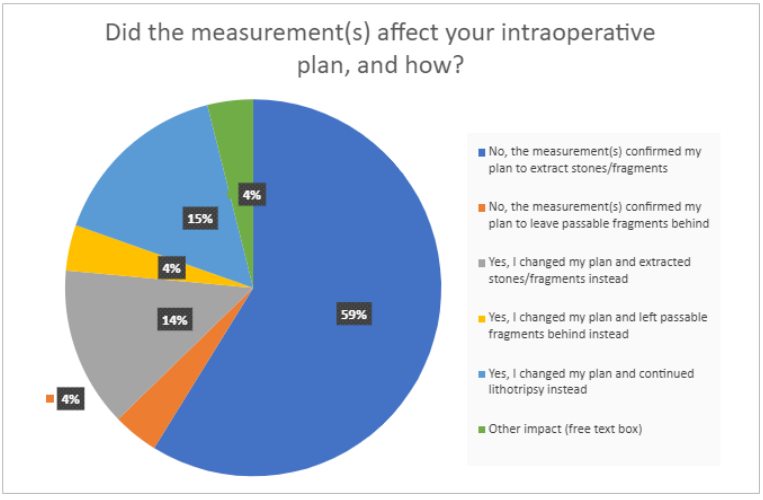


**Conclusion:** The ability to take real-time stone measurements during flexible ureteroscopy changed surgeons' intraoperative decisions in 33% of cases. This may improve procedural efficiency and reduce fragment extraction failures and ureteral injury.

**ABSTRACT # 33**

# A BENCHTOP KIDNEY MODEL FOR MEASURING TRANSIENT INTRARENAL PRESSURE DURING SIMULATED URETEROSCOPY

Alycia Abbott, Jessica Williams, Candace Rhodes, Aditi Ray
Boston Scientific, Inc

**Introduction:** Increased pressures in the upper urinary tract during endourological procedures are suspected to increase post-operative complications [1, 2]. Previously, we have presented a benchtop model that enables study of intrarenal pressure (IRP) throughout steady state periods of fluid irrigation during simulated ureteroscopy [3]. However, changes to irrigation flow rate including turning on/off flow and flushing occur during ureteroscopy and can cause temporary fluctuations in IRP. Here we present the ability of the bench model to enable study of IRP during transient flow events of simulated ureteroscopy.

**Methods:** The Boston Scientific Bench (BSB) kidney model consists of a chamber (with a 3-D printed "kidney" insert) ringed by sensors with outflow paths available through use of a UAS and/or through use of valves. Experiments were conducted with a UAS (10/12F or 11/13F) and with/without a tool in the working channel (1.3F Flexiva™ 200 Laser Fiber). Irrigation during flow on/off scenarios was provided by an automated pressure pump (30-300 mmHg) while a prototype fluid management system provided irrigation during different flush scenarios. The IRP was monitored through use of the Lithovue Elite™ Single-Use Digital Flexible Ureteroscope System with intrarenal pressure monitoring. The data from the BSB was compared to data collected in a preclinical porcine (PCP) model and was evaluated for IRP values (i.e. mean, peak) produced as well as time durations to achieve IRP values.

**Results:** On average, the BSB produced mean IRP values within 4 and 1 mmHg of the PCP IRP values during various flow on/off scenarios with 10/12F and 11/13F UAS, respectively (Table 1). The time it took to achieve those IRP values with an 11/13F UAS was within 2 s for the two models. During flush scenarios of different magnitudes and durations with an 11/13F UAS and with/without a tool in the working channel, the BSB model produced IRP values within 13 mmHg of the PCP model. Both models had comparable time ranges to produce the peak IRP during a flush event. During flush scenarios with a 10/12F UAS and with/without a tool in the working channel, the BSB produced reasonably similar IRP values to the PCP after modification to the BSB set-up where a valve was partially opened to allow additional outflow. This additional outflow path in the BSB enables adjustment for various physiological parameters.

| Transient Scenario | Sheath Size (F) | Average Difference in IRP (mmHg) | Average Difference in Timing (s) |
|---|---|---|---|
| Flow On/Off | 11/13 | 1 ± 0.8 | 1.9 ± 3.2 |
| Flush | 11/13 | 13 ± 4 | 3.5 ± 2.6 |
| Flow On/Off | 10/12 | 4 ± 1.4 | 13 ± 8.5 |
| Flush | 10/12 & valve | 18 ± 9 | 0.5 ± 0.3 |

Table 1: Average difference in IRP (mmHg) and time to achieve IRP values (s) between BSB and PCP models. Representative data with use of 11/13F and 10/12F UAS and no tools in place.

**Conclusion:** IRP values and times to achieve those values produced by the BSB model during fluid transition periods were reasonably similar to those measured from an *in vivo* PCP model. The comparable behavior was achieved in differing outflow and tool use scenarios which enables investigation of how ancillary devices impact IRP during ureteroscopy procedures. Although IRP is the focus of this abstract, the additional sensors in the BSB can help characterize the relationships between pressure, flow rate, and temperature during both transient and steady state ureteroscopy scenarios.

**Disclaimers***:* Prototype fluid management system used in this study was a concept device/technology, which was not available for sale at the time the study was conducted. Bench testing results may not necessarily be indicative of clinical performance. Testing was performed by Boston Scientific. Data on file.

**ABSTRACT # 34** **TOP 10 ABSTRACT**

# PROSPECTIVE EVALUATION OF EFFICACY, SAFETY, CUMULATIVE LASER ENERGY, AND STONE-FREE RATES IN THE POST-MARKET THULIUM FIBER LASER (SOLTIVETM SUPERPULSED LASER SYSTEM) REGISTRY: INSIGHTS FROM TEAM OF WORLDWIDE ENDOUROLOGICAL RESEARCHERS (T.O.W.E.R.) RESEARCH CONSORTIUM

Ben H. Chew[1], Mitchell R. Humphreys[2], Wilson R. Molina[3], Bodo E. Knudsen[4], Mantu Gupta[5], Duane D. Baldwin[6], Kyochul Koo[7], Victor KF. Wong[1], Peter Kronenberg[8], Palle Osther[9], Olivier Traxer[10]

[1] University of British Columbia, [2]Mayo Clinic Arizona, [3]Kansas University Medical Center, [4]Ohio State University, [5]Mount Sinai West, [6]Loma Linda University Medical Center, [7]Yonsei University, Seoul, [8]Hospital CUF Descobertas, [9]University Southern Denmark, [10]Sorbonne University Tenon Hospital

**Introduction:** Thulium fiber laser (TFL) has emerged as an effective tool for endoscopic laser lithotripsy since its introduction in 2019. In this prospective, international clinical registry, the Endourological Society's T.O.W.E.R. Research Consortium evaluated the ablative performance, stone-free rates (SFRs), and safety of the first commercially available TFL system, SOLTIVE$^{TM}$ SuperPulsed Laser System (Gyrus ACMI, Brooklyn Park) in a large patient cohort.

**Methods:** 423 patients undergoing ureteroscopy for ureteral and/or renal stones using the TFL were prospectively recruited and treated across eight international institutions between 12/2021- 4/2023. Baseline clinical characteristics, intraoperative lithotripsy efficiency, (adverse events, and post-operative outcomes were collected. Kidney and ureteral stones were analyzed according to stone volume and density. Adverse events and SFRs were assessed at 1 and 3 months.

**Results:** The stone free rates at 3 months are listed in figure 1. Stone ablation speed is statistically comparable across all stone densities within each stone location, (p= 0.41, p=0.125) for kidney and ureter, respectively (figure 2). Serious adverse events (SAEs) occurred in 3.8% (16/423) of patients and were all due to infection with 2 being ureteral stricture (deemed not related to the laser procedure).

**Conclusion:** The thulium fiber laser (SOLTIVE$^{TM}$ SuperPulsed Laser System is effective in ureteroscopic lithotripsy for stone disease, with low complications and good SFRs and ablation speeds (0.62 (0.31-1.45) mm$^3$/s) across all stone densities. Stone ablation speeds are consistent through all 4 quartiles of stone densities indicating the TFL is an effective laser for all stone types.

Figure 1. Stone Free Rate

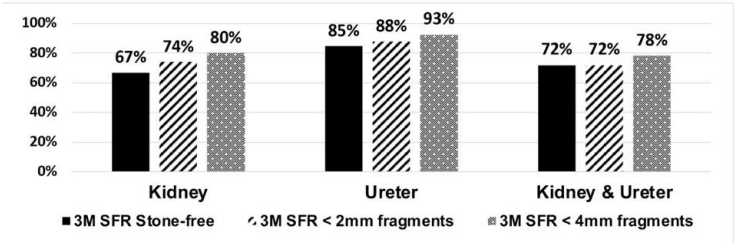


Figure 2. Stone Ablation Speed by Stone Density (mm3/s)

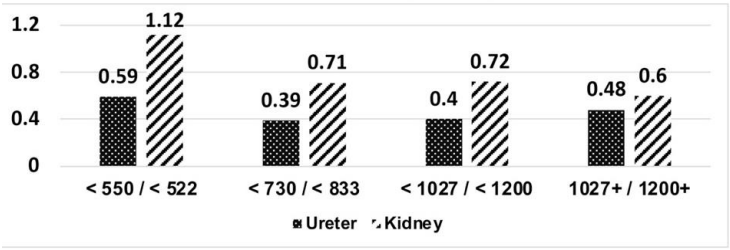

**ABSTRACT # 35**

## TRI-LAYER URETERAL STENTS, WITH ANTI-ENCRUSTATION SURFACE, OFFER IMPROVED COMFORT: RESULTS FROM AN INTERNATIONAL STENT REGISTRY

Ben H. Chew[1], Connor M. Forbes[1], K.F. Victor Wong[1], Runhan Ren[1], Dirk Lange[1], Alexander Glaser[2], Kazumi Taguchi[3], Ojas Shah[4], Edouard Tariel[5], Channa Amarasekera[6], Shuzo Hamamoto[7], Wilson R. Molina[8], John J. Knoedler[9], Marcelino E. Rivera[10], Karen L. Stern[11], Mitchell R. Humphreys[11], Michael Borofsky[12], Amy E. Krambeck[6]

[1]University of British Columbia, Vancouver, BC, Canada, [2]Northwestern University, Glenview, IL, [3]Nagoya University, Nagoya, Japan, [4]ColumbiaUniversity, New York, NY, [5]Centre Hospitalier, St Grégoire, France, [6]Northwestern University, Chicago, IL, [7]Nagoya City University, Nagoya, Japan,[8]Kansas University, Kansas City, KS, [9]Pennsylvania State University, Hershey, PA, [10]Indiana University, Indianapolis, IN, [11]Mayo Clinic Arizona, Phoenix, AZ [12]University of Minnesota, MN

**Introduction:** The Tria$^{TM}$ stent has novel Percushield$^{TM}$ technology on both the inner and outer surfaces of a Percuflex$^{TM}$ stent designed to resist salt ($Mg^{2+}$ and $Ca^{2+}$) adherence in an attempt to reduce encrustation. We determined the technical success, complications and patient symptoms in a prospectively collected database to determine if Tria$^{TM}$ stents improved encrustation, infection and comfort compared to other stents.

**Methods:** An international prospective registry with several stent types was conducted in USA, Canada, Japan, France from 2020-2023. Patient reported data included the PROMIS Pain Intensity (3a) and Pain Interference (6b) scores which were obtained at time of index procedure, stent removal and post stent removal. Non Tria stents included Percuflex, Percuflex Plus, Contour, and Polaris (Loop & Ultra) stents.

**Results:** Of 359 patients, 271 had a unilateral stent placed for stone management procedures. The Tria vs non-Tria groups were comparable: ages 55.9± 15.0, 58.7± 13.8y, 57.8% and 56.4% male, 42.2% and 43.6% female, BMI 28.9 ± 8.1, 29.7± 7.9 kg/m$^2$, and indwell times 11.8± 14.4 and 9.9± 12.6 d, respectively. Pain intensity (p=0.052) and pain interference scores (p=0.025) were lower for patients with Tria vs non-Tria stents at the time of stent removal. Tria patients reported slightly lower pain scores at the time of stent removal compared to their baseline, while non-Tria subjects reported a slight increase in both domains, but both were insignificant (p=0.3390, p=0.0864). Non Tria subjects reported significantly larger decreases in both domains at post stent removal compared to stent removal visit (p=0.0245, p=0.0216). Higher age was correlated with lower pain scores (p=0.041). Specific sub-analysis shows that Tria stents had lower interference and intensity scores compared to Percuflex and Percuflex Plus stents at the time of stent removal (p<0.0001, p=0.0002). There was no difference in infections and encrustation between groups (p=0.45).

**Conclusion:** Tria stents were more comfortable than other tested stents at the time of stent removal and post-stent removal in both pain intensity and interference scores. There was no difference in encrustation or urinary tract infections between groups.

**ABSTRACT # 36**

## THE USE OF 3-D PRINTING IN THE PLANNING OF COMPLEX ROBOTIC UROLOGIC SURGERY

Ryan L. Buettner, MD[1], Morgan McCain, Ronald Hidalgo, MD[2], Bradley Schwartz, DO[1]
[1] Southern Illinois University School of Medicine, Springfield, Illinois
[2] Springfield Memorial Hospital, Springfield, Illinois

**Introduction:** Three-dimensional printing (3DP) is an additive manufacturing process by which a digital image is translated into a 3D object. Cross-sectional imaging can be used to create 3D models of patient pathology to aid in surgical planning. This becomes particularly useful when approaching aberrant or complex anatomy. We sought to compare surgical outcomes of patients who underwent complex robotic urologic surgery with and without the aid of a 3DP model.

**Methods:** Patients were selected to have a 3DP model created prior to undergoing complex robotic urologic surgery at the primary surgeon's discretion. An IRB-approved, retrospective review was performed. Patients who had a 3DP model created prior to undergoing complex robotic urologic surgery were compared to patients who did not have a 3DP model created prior to undergoing similar surgeries. The study and control groups were compared using Fisher's method.

**Results:** A total of 5 study patients and 10 control patients were analyzed. Both groups were similar in gender, BMI, preoperative serum creatinine (sCr), and preoperative GFR. There were no statistically significant differences between the study group and the control group, respectively, in nephrometry scores (mean 7.67 v 6.25, p = 0.3361), OR time (mean 233.2 min v 175.2 min, p = 0.0959), clamp time (mean 36 min v 23 min, p = 0.1318), estimated blood loss (mean 152mL v 124 mL, p = 0.7457), length of stay (mean 1.8d v 1.4d), postoperative sCr (mean 1.00 v 0.98, p = 0.9435), postoperative GFR (mean 83.0 v 76.2, p = 0.5910), or negative surgical margin status (p = 0.9999). Neither group experience excessive bleeding, conversion to open, bowel injury, ureteral injury, vascular injury, or conversion to radical nephrectomy.

**Conclusion:** With this pilot study we did not observe a statistically significant advantage when using preoperative 3D modeling. However, subjectively the surgeons felt the models were helpful in visualizing the pathology, vasculature, and anomalies during surgery after "seeing" them preoperatively. More prospective randomized data will be helpful in determining if this technology will make a difference in outcomes.

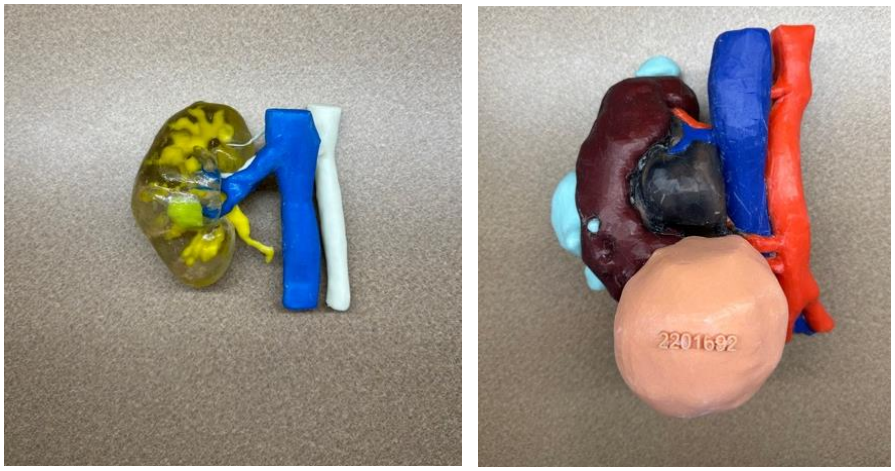


Figure 1. Examples of 3DP models.

**ABSTRACT # 37**

## IMPLEMENTATION OF A NOVEL ELECTROMAGNETIC DEVICE IN PROSTATE CANCER DIAGNOSTIC PATHWAY: COMPARISON WITH MULTIPARAMETRIC MRI AND DIGITAL RECTAL EXAMINATION

Carlo Bellorofonte[1], Tommaso Calcagnile[2], Davide Perri[2], Andrea Pacchetti[2], Federica Mazzoleni[2], Lorenzo Berti[3], Giorgio Bozzini[2]

[1] Columbus Clinic Center, Milan, Italy [2] Department of Urology, ASST Lariana, Sant'Anna Hospital, San Fermo della Battaglia (CO), Italy [3]Department of Urology, ASST Valle Olona, Busto Arsizio Hospital, Busto Arsizio (VA), Italy

**Introduction:** Prostate cancer (PCa) is the most frequent tumor afflicting men after the age of 50. Whether the diagnosis of prostate cancer is only allowed by performing a biopsy, the currently validated tests capable of raising the suspicion of PCa (e.g. digital rectal examination (DRE) and multiparametric MRI (mpMRI) and PSA testing) may result invasive, thus limiting patient's compliance. This highlights the need for development of novel minimally invasive diagnostic tools, with the target to become as accurate as the traditional ones. The current paper aims to provide an evaluation of Scanget® (TXT Health Probe, Figure 1), an electromagnetic device used in non-invasive detection of PCa. Scanget® equipment consists of a probe which emits signals that passes through the tissues, and a receiver that detects the electrical differences based on how the waves are absorbed and polarized by healthy or pathological cells.

**Methods:** A retrospective analysis of prospectively collected data of 129 patients from a single center (Columbus Clinic, Milan, Italy) was carried out. Inclusion criteria were prostate biopsy eligibility and age ≥18 years. Every patient underwent PSA testing, mpMRI, DRE and Scanget® test, with the last two carried out by a single expert operator (CB). At the end, transperineal fusion prostate biopsy was performed in all cases. Sensitivity, specificity, positive (PPV) and negative predictive values (NPV) were calculated and compared to assess the diagnostic ability of mpMRI, DRE and Scanget® test. A two-sided p-value of less than 0.05 was considered statistically significant.

**Results:** Mean PSA level was 11.6 ng/ml; 84 out of 129 (65.1%) presented with a positive mpMRI (defined as evidence of one or more PIRADS ≥3 lesions). DRE resulted suspect in 59 out of 129 individuals (45.7%), whereas Scanget® test was positive in 78 cases (60.5%). No side effects were observed for all the three tests included in the analysis.

At final histopathology, PCa was found in 68 out of 129 patients (52.7%). Scanget® test showed a specificity of 0.8, a PPV of 0.85, a sensitivity of 0.97 and a NPV of 0.96, with the last two performing significantly better than DRE (p=0.04 and p=0.03 respectively). On the other hand, no statistically significant differences in specificity (p=0.07), sensitivity (p=0.08), PPV (p=0.1) and NPV (p=0.09) were found when comparing Scanget® test with mpMRI.

**Conclusion:** In conclusion, Scanget® is a tool likely to identify PCa without requiring the patient to undergo any invasive procedure, hence increasing his compliance. Preliminary Scanget® findings demonstrated higher sensitivity and NPV than DRE, and outcomes comparable to mpMRI in raising suspect of PCa. Nevertheless, limitations are still present: Scanget® is not able to guide to the target area during fusion biopsies, requires to be performed by skilled operators and a cost analysis is lacking. Further iterations and a prospective randomized clinical trial are needed to confirm the initial promising findings.

**ABSTRACT # 38**

# EVALUATING EFFICACY OF PERCUTANEOUS PROCEDURES PLANNED VIA AUGMENTED REALITY

Lucille G Cheng, BA[1], Shyam Patnaik, MD[2], Stephen P. Canton, MD[3], Jacob Biehl, PhD[3], Edward Andrews, MD[3], Tatum Tarin, MD[2]

[1] University of Pittsburgh School of Medicine, Pittsburgh, PA

[2] Department of Urology, University of Pittsburgh Medical Center, Pittsburgh, PA

[3] Surreality Lab, University of Pittsburgh, Pittsburgh, PA

**Introduction:** In urological procedures with percutaneous approaches, targeting is often cited as the most challenging part due to imaging limitations, difficulties determining puncture site, and issues maintaining an accurate trajectory [1][2][3]. Advancements in augmented reality (AR) have allowed for the overlay of digital information, such as a 3D volumetric rendering of patient scans or virtual planned trajectories, over the physical world, such as a patient [4]. In this feasibility study, we explore the usability of AR-guided percutaneous puncture trajectories on renal targets.

**Methods:** CT imaging of two supine male cadaveric torsos was uploaded to the SurgicalAR system (Medivis, New York, NY). A 3D volumetric hologram was projected through the see-through visor of the HoloLens 2 (Microsoft, Seattle, WA). The hologram was registered to the cadaver using a point-to-point framework relying on pre-verified cadaveric fiducials matched to virtual counterparts. Using SurgicalAR, virtual trajectories towards pre-selected renal targets were planned with the torsos in supine position; these trajectories were projected through the HoloLens 2 visor. Needle probes were then inserted following the virtual planned trajectory, and radiopaque dye was injected into the entry points. The cadavers were rescanned to highlight needle tracts. Data on time to register and plan trajectories was measured.

**Results:** Using the AR system, seven virtual trajectories across two cadavers were planned. Time to register the 3D volumetric imaging over the cadaveric torso was approximately 5 minutes 24 seconds. Mean time to plan trajectories was approximately 1 minute (range: 7 seconds, 4 minutes). Targets were selected with the goal of easier reproduction for future study and included the superior and inferior poles of kidneys and stone in the left kidney of one cadaver. Trajectories were planned similar to those performed for supine percutaneous nephrolithotomy, aiming for the space between the 12$^{th}$ rib and iliac crest. Aided by virtual trajectories planned using 3D volumetric imaging, we were successful in hitting our kidney targets without damaging surrounding colon or other structures.

**Conclusion:** To the best of our knowledge, we present the first feasibility study examining AR-guided percutaneous procedures using 3D volumetric patient scans. With the help of the AR guidance, we were able to avoid hitting adjacent structures such as bowel or bone. This proof of concept highlights the potential for novel approaches to accessing the kidney beyond the classical landmarks, where percutaneous access can be achieved in unconventional locations with the assistance of AR. Future research with a larger cohort of cadavers and patient trials is warranted.

***Figure 1*** *Cadaveric torso with AR scan overlaid, as seen through HoloLens 2.*

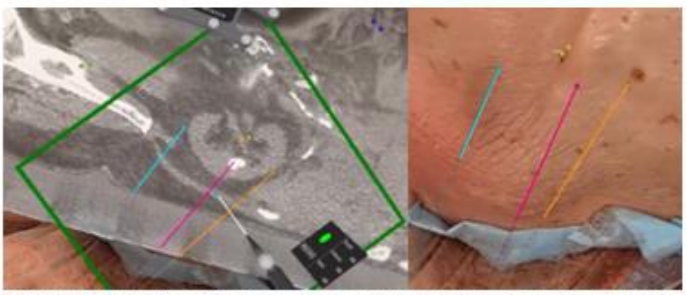

***Figure 2*** *Side-by-side comparison of planned trajectories toward targets (left) vs the same torso with imaging removed (right).*

***Figure 3*** *Post-dye CT of left kidney.*

**ABSTRACT # 39**

## FUNDAMENTALS, APPLICATIONS, AND LIMITATIONS OF AUGMENTED REALITY IN UROLOGICAL SURGERY: A PRACTICAL PRIMER FOR THE PRACTICING PHYSICIAN

Lucille G Cheng, BA[1], Vivian L Wang, BS[1], Shyam Patnaik, MD[2], Tatum Tarin, MD[2]
[1] University of Pittsburgh School of Medicine, Pittsburgh, PA
[2] Department of Urology, University of Pittsburgh Medical Center, Pittsburgh, PA

**Introduction:** Augmented reality (AR) refers to the process of superimposing digital information (e.g. preoperative images) on top of the physical world. Along with its interactive counterpart, mixed reality (MR), AR has become an area of sustained research interest in the urological surgery space. In this narrative review, we provide both a primer for how AR-guided surgical technology works at a fundamental level as well as a discussion of how recent studies will reduce current issues limiting wider adoption.

**Methods:** We searched online databases Web of Science, PubMed, and Embase using the query ("augmented reality" OR "mixed reality") AND ("urology") in February 2024. Studies were reviewed if they met the following criteria: original research, peer-reviewed, published in English, and evaluated the usage of augmented reality in a urological surgery setting.

**Results:** 130 articles were reviewed in total. In order to successfully merge a virtual image to its physical counterpart, most AR workflows consist of three key areas of investment: accurate *mapping* of the physical landscape into a geometric virtual reconstruction; *locating* the AR device within this landscape; and *registering* or *merging* the virtual and physical objects accurately. Advancements in computer vision have allowed for advancements in automatic *registration*, particularly in robot-assisted procedures. Meanwhile, the user experience for physicians has progressed from primarily static data overlays using custom proprietary devices to interactive holograms using widely available commercial technology. This has corresponded with consumer technology releases, such as the Google Glass (Google, Mountain View, CA) and Microsoft HoloLens (Microsoft, Redmond, WA), which have allowed for a head-mounted display platform on which to display augmented reality interventions. The most common organ systems where AR technologies have been applied successfully in urological settings were kidney and prostate interventions, with partial nephrectomy and robot-assisted laparoscopic prostatectomy being the most studied procedures, respectively. Most studies reviewed were feasibility studies on phantoms, with the first clinical studies noted in 2018. The most often cited limitations impacting further intraoperative adoption were technological difficulties distinguishing soft tissue and user experience challenges interacting with holographic overlays.

**Conclusion:** Augmented reality in urological surgery is an exciting field of study. To make the most of these innovations and contribute to improving AR technology in clinical settings, practicing urologists must understand both the fundamentals of augmented reality as well as its current applications and limitations.

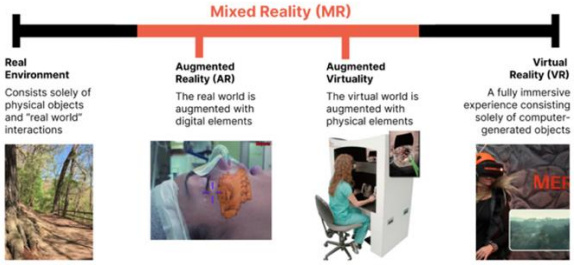


***Figure 1.*** *Overview of augmented reality as it falls on the reality-virtuality continuum described by Milgram and Kishino (1976).*

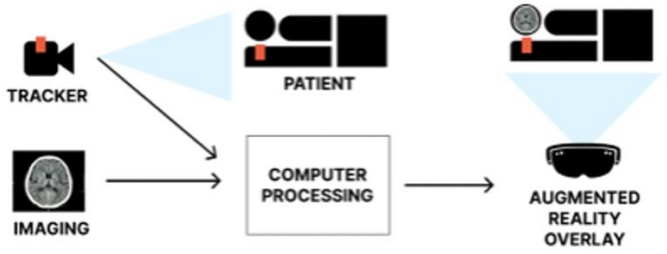


***Figure 2.*** *Schematic workflow of a simplified augmented reality workflow in a surgical context, where patient imaging (virtual) appears superimposed over the patient (physical) when viewed through a head-mounted display (HMD).*

**ABSTRACT # 40** **BEST ABSTRACT AWARD**

# AUGMENTED REALITY-GUIDED TRANSPERINEAL PROSTATE BIOPSY: SHIFTING THE PARADIGM

Lucille G Cheng, BA[1], Shyam Patnaik, MD[2], Stephen P. Canton, MD[3], Jacob Biehl, PhD[3], Edward Andrews, MD[3], Tatum Tarin, MD[2]
[1] University of Pittsburgh School of Medicine, Pittsburgh, PA
[2] Department of Urology, University of Pittsburgh Medical Center, Pittsburgh, PA
[3] Surreality Lab, University of Pittsburgh, Pittsburgh, PA

**Introduction:** Transrectal ultrasound guided (TRUS) prostate biopsies are the gold standard for diagnosis of prostate cancer, the most common cancer among men in the United States [1][2]. However, discomfort associated with the transrectal probe can lead to patient reluctance to follow-through with prostate biopsies [3]. Augmented reality (AR) has emerged as a paradigm-shifting technology in surgery by superimposing digital information (i.e. 3D volumetric renderings of patient scans) on top of the physical world (i.e. the respective patient's body) [4]. In this proof of concept, we explore the feasibility of an AR-guided non-TRUS transperineal prostate biopsy.

**Methods:** CT imaging of two supine male cadaveric torsos was uploaded to the SurgicalAR system (Medivis, New York, NY) and a 3D volumetric hologram was projected through the see-through visor of the HoloLens 2 (Microsoft, Seattle, WA). The hologram was registered to the cadaver using a point-to-point framework relying on pre-identified cadaveric landmarks matched to virtual counterparts. While wearing the HoloLens and using SurgicalAR, virtual trajectories towards the pre-selected prostate targets were planned by first selecting a prostate target and subsequently selecting a superficial entry point. The trajectories were then projected through the visor. A needle was inserted following the virtual plans and 1cc of radiopaque dye was injected. The cadavers were rescanned to highlight dye tract and target.

**Results:** Three trajectories were planned using the AR-system. In two of the trajectories, the target and entry points were both planned with the senior author positioned caudally; in the other trajectory, the senior author planned the target while positioned rostrally and the entry point while positioned caudally. Following the latter trajectory, the prostate target was hit successfully without damage to local structures.

**Conclusion:** To the best of our knowledge, we present the first cadaveric study of non-TRUS guided transperineal prostate biopsy using AR guidance. This feasibility study paves the way for future studies and clinical trials using AR in place of TRUS to guide transperineal prostate biopsy.

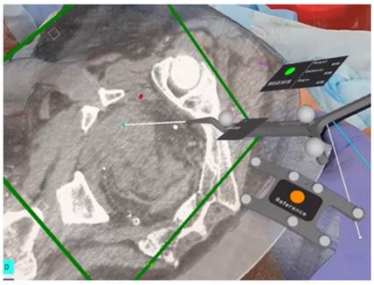

***Figure 1.*** *Placing a virtual trajectory targeting left lobe of prostate.*

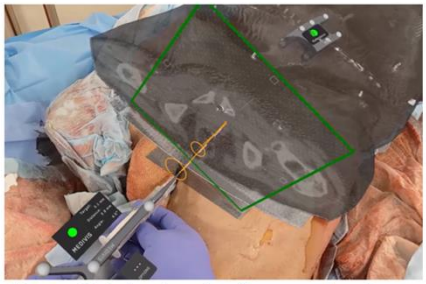

***Figure 2.*** *Injecting dye from perineal entry point following AR-guided trajectory.*

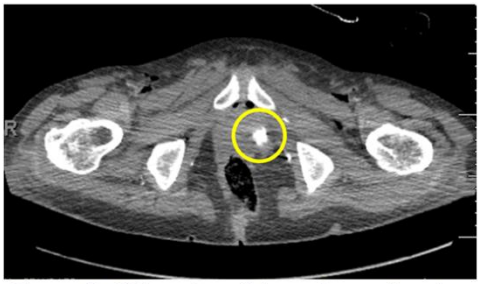

***Figure 3.*** *CT imaging of the cadaver after dye was successfully injected into prostate target.*

**ABSTRACT # 41**

## PROTOTYPE PASSIVE DRIVER AND MAGNETIC RESONANCE ELASTOGRAPHY TO IDENTIFY PROSTATE TISSUE PROPERTIES

Cody J. Johnson[1,2], Juan P. Gonzalez-Pereira[1,2], Timothy J. Hall[1,3], William A. Ricke[4], Vikas Gulani[5,6], Matthew Grimes[4], Yun Jiang[5,6], Alejandro Roldan-Alzate[1,2], Shane A. Wells[5,6], Christopher L. Brace[1,3]

University of Wisconsin Madison – Departments of [1]Radiology, [2]Mechanical Engineering, [3]Medical Physics, [4]Urology
University of Michigan – Departments of [5]Radiology and [6]Urology

**Introduction:** There is a paucity of non-invasive tests for the diagnosis of prostate inflammation and fibrosis. Therefore, novel diagnostics are a critical need to facilitate improved disease phenotyping and guide treatment related decisions. Magnetic resonance elastography (MRE) is a non-invasive imaging technique for quantitatively assessing the in-vivo mechanical properties of tissue, akin to palpation by a passive driver [1]. However, this technology has almost been exclusively used in the liver to detect and differentiate between different levels of hepatic fibrosis [2,3,4,5] resulting in an untapped potential for its use in the prostate. Therefore, using a prototype prostate passive driver this research aims to develop and implement a novel, non-invasive image-based test that quantifies biomarkers of the prostate that will optimize clinical management.

**Methods:** In this HIPAA compliant, IRB approved prospective clinical trial, 14 male subjects (n=30 planned) have been recruited. Biometric data (BMI, abdominal circumference, uroflowmetry) and symptom index scores (AUA-SI, LURN-SI29) were obtained. Men were fitted with a prototype prostate-specific passive driver and multiparametric MRI (mpMRI) was performed on a clinical 3.0T scanner (GE Healthcare, WI). mpMRI included three prostate MRE (pMRE) acquisitions at the following active driver (Resoundant, MN) settings: 100Hz 40amp, 100Hz 70amp, and 100Hz 70amp (repeat). Regions-of-interest were placed on the transition zones (TZ) and peripheral zone (PZ) stiffness maps at multiple locations (Figure 1B-D). Prostate, TZ, and PZ volumes, and post-void residual (PVR) were measured using the true axial and sagittal T2W images.

**Results:** Imaging sessions rendered high fidelity, full field of view images of the prostate, bladder, and abdomen in all subjects. The results of one subject are illustrated here. The 3D whole prostate, TZ, and PVR volumes were 18.9cc, 6.6cc, and 25.5cc, respectively. Axial T2W images demonstrated stromal-predominant BPH-related changes in the TZ with a 35% higher tissue stiffness than the normal PZ (left). Hypointense T2-weighted signal in the right PZ on axial T2W without restricted diffusion or suspicious enhancement (not shown) was compatible with prostatitis (Figure 1A). pMRE showed a 25% higher tissue stiffness in the right PZ region of inflammation (prostatitis) compared to the normal left PZ (Figure 1E) suggesting that MRE provides a quantitative measurement of a qualitative observation. Lastly, test-retest pMRE demonstrated minimal (~2%) bias suggesting reproducibility of this methodology.

**Conclusion:** Our initial observations reveal the unique power of pMRE as a non-invasive, reproducible, image-based biomarker that may provide novel insights into the tissue properties of the prostate.

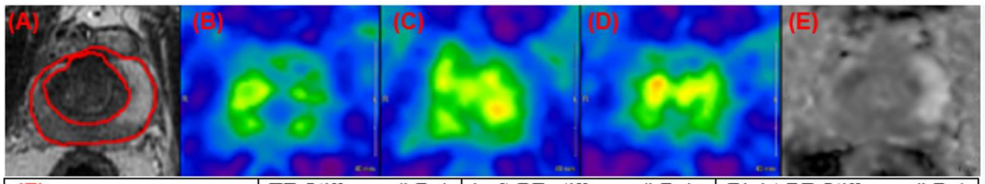


| (F) | TZ Stiffness (kPa) | Left PZ stiffness (kPa) | Right PZ Stiffness (kPa) |
|---|---|---|---|
| 100Hz 40amp | 3.319 (SD 0.022) | 2.821 (SD 0.097) | 4.007 (SD 0.334) |
| 100Hz 70amp | 4.620 (SD 0.185) | 2.899 (SD 0.055) | 3.527 (SD 0.519) |
| 100Hz 70 amp (repeat) | 4.423 (SD 0.015) | 2.985 (SD 0.121) | 3.458 (SD 0.386) |


Figure 1: Axial T2W (A) and magnetic resonance elastogram (MRE) stiffness maps of the prostate midgland, at the level of the verumontanum. The 3 MRE stiffness maps were obtained at 100Hz 40 amp (B) and 100Hz 70amp (test-retest) (C-D). Abnormally dark right peripheral zone compatible with prostatitis (negative DWI/ADC) (E). Average region-of-interest stiffness calculations are shown in (F). MRI compatible active driver used for MRE.

**ABSTRACT # 42**

## IS SHORTER BETTER? ASSOCIATION BETWEEN PAIN INTENSITY, URETERAL STENT INDWELLING TIME, AND PATIENT FACTORS FROM AN INTERNATIONAL PROSPECTIVE REGISTRY

Connor M Forbes[1], Ben H Chew[1], KF Victor Wong[1], Runhan Ren[1], Alexander P Glaser[2], Kazumi Taguchi[3], Amy E Krambeck[4], Marcelino E Rivera[5], Ojas Shah[6], Edouard Tariel[7], Dirk Lange[1], Channa Amarasekera[4], Shuzo Hamamoto[3], Wilson R Molina[8], John J Knoedler[9], Mitchell R Humphreys[10], Karen L Stern[10]

[1]University of British Columbia, Vancouver, BC, Canada, [2]Northshore University Health System, Chicago, IL, [3]Nagoya City University, Nagoya, Japan, [4]Northwestern University, Chicago, IL, [5]Indiana University, Bloomington, IN, [6]Columbia University, New York, NY, [7]Saint Gregoire, Rennes, France, [8]University of Kansas, Kansas City, KS, [9]Pennsylvannia State University, Pennsylvania, PA, [10]Mayo Arizona, Phoenix, AZ

**Introduction:** Previous studies have found that a shorter stent indwell time is associated with an increase in patient discomfort. We assessed the impact of stent duration and patient-associated factors on pain scores.

**Methods:** An international, prospective database assessing Boston Scientific ureteral stents at 10 centers in 4 countries (USA, Canada, France, & Japan) from 2020-23 was assessed. Primary outcome was pain intensity on day of stent removal using the validated PROMIS Pain Intensity (3a) and Pain Interference (6b) Scores. Patients were grouped by indwell time and pain scores were compared between and within groups. Impact of sex, height vs stent length, and method of stent removal on pain was assessed.

**Results:** Of the 359 patients in the database, 271 patients had one stent placed after ureteroscopy for stones. Indwell time was categorized based on consensus of short (0-6d), medium(7-10d), long(11-29d), and very long (>30d) stent dwell times. No significant difference was detected in pain scores between any of the time groups, (p=0.28). Within the long duration stent group (11-29 days), patients reported less pain the closer they were to 11 days (Figure 2A, p=0.008). Height when stratified by stent length was not significantly associated with pain scores. There was no difference in pain scores for removal with tether versus cystoscopy. Men reported lower pain scores than women (Figure 2B, p=0.015).

**Conclusion:** This study did not detect an overall difference in pain scores at stent removal between groups for stent duration. However, within the "long" stent duration group (11-29 days) a shorter indwell time was associated with improved pain scores. Within the short indwell time group (0-6 day) no difference was found in pain scores between 0 to 6 days. Men reported less pain than women.

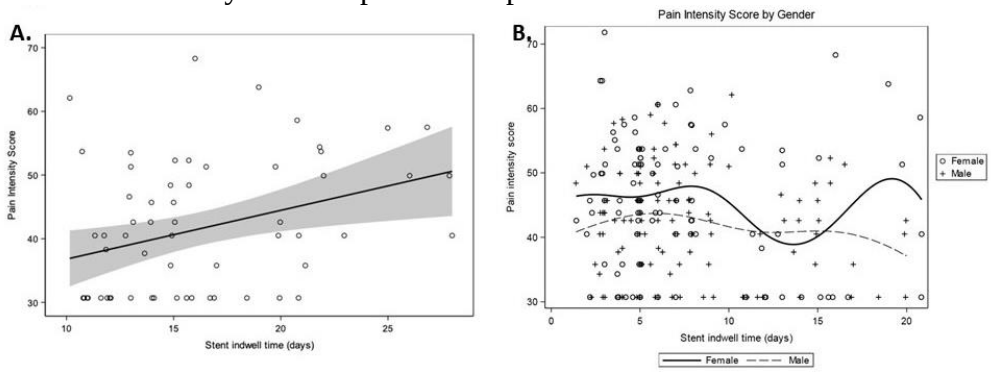


**Figure 2. Indwell time and pain intensity scores. 2A.** Pain intensity scores were lower towards 11d in the 11-29d group(p=0.008). **2B.** Pain intensity scores by gender. Men reported significantly lower pain intensity compared to women (p=0.015).

**ABSTRACT # 43**

## 3D SLICER: DETERMINATION OF ACCURATE UROLITHIASIS VOLUMES

Jacob C. Tsai, Jaime Altamirano-Villarroel, Yi Xi Wu, Seyed Amiryaghoub M. Lavasani, Andrei D. Cumpanas, Seyedamiryala Saadat, Bruce M. Gao, Zachary E. Tano, Pengbo Jiang, Roshan M. Patel, Jaime Landman, Ralph V. Clayman

Department of Urology, University of California, Irvine, USA

**Introduction:** The size of renal calculi is typically reported using two dimensional linear measurements; however, due to each uroliths irregular shape, this assessment often fails to accurately represent the true stone burden. To address this challenge, computed tomography (CT)-based 3D volume (3Dv) measurement software (3D Slicer®) was developed. Herein, we compare the accuracy of CT-based 3Dv and two CT-based ellipsoid formula volumes (EFv) — scalene and prolate ellipsoid formulas (SEF and PEF, respectively) — with "ground truth" stone volumes measured by gas pycnometer (GPv).

**Methods:** GPv of 116 air-dried and pre-weighed human stones from five common stone types (calcium oxalate (CaOx), calcium phosphate (CaPO), uric acid (UA), struvite (ST), and cystine (Cys)) were determined. Each stone, ranging from 14mm$^3$ (4 x 1.8 x 1.9mm) to 200mm$^3$ (8.5 x 4.6 x 5.1mm, median = 64mm$^3$, IQR: 36-93), was placed into a 1.7mL test tube and imaged by a CT scanner without and then within a silicone phantom designed to match physiologic attenuation. Three independent physician reviewers, one with prior 3D Slicer® experience and two with prior EFv experience, calculated the CT based 3Dv, SEF (a x b x c x π x 0.167) and PEF (a x a x b x π x 0.167). Measurements were analyzed by variance (ANOVA), Bland-Altman comparison, Pearson correlation coefficients and paired t-tests.

**Results:** 3Dv displayed greater inter-observer variability than EFv. The 3Dv for UA, ST, and Cys stones in air and phantom was not statistically different from GPv. Similarly, SEF for ST and Cys in air and in the phantom and UA in the phantom was not statistically different from GPv. Finally, PEF measurements for all stones in both mediums were statistically different ($p$<0.05) from the GPv (**Table 1)**. For the experienced 3Dv user, 3Dv was 65% more accurate than SEF ($p$=0.003) and 50% better than PEF ($p$<0.001). However, for all users, the measurement modalities differed from GPv by 63%, 70%, and 54% for 3Dv, SEF and PEF, respectively. The two EAU formulas were not statistically different from 3Dv ($p$=0.117 and $p$=0.095 for SEF and PEF, respectively).

**Conclusion:** The accuracy of 3Dv is dependent on user experience. 3D Slicer® proved to be a superior measurement tool compared to SEF and PEF for small ellipsoid stones in the 14mm$^3$ to 200mm$^3$ size range, but only for the experienced user.

**Table 1.** Pearson Correlations for 3Dv, SEF (*a x b x c x π x 0.167*), and PEF (*a x a x b x π x 0.167*) compared to GPv for five stone types ($p$<0.05 = volume measurement method differed from GPv).

| Stone Composition | Medium | GPv vs. 3Dv | | GPv vs. SEF | | GPv vs. PEF | |
|---|---|---|---|---|---|---|---|
| | | R | *p*-value | R | *p*-value | R | *p*-value |
| Uric Acid | Air | 0.894 | 0.955 | 0.829 | <0.001 | 0.770 | <0.001 |
| | Phantom | 0.912 | 0.451 | 0.845 | 0.813 | 0.811 | <0.001 |
| Calcium Phosphate | Air | 0.899 | 0.010 | 0.813 | <0.001 | 0.683 | <0.001 |
| | Phantom | 0.956 | <0.001 | 0.916 | <0.001 | 0.800 | <0.001 |
| Struvite | Air | 0.962 | 0.293 | 0.949 | 0.451 | 0.767 | <0.001 |
| | Phantom | 0.917 | 0.245 | 0.951 | 0.139 | 0.946 | <0.001 |
| Cystine | Air | 0.976 | 0.916 | 0.955 | 0.164 | 0.899 | <0.001 |
| | Phantom | 0.980 | 0.343 | 0.949 | 0.961 | 0.862 | <0.001 |
| Calcium Oxalate | Air | 0.974 | 0.013 | 0.935 | 0.001 | 0.961 | <0.001 |
| | Phantom | 0.977 | 0.001 | 0.942 | <0.001 | 0.917 | <0.001 |

**ABSTRACT # 44**

# EXPERIMENTAL MODEL OF POSITIONING DEVICE FOR MALE UROGENITAL TRACT BIOPSY IN MINIMALLY INVASIVE AUTOPSY

Pinto, Júlia Alarcon[1,3]; Vieira, Andreia[2]; Filho, Jair Theodoro[4]; Bucceroni, Victor[1,3]; Bressan, Paulo[1]; José Arthur Huffenbacher[3]; Andrade, Caio[1,3]; Andrade, Enrico[1]; Pinto, Gustavo[1,2,3]

[1] Hospital Santa Virgínia (HSV) [2] Instituto de Urologia - Hospital Santa Virgínia [3] Universidade Municipal de São Caetano do Sul (USCS) [4] Serviço de Verificação de Óbito - Hospital das Clínicas (SVOC)

**Introduction:** Globally, the decline in the number of autopsies is a documented reality in the literature, due to the procedure being considered disfiguring [1, Pg. 1]. The modern concept of 'minimally invasive autopsy' (MIA) in medical literature began in 1995, when laparoscopy was used to compare the results of less invasive methods with conventional autopsies [2, Pg. 1]. The postmortem examination can be performed, guided or not, by radiological exams (ultrasonography, computed tomography, magnetic resonance), or by videolaparoscopy, as previously described, which allow guiding and assisting in the positioning of biopsy needles to obtain samples of organs and bodily fluids, as well as minimizing the risk of contamination by forensic professionals [3, Pg. 3]. The MIA technique has gained prominence recently for being a safer and less contaminating method, after forensic experts were exposed to SARS-Cov-2 during conventional autopsies. Therefore, an experimental model of a positioning device to assist in biopsy of the male urogenital tract was developed with the aim of assessing the prevalence of urological diseases and potential associations with causes of death in the adult population.

**Methods:** Low-cost components were acquired for the construction of the positioning device, making it accessible to autopsy services practicing this method. The experimental model is a prototype to be improved and consists of a multi-purpose combination of static, stationary, and robotic-assisted arms and positioners, operating on the ARDUINO platform, to maximize and facilitate the approach via through-cut needles to target organs, such as: prostate (transperineal and transrectal access), kidneys, testicles, glans, cavernous body, and penoscrotal integument.

**Results:** Literature search on platforms such as PubMed reveals very few publications directly related to the topic; however, they indicate reliable, valid results, and suggest compatibility with conventional autopsy. In 2023, over 15,500 autopsies were conducted solely at SVOC - SP - Brazil [4], with a small percentage comprising MIA. This growing technology, besides establishing causes of death after histopathological analysis, can provide accurate information for data collection on the prevalence of diseases of the male urogenital system, often undiagnosed during life.

**Conclusion:** The proposed model is highly feasible, low-cost, and aims to introduce a new methodology for diagnostic assistance in MIA, where it is proposed not only to understand the natural cause of death but also to obtain urogenital anatomopathological samples for subsequent population-based statistical study.

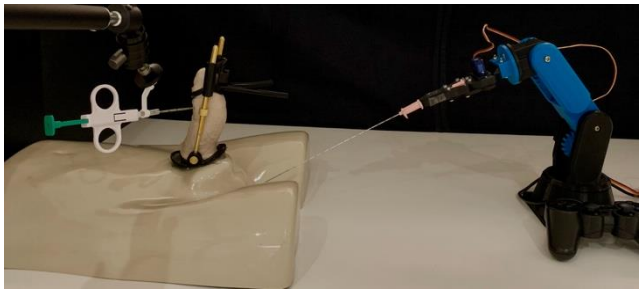

Figure 1: Schematic and experimental model

**ABSTRACT # 45**

# USING MATHEMATICAL MODELING TO INVESTIGATE THE IMPACT OF SUCTION DURING URETEROSCOPY ON RISK OF LASER-INDUCED THERMAL DAMAGE

Jessica Williams, Alycia Abbott, Candace Rhodes, Aditi Ray
Boston Scientific, Inc

**Introduction:** Recent availability and adoption of suction sheaths during ureteroscopy has prompted investigation into their procedural benefits. The addition of suction to ureteroscopic procedures increases the pressure drop between the irrigation mechanism and the end of the fluid pathway, thereby increasing flowrate through the ureteroscope. As higher flowrates have been linked to lower temperatures [1], there is the potential for suction devices to lower temperatures and risk of thermal damage during ureteroscopy [2]. Here, we use mathematical modeling to quantify the relationship between suction pressure and laser firing time to maintain the thermal dose below the commonly accepted damage threshold of 120 minutes ($T_{43}$ = 120 min).

**Methods:** A previous mathematical model relating irrigation pressure to flowrate [3, Pg. 45] was extended to incorporate a commercial suction ureteral access sheath (UAS). The flow resistance value for this sheath was derived via benchtop experiments, where the air vent of the sheath was fully sealed. From this extended mathematical model, a relationship between suction pressure and flowrate was derived, assuming a laser fiber in the working channel of the scope. This flowrate was then mapped to "firing time to reach $T_{43}$ = 120min" using a previously developed mathematical model for temperatures during laser lithotripsy [1]. The representative case used to investigate the relationships between suction setting, flowrate, and firing time was: a 200 m laser fiber firing at 40 Watts, with a 9.5 Fr scope, an 11/13 suction UAS, and 200 mmHg irrigation pressure (with fluid warmed to body temperature).

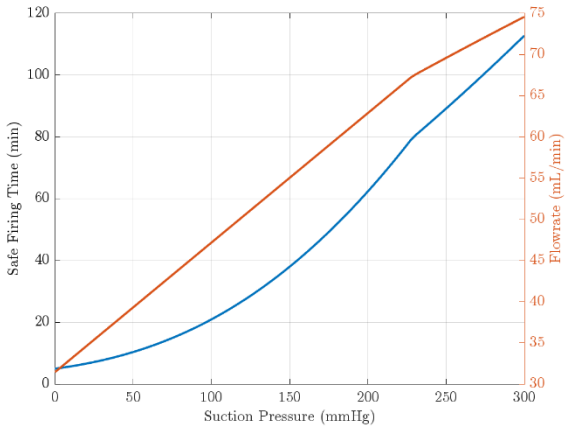


Figure 1: Firing time to reach $T_{43}$=120min (left axis) and flowrate (right axis) as functions of suction pressure.

**Results:** Suction pressure has a nonlinear impact on flowrate (red line and right axis in Figure 1) and an exponential impact on firing time (blue line and left axis in Figure 1). For the example considered here, the firing time with no suction is 5 minutes, the firing time with suction at 100 mmHg is 21 minutes, and the firing time with suction at 200 mmHg is 62 minutes.

**Conclusion:** Connecting the relationships between suction pressure, irrigation flowrate, and firing time allows us to quantify the role of suction in reducing risk of thermal damage. The nonlinear impact of suction pressure on firing time indicates that small increases in suction pressure may provide a significant increase in the time allowed to safely treat kidney stones via laser lithotripsy or enable the use of higher wattage lasers. Combining a mathematical model for ureteroscopy irrigation with a model for temperatures due to laser lithotripsy allows us to understand how emerging technologies which affect fluid delivery rate may impact patient safety.

**Disclaimer:** Mathematical modeling results may not be indicative of clinical results.

**ABSTRACT # 46** **BEST ABSTRACT AWARD**

# NANOPARTICLE COATINGS WITH BROAD SPECTRUM ANTIBACTERIAL AND ANTIBIOFILM PROPERTIES AND LOW TOXICITY

Juan Sebastian Rodriguez-Alvarez MD[1], Yue Xu MSc[2], Smita De MD PhD[1], Jorge Gutierrez-Aceves MD[1], Aaron Miller PhD, Vijay Krishna PhD[1]

[1] Cleveland Clinic Glickman Urological and Kidney Institute, Cleveland, OH, USA
[2] Cleveland Clinic Lerner Research Institute, Cleveland, OH, USA

**Introduction:** Device associated infections (DAI) are important health care associated infections, arising from biofilm formation on their surfaces. [1] Biofilms are extracellular polymeric surfaces that are resistant to antibiotics and immune host responses. Therefore, DAIs often require device removal. Silver (Ag) based coatings have achieved limited success at preventing DAIs, [2] which can be enhanced with the incorporation of gold (Au). [3] Polyhydroxy-fullerene (PHF) is a non-toxic molecule that can also enhance antibacterial properties of Ag nanoparticles (NP) by increasing reactive oxygen species formation. [4, 5] We propose PHF Au-Ag NPs (PAuAgNP) as a potential material coating to prevent DAI and aimed to evaluate its antibacterial and antibiofilm properties, as well as toxicity.

**Methods:** We engineered PAuAgNPs that were then dry-coated on polyurethane (PU) disc surfaces. Coated and uncoated discs were incubated overnight with media containing *Escherichia coli, Enterococcus faecalis, Enterobacter hormaechei, Staphylococcus aureus, Klebsiella oxitoca* and *Staphylococcus epidermidis* isolated from infected penile prostheses or ureteral stents. Free-floating (planktonic) bacteria were sampled from the resulting bacterial broth. Biofilm bacteria was detached in media and sampled. Samples were plated and antibacterial and antibiofilm activity were calculated as the resulting CFU/mL compared to uncoated discs. To evaluate toxicity, we exposed 3T3 murine fibroblasts to media containing varying concentrations of PAuAgNPs and extrapolated viability to calculate median viability loss concentrations. We exposed bacterial strains to similar concentrations to calculate minimal inhibitory concentration (MIC). All experiments were done in triplicates.

**Results:** No bacterial growth (i.e. 100% bacterial load reduction) was observed on coated discs, in both planktonic and biofilm bacteria, for an up to 7.79 log CFU/mL bacterial load reduction compared to uncoated discs ($p<0.0005$ across strains). Median fibroblast viability loss concentration was 3.48 µg/mL. All MICs were below this concentration, the highest being 2.58µg/mL for *E. faecalis.* (Figure)

**Conclusion:** PAuAgNPs have low toxicity and high antibacterial and antibiofilm properties. It shows promise as a material coating that may help prevent DAIs for multiple devices.

**Funding**: CCF RPC grant and CCF Catalyst grant.

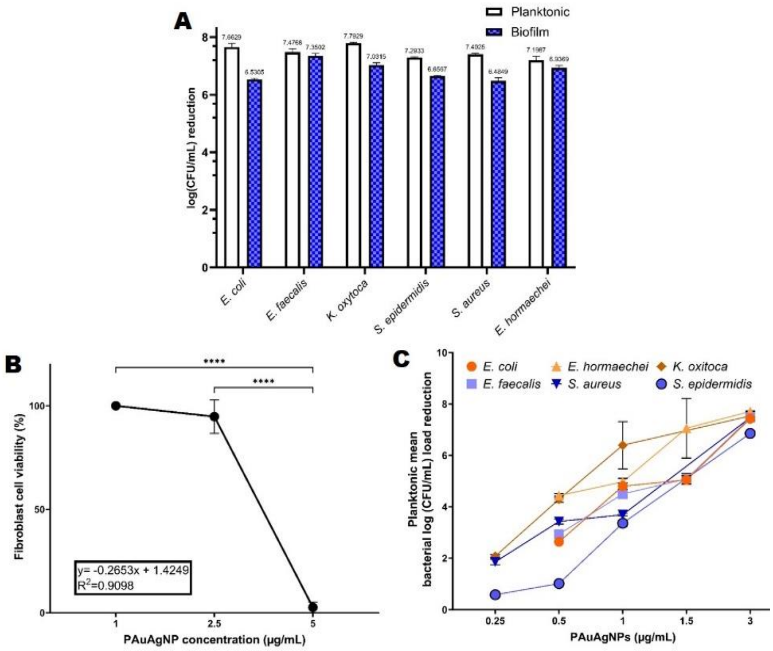


**Antibacterial and antibiofilm efficacy, toxicity and MIC of PAuAgNPs. (A):** Antibacterial and antibiofilm activity as measured by log (CFU/mL) reductions compared to uncoated samples; **(B)** Percent fibroblast viability after exposure to different concentrations; **(C):** MICs for different bacterial strains. ****: $p < 0.0005$

**ABSTRACT # 47**

# HOW TO GET A BETTER PERCUTANEOUS ACCESS: A CAUSAL MODEL FOR ROBOTIC-ASSISTED PCNL

Lauren Friend, Samir Hernandez, Ryan Kappedal, Elif Ayvali, Hedyeh Rafii-Tari
[1]Research & Development, Johnson & Johnson MedTech Surgery, Redwood City, CA

**Introduction:** Machine learning tools are increasingly used to predict procedural outcomes for urologic procedures [1],[2],[3],[4]. These models rely primarily on pre- and post-operative data to make predictions. However, the introduction of robot-assisted percutaneous renal access has allowed for continuous measurement of intraoperative data and the subsequent automated processing of this information into quantitative metrics measuring intra-operative factors. [5] Analysis of such a complex intraoperative dataset requires advancement beyond traditional correlative statistics to *causal* statistical methods.[6] The first step of such an analysis is causal discovery: algorithmically revealing the causal relationships in observational data.[7] By applying causal discovery methodology to observational data collected using the MONARCH™ Platform, Urology the causal patterns that were previously obscured from correlative analysis may be revealed and used to improve percutaneous access technique.

**Methods:** Data for this statistical analysis came from instrument location and orientation in 205 percutaneous access attempts conducted in human cadaver and porcine models using MONARCH™ Platform, Urology. These data were cleaned of outliers, normalized, and scaled. Next, a causal discovery algorithm was applied to the data along with a set of temporally impossible connections extracted from the event sequence robotic dataset. After tuning algorithm hyperparameters, we arrived on a potential Directed Acyclic Graph (DAG) describing the causal relationships of intra-operative parameters.

**Results:** The novel DAG (*Figure 1*) can be used to identify causal pathways existing in the observational dataset. While many were of interest, here we will focus on the relationship between the angle of the needle in the Anterior-Posterior plane at the start of insertion (*Needle AP*), and procedure success binarily defined as gaining access to the desired calyx. In traditional statistics, the existence and strength of this relationship would be determined through correlation using a statistical test such as the point biserial coefficient (*Equation 1*). The data show results of P=0.25 and $r_{pb}$=0.08**,** therefore we do not reject the null hypothesis that these variables are independent. Although these variables are not *correlated*, they do exist in a *causal pathway* as calculated by the causal discovery algorithm and depicted on the DAG.

Equation 1 is the point biserial coefficient calculation.

$$r_{pb} = \frac{\mu_1 - \mu_0}{\sigma_n}\sqrt{\frac{n_1 \cdot n_0}{n^2}}$$

**Conclusion:** This DAG is the first step towards a new generation of causal statistical analyses and predictions. This analysis shows that traditional correlative statistics not only fail to identify key clinical relationships such as Needle AP angle on Successful percutaneous access, but in fact refute them. By using causal discovery methods, the interconnection of variables in a complex and dynamic system such as the MONARCH™ Platform, Urology are revealed. With this DAG, future statistical estimations can be updated to account for confounding variables, increasing the power of observational data. Findings derived from downstream causal inferences welcome a future for urologists to gain percutaneous access with increased efficiency, accuracy, and fewer complications.

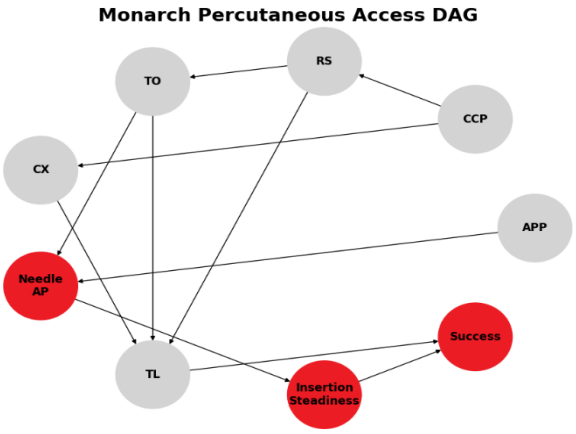


*Figure 1 displays the Directed Acyclic Graph (DAG) created through causal discovery methodology.*

**ABSTRACT # 48**

# QUANTITATIVE PIXEL INTENSITY ANALYSIS FOR CHARACTERIZING HYPOSPADIAS ANATOMY: ENTROPY AND RANGE ASSESSMENT IN FAVORABLE VERSUS UNFAVORABLE CASES

Meghana Noonavath[1], Adam Maxwell[2], Joshua Caldwell[1], Nicolas Fernandez[3]

[1] University of Washington, Seattle, WA, USA. [2] Virginia Tech, Blacksburg, VA, USA. [3] Seattle Children's Hospital, Seattle, WA, USA

**Introduction:** Hypospadias, a common congenital anomaly of the male urethra, presents with varying degrees of anatomical severity, ranging from favorable to unfavorable anatomy [1]. Accurate characterization of hypospadias anatomy is crucial for treatment planning and prognostic assessment. Texture analysis has been used in biomedical imaging to characterize tissues and predict outcomes [2]. Two statistical measures of texture are entropy, a measure of randomness or complexity in pixel intensity distributions, and range, which indicates the spread of pixel intensities [3]. In this study, we aim to investigate the entropy and range of hypospadias images, segmented into four distinct regions: glans, foreskin, urethral plate, and periurethral areas. We hypothesize that patients with favorable or moderately favorable hypospadias exhibit higher entropy and range values compared to those with unfavorable anatomy across all segmented regions.

**Methods:** Digital images from 148 patients with hypospadias were classified by 3 independent experts following the GMS score into "favorable" (54), "moderately favorable" (44) and "unfavorable" (50) cases. For each of the 148 images, the regions of interest were manually segmented separately into "glans," "urethral plate," "foreskin," and "periurethral area" by trained reviewers (Figure). Entropy and range were computed for each segmented region, with higher values reflecting greater entropy and range of pixel intensities. One-way Analysis of Variance was used to compare entropy and range values among favorable, moderately favorable, and unfavorable hypospadias groups for each region.

**Results:** The analysis revealed significant differences in range values across the favorable, moderately favorable and unfavorable groups: Glans (mean range for favorable (0.10), moderately favorable (0.11), and unfavorable (0.08), $p<0.040$), urethral plate (mean range for favorable (0.15), moderately favorable (0.13), and unfavorable (0.11), $p<0.013$), and foreskin (mean range for favorable (0.17), moderately favorable (0.15), and unfavorable (0.12), $p<0.032$). However, no significant differences were observed in entropy values across the different groups.

**Conclusion:** Our findings reveal that patients with favorable or moderately favorable hypospadias demonstrate higher range values in segmented regions compared to those with unfavorable anatomy. Unfavorable hypospadias cases may exhibit more uniform, or “smoother” tissue characteristics, such as scarring or fibrosis, leading to decreased heterogeneity and narrower ranges of pixel intensities (thus corresponding to lower range values). Understanding these pixel intensity characteristics could aid development of quantitative imaging biomarkers for hypospadias diagnosis, prognosis, and treatment evaluation.

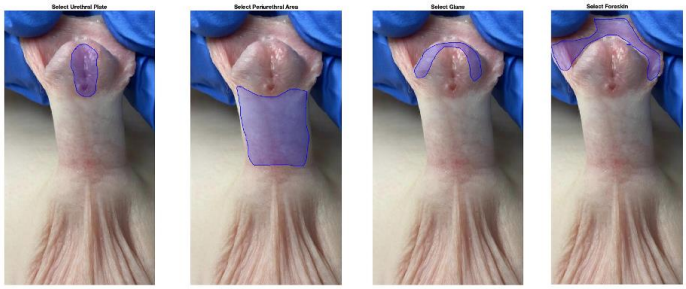

Figure: Hypospadias image segmented into four regions (from left to right: “urethral plate,” “periurethral area,” “glans,” “foreskin.”)

**ABSTRACT # 49**

# MAPPING THE PREDICTIVE LANDSCAPE OF PREOPERATIVE CT WITH DEEP LEARNING ACROSS RENAL TUMOR OUTCOMES

Nicholas E Heller[1], Rebecca A Campbell[1], Andrew M Wood[1], Nour Abdallah[1], Michal Ozery-Flato[2], Vesna Barros[2], Steven C Campbell[1], Nikolaos Papanikolopoulos[3], Robert Abouassaly[1], Christopher J Weight[1]
[1] Cleveland Clinic. [2] IBM Research. [3] University of Minnesota

**Introduction:** With sufficient training data, deep neural networks can learn the relationship between high-dimensional data like cross-sectional images and corresponding labels such as tumor characteristics or patient outcomes. However, the quantity of data needed to achieve a certain level of performance (if possible) is difficult to determine *a priori*. The goal of this work is to characterize the performance of models trained to predict postoperative variables for kidney tumors based on CT images, and how performance relates to the size of the training dataset.

**Methods:** Images and clinical data were collected for 599 renal tumor patients undergoing treatment at a single institution between 2010 and 2021. Regions Of Interest (ROIs) centered around tumors were used to train neural networks to predict six targets. Performance was plotted as a function of training set size, which was systematically varied. Cross-validation was used to evaluate performance across the full cohort, and univariate regression was used to compare AI performance to well-established predictors.

**Results:** In all cases, performance was positively correlated with dataset size, but the nature of this relationship varied. For tumor necrosis and synchronous metastases, very good performance (AUC of around 0.8) is achieved even with very small training sets. For sarcomatoid features, and (interestingly) advanced age, a steady improvement is observed with good performance achieved near n=500. Finally, for hospitalization and benign vs. malignant, a plateau in AUC between 0.6 and 0.65 is observed at roughly n=100, suggesting that predictive performance may have saturated at this value.

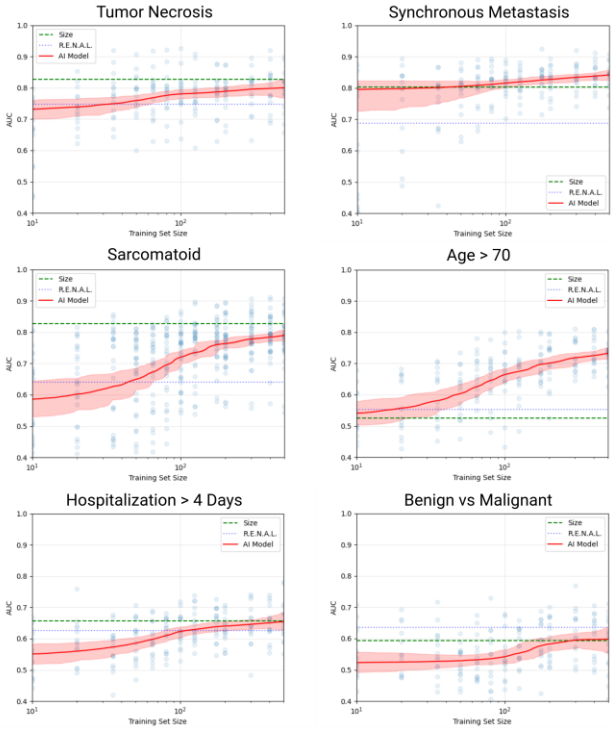


**Figure 1**: The learning curves (red) observed for a deep neural network predicting six labels based on a preoperative CT image. The horizontal green lines represent the AUC achieved by size alone, and the blue lines represent that achieved by the R.E.N.A.L. score.

**Conclusion:** The relationship between training set size and predictive performance shows to what extent postoperative variables associate with morphology in preoperative imaging. Our results suggest that excellent performance is achievable in many cases, and that additional performance improvements may be observed with additional training data. This motivates collaborative research to build the large datasets necessary to significantly reduce overtreatment and improve outcomes for renal tumors through AI.

**ABSTRACT # 50**

## AUTOMATICALLY CURATING REDCap DATABASES USING OPEN-SOURCE LARGE LANGUAGE MODELS: A PILOT STUDY WITH KIDNEY TUMOR PATHOLOGY REPORTS

Nicholas E Heller, Jayant Siva, Jason Scovell, Nicolas Soputro, Rebecca A Campbell, Andrew M Wood, Nour Abdallah, Reza Alaghehbandan, Robert Abouassaly, Christopher J Weight
Cleveland Clinic

**Introduction:** Clinical databases, often collected using REDCap, are the backbone of clinical and translational research. They are typically collected through an arduous process involving the manual extraction of data from a combination of free text and structured data from the electronic medical record (EMR). This process requires a great deal of time and effort, and it introduces the possibility for pernicious errors that often go undetected. It is therefore no surprise that significant effort has been put toward methods to automate this process through natural language processing (NLP). In the last few years, great strides have been made in NLP, largely through the large-scale self-supervised training of transformer models such as OpenAI's "GPT", Google's "Gemini", and Anthropic's "Claude". Open-source models such as Meta's "Llama" and Mistral's "Mixtral" and their fine-tuned derivatives have nearly kept pace with their closed-source counterparts. The goal of this work is to develop a framework in which open-source models can populate REDCap instruments based on free text in the EMR.

**Methods:** A primary design goal was to put the so-called "prompt engineering" in the hands of the domain experts designing the REDCap instrument. A syntax was developed in which the 'Field Label' defines both the note to be parsed and the prompt to be sent to the model. The LMQL package was used to implement token masking and eager validation to enforce constraints on model output, ensuring datatype correctness and membership in dropdown options where applicable. Branching logic defined by the REDCap instrument is used to define which prompts are sent to the model for each record. Copies of each AI-defined variable are used for auditing model's predictions for and random subset of records. Auditors are blinded to AI-predictions through REDCap 'Action Tags' and 'User Roles'. An additional copy of each variable is used for arbitration where the model and the auditor disagree.

**Results:** A small pilot study was performed in which 29 AI-defined variables were extracted from pathology reports describing nephrectomy specimens from 6 patients. These variables included histologic subtype, pTNM stage, grade, tumor size, spatial extent, and others. A 14B parameter fine-tune of the open source Mixtral model was used for extraction. The model achieved an accuracy of 98.9%, greater than the 95.4% achieved by a student. Importantly, this level of accuracy was achieved only after carefully designed prompts, dropdown options, and branching logic were implemented. The "first pass" at prompt engineering yielded only 80.4% accuracy, illustrating the importance of care and practice at this activity.

**Conclusion:** Our results suggest that with open-source language models, REDCap can be extended to achieve human-level accuracy at automatically extracting clinical data from free text found in the EMR. Larger, more convincing studies to demonstrate this are underway. One limitation is that this framework still requires a data analyst (or similar) to build database queries to procure the appropriate free text. This is likely the greatest bottleneck to address to allow for large-scale adoption. Through model improvements, accuracy is expected to increase and the need for such careful prompt engineering is expected to subside.

**ABSTRACT # 51**

# CORRELATION OF PENILE GRAYSCALE PHARMACO-ULTRASONOGRAPHY WITH ERECTILE TISSUE COMPOSITION IN MEN WITH ERECTILE DYSFUNCTION

Noel N. Kim[1], Sue W. Goldstein[2], Irwin Goldstein[2]
[1] Institute for Sexual Medicine, San Diego, CA. [2] San Diego Sexual Medicine, San Diego, CA

**Introduction:** Percentage of smooth muscle and connective tissue within corpora cavernosa (CC) erectile tissue was determined by histomorphometry on tissue samples removed during penile prosthesis insertion. Previous studies have shown that these histomorphometric data correlated with pre-operative pharmacocavernosometry erectile function testing. At 50-55% connective tissue (CT) content, corporal venoocclusive function (CVOF) was found to be normal. When CT content was 60-75%, CVOF significantly worsened in an exponential relationship. Above 75% CT content, there was no recordable CVOF. Grayscale pharmaco-ultrasonography (GPUS) is a less invasive in-office diagnostic assessment for ED than pharmacocavernosometry. It has been previously reported that hypoechoic areas in GPUS are representative of CT content, indicative of tissue fibrosis. In this study, we examined for the first time whether findings on GPUS could correlate with CT content.

**Methods:** Pre-operative proximal shaft axial plane GPUS images were obtained using a 15.4 MHz probe (Aixplorer), gain setting 45%, dynamic range 70dB. Percent hypoechoic area (%HA) within the CC was assessed by computer-assisted image analysis using Image J (Fig. 1). During penile prosthesis surgery, CC tissue from the proximal shaft was biopsied for histological analysis (n=12). Formalin-fixed (10%), paraffin-embedded tissue sections (5 μm) were stained with Masson's trichrome. Photomicrographs were also analyzed by Image J using the Masson trichrome vector of the color deconvolution plugin.

**Results:** % HA was poorly correlated to % CT area by linear regression analysis (r2 = 0.287). However, a non-linear regression model (exponential growth curve) provided a better fit (r2 = 0.672) with an inflection point at 40% CT area (Fig. 2). The abrupt shift is similar to the previously reported CVOF curve using pharmacocavernosometry.

**Conclusion:** Estimation of % HA on GPUS images may be a useful, non-invasive assessment of CT content to predict CVOF. Larger cohorts of ED patients are needed to verify the clinical utility of GPUS.

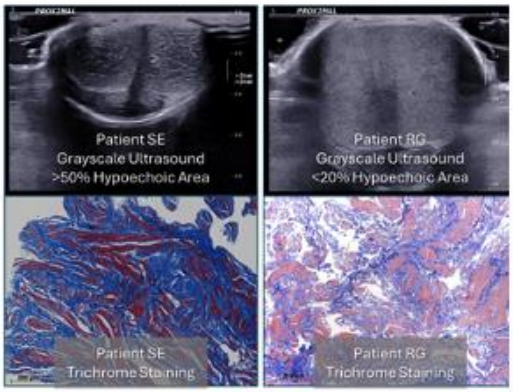


**Figure 1**: Representative grayscale ultrasound and trichrome staining.

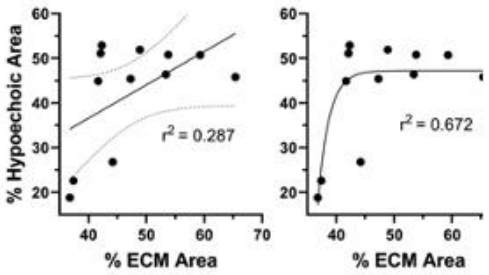


**Figure 2**: Correlation between percent hypoechoic area and connective tissue content (%ECM).

**ABSTRACT # 52**

# DEISGN AND PERFORMANCE EVALUATION OF A TRANSRECTAL HISTOTRIPSY DEVICE FOR PROSTATE ABLATION

Pavel B. Rosnitskiy[1], Gilles P.L. Thomas[2], Tatiana D. Khokhlova[1,2], Vera A. Khokhlova[2], Oleg A. Sapozhnikov[2], George R. Schade[3]

[1] Department of Gastroenterology, [2]Center for Industrial and Medical Ultrasound, Applied Physics Lab, [3]Department of Urology, University of Washington, Seattle, Washington, USA

**Introduction:** Ultrasound (US)-guided transrectal boiling histotripsy (BH) ablation of the prostate may offer benefits over currently utilized focal therapies due to its non-thermal mechanism and high-resolution real-time visualization on B-mode US. Its feasibility in a canine model was recently demonstrated with a robotically controlled single-element transducer. However, a multi-element transducer for electronic beam steering over the ablation volume would be preferable to enable automation and improve safety and ablation rate. Such design is challenging due to the anatomical constraints on the probe size. Our goal was to design and fabricate a clinical prototype array and test its performance in BH ablation of *ex vivo* tissue.

**Methods:** A novel randomized mosaic pattern approach (Fully Populated Array) was used to design a 1.5 MHz 128-element array transducer with a central opening for an US imaging probe. Of the 1000 test patterns generated, the one maximizing the electronic steering range, as estimated with numerical modelling of the US field, was selected for fabrication (Fig.1a). The output of the fabricated array was characterized with transient acoustic holography. Both the BH array and the US imaging probe were driven with a power-enhanced Verasonics Vantage system to produce 1 – 10 ms BH pulses with peak acoustic power of up to 2 kW at 1% duty cycle, synchronized with B-mode US imaging. A subset of the element pattern was fabricated separately and subjected to destructive testing with pulsed excitation with excessive voltage amplitudes to identify the safe range of operation and potential modes of failure.

**Results:** The BH beam steering range resulting from different mosaic patterns differed only by 2 mm axially and 1 mm laterally; the characteristic steering range along *z* and *x* was 35–65 and ±6 mm respectively (Fig.1b). The 128-element array was diced from curved piezoelectric material with a 200-micron kerf, and the electroacoustic efficiency was over 72%. The primary mode of failure was electrical breakdown between elements at >650 volts peak-to-peak difference. This was successfully mitigated by filling the kerfs with insulating material without affecting the mechanical cross-talk between elements. The electronic beam steering range and focal pressure levels were close to those predicted numerically. Volumetric BH lesions corresponding to the steering range were successfully generated in *ex vivo* tissue.

**Conclusion:** We designed and built a multi-element transrectal BH array using randomized mosaic patterning that provides clinically relevant electronic beam steering range and output power. Future studies will further evaluate its safety and performance in *ex vivo* and *in vivo* preclinical studies in preparation for first in human trials.

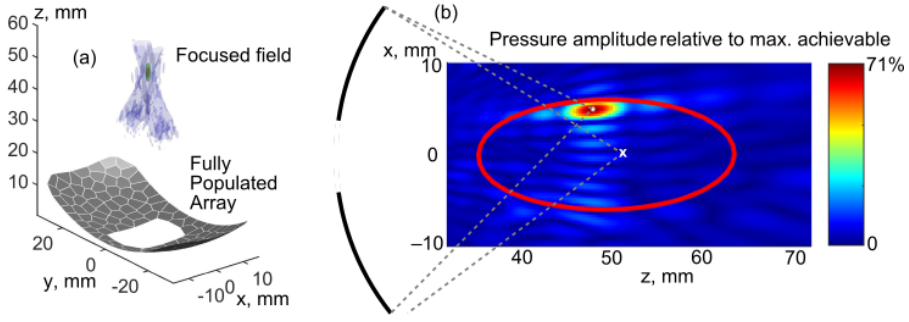


Fig 1. (a) Design of the transrectal 128-element array for volumetric boiling histotripsy (BH) of the prostate. (b) Red contour outlines the safe and efficient electronic beam steering region.

**ABSTRACT # 53**

## SINGLE-USE DIRECT IN-SCOPE SUCTION (DISS™) FLEXIBLE URETEROSCOPE IN SUCTIONING OF DISINTEGRATED RENAL STONES

Geavlete B.[1,2,3], Mares C.[2,3], Multescu R.[1,2], Iordache V.[1,2], Geavlete P.[1,2,3]
[1]Sanador Hospital,
[2] Saint John Emergency Clinical Hospital, Department of Urology, Bucharest, Romania
[3] Carol Davila University of Medicine, Bucharest, Romania

**Introduction**: Flexible ureteroscopy (fURS) increases now-a-days its performances in the treatment of renal lithiasis, offering the best results in relation to the safety of the surgical act. In the last decade, the remarkable technological advances have made possible the creation of more miniaturized and better performing instruments in the desired success of the stone-free status. Direct In-scope Suction (DISS™) from Pusen™ offers the advantage of a miniaturized, efficient instrument with the possibility of real-time suction of the fragments resulting from laser dusting, offering the opportunity to obtain the true stone-free status in real time at the end of the lithotripsy procedure.

**Method**:
We performed laser disintegration in 15 cases with pyelocaliceal kidney stones, particularly easy (normal anatomy), considering the reduced size of the ureteroscope (7.5 Fr). The maximum dimensions of the stones were between 9 and 19 mm, average 13.46 mm, HU between 905 and 1.205. Gender ratio was M=5 (33.3%), W=10 (66.6%). Average age was 50.9 years. We used single-use flexible Pusen 3033AH 7.5 Fr with suction DISS™, Flexor® Ureteral Access Sheath 10/12F and System laser TFL (Thulium Fiber Laser) 60 W, Quanta System. In all cases, TFL was practiced in dusting mode, constantly aspirating all the dust resulting during the intervention. Intrarenal pressure (IRP) was measured in all cases.

**Results**: The operative time (OP) was between 25 min and 75 min (average 42.5 min). DISS™ system was used both during the lithotripsy, improving visualization, and at the end to achieve a stone-free status in real time. We didn't use postoperative JJ stent. The stone free rate at 3 weeks was 93.3% (14 patients); 1 single patient had a residual fragment of 4.1 mm. noncontrast CT evaluation (pre- and post-operatively) was used in all patients. Median IRPs was 16.0 mmHg (5.8-33.1). When the instrument was withdrawn, we didn't find any superficial injury of the ureter. In 1 case (6.6%) we described mild hematuria for 9 hours (Clavien I), without requiring an additional night of hospitalization. In all cases 24hour hospitalization was practiced. No urinary tract infections (UTI) were found. No other complication was determined in the studied group.

**Conclusions**: This new real-time aspiration technology (single-use flexible Pusen 3033AH 7.5 Fr with suction DISS™) offers both the advantage of a better visualization intraoperatively and consequently a shorter procedure time, as well as the opportunity to achieve true stone-free status at the end of the intervention with less complications and no JJ stent after procedure.

**ABSTRACT # 54**

## COMBINED DIRECT IN-SCOPE SUCTION (DISS™) FLEXIBLE URETEROSCOPE WITH BENDABLE ACCESS SHEATH FOR COMPLETE STONE REMOVAL

Geavlete B.[1,2,3], Mares C.[2,3], Multescu R.[1,2], Iordache V.[1,2], Geavlete P.[1,2,3]
[1]Sanador Hospital
[2] Saint John Emergency Clinical Hospital, Department of Urology, Bucharest, Romania
[3] Carol Davila University of Medicine, Bucharest, Romania

**Introduction**: Flexible ureteroscopy has undergone significant improvements in the last decade, offering smaller, more efficient instruments with extremely useful properties such as in-scope aspiration (DISS™), which used together with bendable access sheaths have greatly improved postoperative stone-free rates.

**Method**: We performed laser disintegration in 14 cases with pyelocaliceal kidney stones (maximum dimensions between 18 mm and 31 mm, 1.125 to 2.410 $mm^3$, HU between 1,130 and 1,410). Gender ratio was M=5, W=9. Average age 54.3 years. 5 patients (35.7%) were previously stented. In all cases, the pyelocaliceal access was successful. We used single-use fURS using Pusen 3033AH 7.5 Fr single-use with suction DISS™, ClearPetra® Wellead Flexi Ureteral Access Sheath 10/12F and System laser TFL (Thulium Fiber Laser) 60 W, Quanta System. Intrarenal pressure (IRP) was measured in all cases.

**Results**: The DISS™ system was used both during the lithotripsy, improving visualization, and at the end to achieve a complete stone-free status in real time. For large renal stones (over 1,000 $mm^3$) combined suction and access sheath aspiration was used. Especially in such cases, this new technique gave us better irrigation control, improved visualization and aspiration of the stone fragments resulted from lithotripsy. Median IRPs was 19.5 mmHg (10.3-39.5). Operative time (OP) was between 35-85min (average 48.5min). In 4 cases (28,5%) postoperative JJ stent was placed for 2 weeks. In 3 cases (21.4%) mild hematuria was described (Clavien I-II). In uncomplicated cases 24h hospitalization was necessary. The stone free rate (SFR) at 3 weeks noncontrast CT (pre- and post-operatively) was 92.9% (13 patients); 1 single patient had multiple residual fragments (4-5.2 mm.). No urinary tract infections (UTI) were found. No other complication was determined in the studied group.

**Conclusion**: The major advantage of combining fURS with in-scope aspiration together with bendable flexible access sheets is that it offers an improved intrarenal visualization by aspirating the dust resulting from lithotripsy, it ensures the true stone-free status of patients in selected cases, aspirating all fragments resulting under direct endoscopic visualization. Especially for large renal stones this new technique seems to be very effective.

**ABSTRACT # 55**

## NEW TECHNOLOGIES IN FLEXIBLE URETEROSCOPY—WHAT IS THE LIMIT NOW OF THE ONE SESSION STONE REMOVAL?

Geavlete B.[1,2,4], Popescu R.[3,4], Buzescu B.[2,4], Mares C.[2,4] Geavlete P.[1,2,4]
[1] Sanador Hospital
[2] Saint John Emergency Clinical Hospital, Department of Urology, Bucharest, Romania
[3] Theodor Burghele Clinical Hospital, Department of Urology, Bucharest, Romania
[4] Carol Davila University of Medicine, Bucharest, Romania

**Introduction.** The objective of this study was to evaluate the results of single-use flexible ureteroscopic lithotripsy and one of the latest Thulium Fiber Laser in patients with kidney stones between 2 and 3 cm. using a flexible vacuum-assisted ureteral access sheath (FV-UAS) versus standard ureteral access sheath (SUAS).

**Material and methods.** We conducted a retrospective analysis of 97 consecutive patients who had big solitary kidney stones (with a stone burden ranging from 2 to 3 cm) throughout the period from January 1, 2022, to December 31, 2023. We used single-use flexible ureteroscopes (7.5 F., Pusen PU3033A and 7.5 F. HugeMed HU30S), ClearPetra® Wellead Flexi Ureteral Access Sheath, Flexor® Ureteral Access Sheath and Dornier Thulium Laser – Thulio (pulsed Tm:YAG, Dornier, Germany). The patients were categorized into two groups: group 1 (50 patients) underwent retrograde flexible ureteroscopic lithotripsy with FV-UAS, whereas group 2 (47 patients) underwent lithotripsy with SUAS. Stone characteristics and anatomical data were observed based on the computed tomography (CT) and/or KUB (Kidney-Ureter-Bladder) radiography imaging archive.

**Results.** For statistical analysis, we used the p-value for Student's t-test and the Mann-Whitney U test. The patient demographics, preoperative clinical characteristics, and renal stone properties of both groups were comparable and showed no significant differences. Regarding the location of the stones, the distribution was as follows: for the FV-UAS group, 22 (44%) lower calyx, 13 (26%) renal pelvis, 11 (22%) middle calyx and 4 (8%) superior calyx, and for the SUAS group, 18 (38,3%) lower calyx, 12 (25,53%) renal pelvis, 9 (19,15%) superior calyx and 8 (17,02%) middle calyx. Compared to the SUAS group, the FV-UAS group demonstrated significantly higher stone-free rates 90% vs 74,47%; P=0,044). Compared to the SUAS group, the FV-UAS group exhibited significantly shorter operative times (83,9 min vs. 73,2 min; $P < 0.01$). In all cases non-contrast CT was used at 1 month. The SUAS group had a significantly higher incidence of fever (11.9% vs. 5.9%; $P = 0.001$)

**Conclusion.** With the new flexible ureteroscopy technologies, we are able to safely manage increasingly larger stones. According to our outcome, compared to SUAS during RIRS for treating bigger renal stones, FV-UAS has a higher SFR. In addition, FV-UAS has contributed to shorter operative time and fewer complications.

**ABSTRACT # 56**

## FLEXIBLE URETEROSCOPY LITHOTRIPSY IN STAGHORN CALCULI: BENDABLE VERSUS TRADITIONAL ACCESS SHEATH

Geavlete B.[1,2,4], Popescu R.[3,4], Buzescu B.[2,4], Mares C.[2,4] Geavlete P.[1,2,4]
[1] Sanador Hospital
[2] Saint John Emergency Clinical Hospital, Department of Urology, Bucharest, Romania
[3] Theodor Burghele Clinical Hospital, Department of Urology, Bucharest, Romania
[4] Carol Davila University of Medicine, Bucharest, Romania

**Introduction.** Staghorn calculi represent one of the most challenging situations in urolithiasis. Despite the technological advances in flexible ureteroscopy, the gold standard treatment indicated by the current guidelines is still PCNL. This study compares the results of two types of access sheaths used to treat staghorn stones.

**Materials and Methods.** This retrospective study included 53 staghorn stones Type A and B (volumes between 1,300 and 29,000 $mm^3$) treated using flexible ureteroscopy, between 01.01.2020 and 31.12.2023. All the surgeries were performed by the same experienced surgeon. The surgical equipment consisted of 7.5 Fr Single-Use ureteroscopes (7.5 F., Pusen PU3033A and HugeMed HU30S), Thulium laser fiber (SoltiveSuperPulsed), and two different types of access sheaths (ClearPetra® Welllead Flexi Ureteral Access Sheath and YiGaoMed, Hangzhou, China). We used the following settings: "fine dusting" 0.15 J/100 Hz and for "dusting" 0.5 J/30 Hz. The mean laser efficacy laser efficacy was 8.7 $J/mm^3$ and the average ablation speed was 1.2 $mm^3/s$. The enrolled patients were divided into two groups. In the First Group (Group I) there were used standard access sheaths (10/12 Fr. and 11/13 Fr.), and in the Second Group in which was used vacuum-aspired access sheaths (10/12 and 11/13 Fr.). Several parameters were evaluated, including pre-stenting, mean operative time, number of performed sessions, complications, and stone-free rate. Students' t-tests and Mann-Whitney U tests were used to compare the results.

**Results.** The demographic statistics revealed a mean age of 51.03 years old in Group 1 and 53.12 in Group 2, while the sex distribution showed an increased prevalence for male sex (57.14% males in Group 1 and 64% in Group 1). Previous surgical infections were also analysed. These data showed 71.43% of infections in the first group and 60% in the second one. The most frequent isolated bacteria were *Proteus* (40%- 8 cases) in Group 1 and *E. coli* (40% - 6 cases) in Group 2. In terms of pre-stenting, most of the cases had previously placed Double J Stent (Cook and Coloplast), but without any statistical significance (Group 1:82.14% - 23 cases, Group 2:72%- 18 cases; p=0.388). The mean number of performed sessions was lower in the second group, with statistical significance (Group 1: 3.03 sessions, Group 2: 2.76 sessions, p=0.0051). There were observed differences between the overall surgical time (Group 1: 305.86 min. *vs.* Group 2: 259.26 min., p=0.0002). Also, some differences in favour of vacuum-assisted sheath were revealed regarding complications (Group 1: 28 complications – 32.94% for an overall nr. of procedures- 85 *vs.* Group 2: 13 complications – 18.84% for an overall nr. of procedures – 69). Most of the complications were Clavien 1 and 2. Regarding the stone-free rate (complete cleaning), this study showed some differences with statistical significance (Group 1: 73.57% Stone-Free rate *vs.* Group 2: 91% Stone-Free rate, p=0.0007), non-contrast CT has been used pre- and postoperatively.

**Conclusion.** The present results revealed good achievements of flexible ureteroscopy for treating staghorn calculi in repeated procedures. The vacuum-assisted access sheath showed improved outcomes regarding the overall surgical time, immediate postoperative complications rate and Stone-Free rates for this type of pathology.

**ABSTRACT # 57**

## BENDABLE SUCTION URETERAL ACCESS SHEATH: A COMPARISON WITH STANDARD URETERAL ACCESS SHEATH IN RENAL STONE URETEROSCOPIC TREATMENT

Geavlete P.[1,2,3], Multescu R.[1,2], Buzescu B. [2,3], Iordache V.[1,2], Geavlete B.[1,2,3]

1 Sanador Hospital
2 Saint John Emergency Clinical Hospital, Department of Urology, Bucharest, Romania
3 Carol Davila University of Medicine, Bucharest, Romania

**Introduction**: Improving the stone-free rate is a major objective during the retrograde flexible ureteroscopic approach for pyelocaliceal lithiasis. The flexible tip suctioning ureteral access sheath is an accessory instrument with great potential that has recently entered in the therapeutic armamentarium of this intervention. The aim of the study was to evaluate this sheath model by comparison to the standard model.

**Material and methods.** We evaluated 88 patients who underwent retrograde flexible ureteroscopic approach for single pyelocaliceal stones: 44 consecutive patients in whom we used ClearPetra® Wellead Flexi Ureteral Access Sheath 10/12F access sheath (Well Lead Medical Co, Guangzhou, China) and 44 consecutive patients in whom the retrograde flexible ureteroscopic approach was performed with a standard 10/12F access sheath (Flexor® Ureteral Access Sheath). We used Dornier Thulium Laser – Thulio (pulsed Tm:YAG, Dornier, Germany). The mean operative time, the stone-free rate on the first postoperative day and at 1 month, and the complication rate were evaluated. Assessment of the stone-free status was performed using ultrasonography and KUB on the first postoperative day, respectively by non-contrast CT examination at one month postoperatively.

**Results**: The average size of the stones was similar: 14 mm (7-19 mm) in group 1, respectively 15 mm (7-22 mm) in group 2 (p=0.14). The average operative time was longer in the suction ureteral access sheath group: 29 minutes versus 25 minutes in group 2 (p=0.004). Stone-free rates on the first postoperative day were 97.7% in group 1 versus 88.6% in group 2 (p=0.044), and those at one month postoperatively were 97.8%, respectively 95.5% (p=0.32). Intra- and postoperative complications occurred in 27.3% in group 1 (all Clavien I and II), and 29.6% in group 2 (Clavien I and II in all cases except one in which a Clavien III complication was encountered).

**Conclusions**: The flexible access sheath with vacuum allows rapid achieving of the stone-free status. Although not statistically significant, the complication rate was lower in patients in whom the flexible sheath was used.

**ABSTRACT # 58**

## IRRIGATION FLUID BACK-FLOW IN NEW BENDABLE URETERAL ACCESS SHEATH USED WITHOUT SUCTION DURING FLEXIBLE URETEROSCOPIC APPROACH OF RENAL STONES

Geavlete P.[1,2,3], Multescu R.[1,2], Buzescu B. [2,3], Iordache V.[1,2], Geavlete B.[1,2,3]

[1]Sanador Hospital
[2.] Saint John Emergency Clinical Hospital, Department of Urology, Bucharest, Romania
[3]. Carol Davila University of Medicine, Bucharest, Romania

**Introduction:** The suction ureteral access sheaths (bendable, with vacuum) are nowadays the newest accessory instruments, more and more used in the flexible ureteroscopic approach of renal stones. The aim of the study was to evaluate the effectiveness of using this access sheath model without suction in the prevention of septic complications.

**Methods:** We evaluated 30 patients who underwent retrograde flexible ureteroscopic approach with the ClearPetra® Wellead Flexi Ureteral Access Sheath 10/12F access sheath but without suction and 30 patients who underwent retrograde flexible ureteroscopic approach with a standard 10/12F access sheath (Flexor® Ureteral Access Sheath). We used System laser TFL (Thulium Fiber Laser) 60 W, Quanta System. There were only solitary kidney stones with a stone burden ranging from 1.32 to 2.33 cm. We assessed the overall rate of complications, as well as the rate and severity of septic complications.

**Results**: The standard access sheath (Flexor® Ureteral Access Sheath) was positioned with the distal end just below the ureteropelvic junction, while the flexible sheath was advanced to the proximity of the calculus (in the pyelocaliceal system). So, the inflow could controlled and verified comparing with the outflow (with no high pressure and heating). The overall complication rate was 26.7% after the use of the flexible sheath versus 23.3% in the group in which the standard sheath was used. However, when analyzing only the incidence of septic complications, they occurred in 6.7% in the flexible sheath group versus 16.6% in the standard sheath group. The distribution by severity was as follows: 100% Clavien I and II complications in group 1, compared to 80% Clavien I and II complications and 20% Clavien III complications in group 2.

**Conclusion**: The optimized drainage of irrigation fluid provided by the flexible ureteral access sheath, even when used without suction, appears to provide a protective effect over the standard access sheath. The evaluation of a larger number of cases is necessary for a better understanding of this effect.

**ABSTRACT # 59** **TOP 10 ABSTRACT**

# SAFETY AND EFFICACY OF ELECTROMOTIVE DRUG ADMINISTRATION IN THE RENAL PELVIS: FIRST IN-VIVO PORCINE REPORT

Seyedamirvala Saadat, Bruce M. Gao, Seyed Hossein Hosseini Sharifi, Yi Xi Wu, Zachary E. Tano, Seyed Amiryaghoub M. Lavasani, Jacob C. Tsai, Andrei Cumpanas, Sohrab N. Ali, Erika Martinez-Carcamo, Mahra Nourbakhsh, Pengbo Jiang, Roshan M. Patel, Michael Daneshvar, Jaime Landman, Ralph V. Clayman
Department of Urology, University of California, Irvine, Orange, CA

**Introduction:** Safe and efficient localized drug administration to the renal pelvis is an unmet need in urologic oncology given the rapid clearance and dilution of any instilled medication secondary to the ongoing flow of urine. Previously, we demonstrated that applying electromotive drug administration (EMDA) to the ureter would drive a small positively charged molecule into the ureteral wall. Accordingly, we sought to investigate the safety and efficacy of EMDA in the renal pelvis.

**Methods:** The proximal ureters of a female Yorkshire pig were sharply transected 2 inches distal to the ureteropelvic junction. An 8 Fr dual lumen catheter and a non-insulated 0.5 mm silver wire jacketed by a 5 Fr catheter with fenestrations in three rows (0.3 mm apart) on its 5 cm distal end were inserted into both renal pelvises and secured using a 2-0 silk suture (Figure 1). A dispersive pad was affixed to the ipsilateral flank and connected to the EMDA generator (*Physion® Mini 30N2*). Methylene blue [0.1%], a positively charged, water-soluble stain with a molecular weight of 334 Da, was infused via the dual lumen catheter at a rate of 5 ml/min using a drug infusion pump; the other lumen was left open for gravity drainage. A positive pulsed direct current of 4 mA was applied for 20 minutes in the experimental renal pelvis. The same infusion without EMDA was performed on the contralateral kidney as a control. The pig was euthanized, and both kidneys were excised for histopathological analysis.

**Results:** As displayed in Figure 2, hematoxylin and eosin (H&E) staining revealed slight denudation of urothelial cells, but no injury to the deeper tissues. Frozen sections of the experimental renal pelvis showed dense, diffuse methylene blue penetration into the urothelium and lamina propria. In contrast, the control kidney exhibited faint methylene blue staining in the urothelium with limited penetration.

**Conclusion**: EMDA enhanced the penetration of a small, water-soluble charged molecule into the urothelium and lamina propria of the porcine renal pelvis.

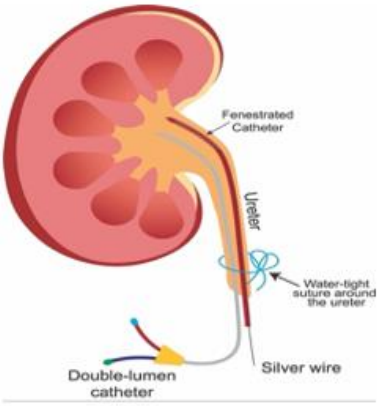


**Figure 1.** Schematic of EMDA procedure in the renal pelvis. A silver wire insulated within a distally fenestrated 5 Fr catheter and an 8 Fr double-lumen catheter were inserted into each renal pelvis and secured with a 2-0 silk suture.

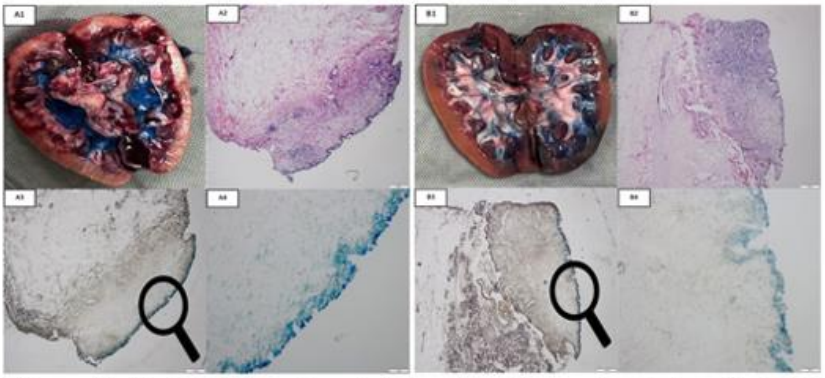

**Figure 2**. A) Methylene blue infusion into the renal pelvis with EMDA activation. A1) Intense macroscopic staining of renal pelvis. A2) H&E staining shows a normal architecture with no signs of acute injury. A3-A4) Deep blue staining of urothelial mucosa into the lamina propria of the renal pelvis.
B) Methylene blue infusion into the renal pelvis with EMDA activation.
B1) Faint macroscopic staining of renal pelvis. B2) H&E staining shows a normal architecture with no signs of acute injury. B3-B4) Minimal staining of the urothelium with scant methylene blue in lamina propria of the renal pelvis.

**ABSTRACT # 60**

## PROSTATE CANCER DETECTION VIA TRANSURETHRAL INTRODUCTION OF PRE-CONDITIONED ANT COLONIES

David Smith[1], John Nguyen[1,2], Kim Wang[2], Maria Silva[2]
[1] Westhaven Institute Department of Entomology. [2] Pellionisz Center for Scientific Excellence

**Introduction:** Diagnosis of prostate cancer (PCa) via canine and insect intermediaries is feasible [PMC7888653, PMC8914326]. However, sensitivity is often limited by dilution and decay of urine biomarkers. Diagnostic accuracy could be improved by direct exposure of ant colonies to *in vivo* prostate tissue. We therefore developed a transurethral ant delivery system for optimized PCa detection.

**Methods:** Ants (*formica fusca)* were conditioned to detect PCa through association of food rewards with true-positive urine samples. 40 patients with GG2-3 PCa and 40 age-matched healthy volunteers with PSA ≤ 3 were recruited. A transurethral catheter was advanced to dwell at the verumontanum (Fig A) while the catheter's proximal end was placed in the entry chamber of an ant colony (Fig B). As ants traversed the catheter, the flow of ants per minute (APM) was estimated using a LED and photodiode (Fig D). It was hypothesized that APM would be elevated for colonies excited by exposure to PCa-bearing prostates.

**Results:** PCa-positive patients attracted significantly more ants per minute than the control group (median 214 APM versus 8 APM, rank sum p<0.001)(Fig C). At an 80 APM threshold, sensitivity was 38/40 (95%) and specificity was 37/40 (92.5%). Adverse events included hematuria (4/80), hematospermia (7/80), hexapoduria (39/80), hexapodospermia (62/80), and self-reported anxiety, e.g. "getting antsy" (69/80). In one case, ants were observed to ingest a sizable volume of prostate tissue around the tumor (Fig E-F).

**Conclusion:** Transurethral introduction of ants to *in vivo* prostate tissue is a promising, minimally invasive, and accurate means of cancer diagnosis. Furthermore, it shows potential as a novel method of self-directed and cancer-specific tumor morcellation, a "focal ablANTion." Future work will investigate ant-based detection and treatment of *in vivo* bronchial, nasal, colorectal, and gynecological cancers.

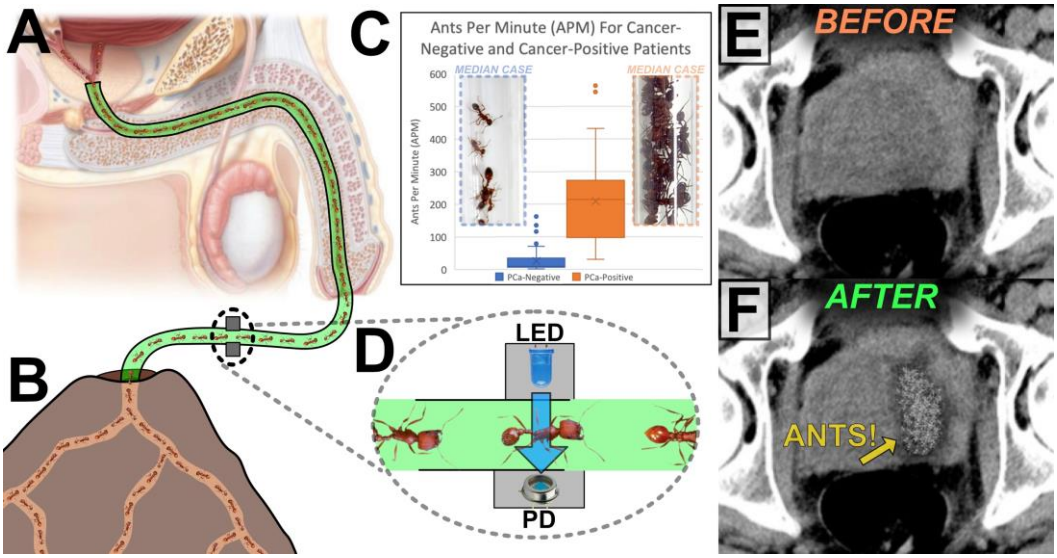


Figure: (A) catheter distal end in the verumontanum; (B) catheter proximal end in ant colony entry chamber; (C) ants per minute for PCa-positive and PCa-negative patients 5 minutes after catheter introduction, with representative photographs; (D) LED-photodiode used to estimate ants per minute (APM); (E-F) CT scan showing ant-mediated morcellation of tumor.

**ABSTRACT # 61**

# *IN VITRO* SIMULATION OF CAVITATION BEHAVIORS IN BURST WAVE LITHOTRIPSY (BWL)

Wayne Kreider[1], Adam D. Maxwell[1,2], Yak-Nam Wang[1], Christopher Hunter[1], Ga Won Kim[1], Jeff Thiel[1], Stephanie Totten[1], Ziyue Liu[3], Michael R. Bailey[1,2]

[1] CIMU, Applied Physics Laboratory, University of Washington, Seattle, Washington
[2] Department of Urology, University of Washington, Seattle, Washington
[3] Department of Biostatistics, Indiana University, Indianapolis, Indiana

**Introduction:** Burst wave lithotripsy (BWL) is an ultrasound-based modality for breaking kidney stones and is currently in clinical trials. In BWL treatments with relatively high rates of energy delivery, it is possible to exceed a cavitation threshold above which sustained bubble clouds are excited. The presence of such sustained cavitation activity has been shown to correlate with hemorrhagic tissue injury [May2017][Wang2021] as well as shielding of the stone to reduce comminution effectiveness [Maeda2018] [Kim2021]. Consequently, understanding and testing how cavitation activity can be mitigated is an important part of the development and refinement of BWL treatment protocols.

**Methods:** A calyx phantom made of polyvinyl chloride (PVC) was developed [**Figure**, panel (1)]. Key features include a cover to maintain a confined fluid volume; a smooth surface on the PVC cover to avoid cavitation on its proximal surface; and the use of degassed water (45-50% oxygen saturation) within the phantom. BWL treatments at 350 kHz were delivered to the phantom at a clinical pressure level (6.2 MPa) for different pulse parameters (length 5–160 cycles, repetition rate 5–160 Hz). Treatments were monitored using B-mode ultrasound and Doppler power to visualize the location and extent of cavitation [**Figure**, panels (2, 3, 4)], with thresholds identified by movement of the cavitation activity away from the stone. From in vitro observations, three treatment protocols of interest were identified for in vivo testing. In vivo experiments involved 6 pigs and a total of 26 distinct treatment sites that targeted the renal collecting space. At each site for a given combination of pulse parameters, a series of 5 minute treatments was delivered to determine pressure amplitudes above and below the threshold for sustained cavitation (as determined from the same imaging used in vitro). This procedure was repeated at each site for all three parameter combinations, and the treatment order was randomized across different sites.

**Results:** Three parameter combinations of interest were identified as follows: (A) 20 cycle pulse length, 10 Hz rate as default clinical parameters with minimal cavitation; (B) 80 cycles, 5 Hz as an accelerated energy delivery rate that may enhance stone breaking with minimal cavitation; (C) 20 cycles, 20 Hz as a combination expected to have a lower cavitation threshold. Explicit thresholds were not always observed because the maximum available pressures did not always produce sustained cavitation. For statistical analysis, this limitation was handled by a shared frailty model; the overall modeling framework was a Cox proportional hazard model (as pressure-to-cavitation threshold). For pairwise comparisons of the three parameter combinations, threshold (A) was greater than (C) [p-value 0.0003]; threshold (B) was greater than (C) [p-value 0.0016]; and thresholds (A) and (B) were not statistically different [p-value 0.36].

**Conclusion:** Ultrasound imaging observations of the extent and location of cavitation activity can reliably detect the onset of cavitation in a calyx phantom as well as under in vivo conditions. Because observed in vivo thresholds for three different BWL parameter combinations follow the same trends predicted by in vitro observations, this phantom can be a useful tool to explore cavitation behaviors in alternative BWL treatment protocols.

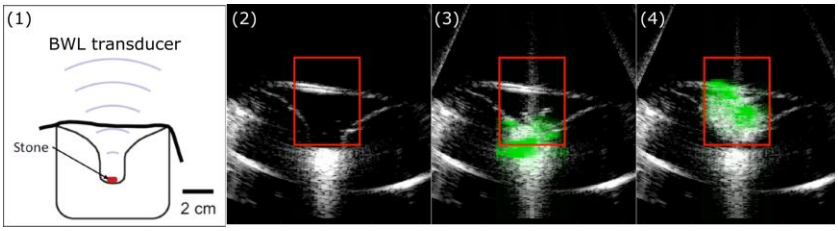


**Figure:** Panels from left to right: (A) schematic of the in vitro arrangement for delivery of BWL to the calyx phantom; (B) B-mode image prior to BWL; (C) B-mode image with superposition of Doppler power in green to show initial cavitation just above the stone; (D) analogous image as cavitation cloud migrates toward the transducer.

# ENGINEERING AND UROLOGY SOCIETY OFFICERS:

**PRESIDENT**
Jihad Kaouk

**SECRETARY**
Margaret Pearle

**TREASURER**
Chandru Sundaram

**COUNCILOR**
Louis Kavoussi

**EXECUTIVE DIRECTOR**
Dan Stoianovici

**ADVISORY BOARD**
Jeffrey Cadeddu

Ralph Clayman

Jean de la Rosette

Misop Han

Pilar Laguna

Thomas Lawson

Manoj Monga

Pierre Mozer

Stephen Nakada

Jens Rassweiler

Koon Ho Rha

William Roberts

Arthur Smith

Li-Ming Su

Gerald Timm

Hessel Wijkstra

Kevin Zorn

# AWARDS:

## BEST ABSTRACT AWARDS:

### NANOPARTICLE COATINGS WITH BROAD SPECTRUM ANTIBACTERIAL AND ANTIBIOFILM PROPERTIES AND LOW TOXICITY

Juan Sebastian Rodriguez-Alvarez MD[1], Yue Xu MSc[2], Smita De MD PhD[1], Jorge Gutierrez-Aceves MD[1], Aaron Miller PhD, Vijay Krishna PhD[1]

[1] Cleveland Clinic Glickman Urological and Kidney Institute, Cleveland, OH, USA, [2] Cleveland Clinic Lerner Research Institute, Cleveland, OH, USA.

### AUGMENTED REALITY-GUIDED TRANSPERINEAL PROSTATE BIOPSY: SHIFTING THE PARADIGM

Lucille G Cheng, BA[1], Shyam Patnaik, MD[2], Stephen P. Canton, MD[3], Jacob Biehl, PhD[3], Edward Andrews, MD[3], Tatum Tarin, MD[2].

[1] University of Pittsburgh School of Medicine, Pittsburgh, PA. [2] Department of Urology, University of Pittsburgh Medical Center, Pittsburgh, PA. [3] Surreality Lab, University of Pittsburgh, Pittsburgh, PA

# AWARDS:

## TOP 10 ABSTRACTS:

**THE EFFECT OF PROSTATE SIZE AND NUMBER OF CORES AT SYSTEMATIC PROSTATE BIOPSY**
Michael E. Rezaee[1], Misop Han[1], Katarzyna J. Macura[3], Bruce Trock[1],Amin Herati[1], Christian Pavlovich[1], Dan Stoianovici[1,2]. [1]Brady Urological Institute [2]Robotics Laboratory, [3]Department of Radiology, Johns Hopkins University

**IMPACT OF INTEGRATED, REAL-TIME DIGITAL MEASUREMENT ON SURGEON DECISION MAKING IN URETEROSCOPIC STONE SURGERY:** Alexander Krueger, B.S.[1], Drew Marie Smith[2], Andrew T. Parzych, B.S.[2], Robert Qi, MD[2], Aaron M. Potretzke, MD[2], Dan Stoianovici, PhD[3], David Holmes III, Ph.D.[4,5], Mark Lifson, Ph.D.[6], Kevin Koo, M.D., M.P.H.[2] [1]Mayo Clinic Alix School of Medicine Rochester; [2]Mayo Clinic Department of Urology; [3]Johns Hopkins University, Baltimore, MD[4]Physiology & Biomedical Engineering; [5]Biomedical Imaging Resource; [6]Center for Digital Health;

**SAFETY AND EFFICACY OF ELECTROMOTIVE DRUG ADMINISTRATION IN THE RENAL PELVIS: FIRST IN-VIVO PORCINE REPORT:** Seyedamirvala Saadat, Bruce M. Gao, Seyed Hossein Hosseini Sharifi, Yi Xi Wu, Zachary E. Tano, Seyed Amiryaghoub M. Lavasani, Jacob C. Tsai, Andrei Cumpanas, Sohrab N. Ali, Erika Martinez-Carcamo, Mahra Nourbakhsh, Pengbo Jiang, Roshan M. Patel, Michael Daneshvar, Jaime Landman, Ralph V. Clayman. Department of Urology, University of California, Irvine.

**DEVELOPMENT OF A NOVEL LUBRICITY EVALUATION MODEL FOR URETERAL ACCESS SHEATHS**
Brandon Camp[1], Andrei D. Cumpanas[1], Kevin Moreno-Ruiz, Zachary E. Tano[1], Bruce M. Gao[1], Jaime Landman[1], Ashlie Martini[2], Ralph V. Clayman[1] [1] Department of Urology, University of California, Irvine. [2] Department of Mechanical Engineering, University of California, Merced

**WHERE IS MY NEEDLE? USE OF A NEEDLE TIP INDICATOR FOR PERCUTANEOUS RENAL ACCESS IN ROBOTIC-ASSISTED PCNL:** Saif Sayed PhD[1], Camilla Gomes MD[1,2], Brandon Cowan MD[1,2], Menglong Ye PhD[1], Elif Ayvali PhD[1], Hedyeh Rafii-Tari PhD[1]. [1] Johnson and Johnson, Inc, Redwood City, CA 94065 [2] Department of Surgery, University of California, San Francisco, CA 94143

**THE MEASUREMENT OF INTRARENAL PRESSURE IN URETEROSCOPY WITH LASER LITHOTRIPSY: A PROSPECTIVE TRIAL:** Jamie Finegan, Jonathan Katz, Jonathan Berger, Seth Bechis, Manoj Monga, Roger Sur. University of California, San Diego

**A NOVEL LLM-MEDIATED DATA EXTRACTION TOOL: A COMPARATIVE STUDY IN PATIENTS WHO UNDERWENT RADICAL PROSTATECTOMY:** William S. Azar[1], Dylan M. Junkin[2], Nicholas Williams[2], Sahil H. Parikh[1], Charles Hesswani[1], Kyle C. Schuppe[1], Christopher R. Koller[1], Daniel Nethala[1], Neil Mendhiratta[1], Alexander P. Kenigsberg[1], Sandeep Gurram[1], Peter A. Pinto[1]. [1] Urologic Oncology Branch, National Cancer Institute, National Institutes of Health, MD, USA; [2] Palantir Technologies, CO, USA. [1] Urologic Oncology Branch, National Cancer Institute, National Institutes of Health, Maryland, USA. [2] Palantir Technologies, Colorado, USA

**PROSPECTIVE EVALUATION OF EFFICACY, SAFETY, CUMULATIVE LASER ENERGY, AND STONE-FREE RATES IN THE POST-MARKET THULIUM FIBER LASER (SOLTIVETM SUPERPULSED LASER SYSTEM) REGISTRY: INSIGHTS FROM TEAM OF WORLDWIDE ENDOUROLOGICAL RESEARCHERS (T.O.W.E.R.) RESEARCH CONSORTIUM**
Ben H. Chew[1], Mitchell R. Humphreys[2], Wilson R. Molina[3], Bodo E. Knudsen[4], Mantu Gupta[5], Duane D. Baldwin[6], Kyochul Koo[7], Victor KF. Wong[1], Peter Kronenberg[8], Palle Osther[9], Olivier Traxer[10]
[1] University of British Columbia, [2]Mayo Clinic Arizona, [3]Kansas University Medical Center, [4]Ohio State University, [5]Mount Sinai West, [6]Loma Linda University Medical Center, [7]Yonsei University, Seoul, [8]Hospital CUF Descobertas, [9]University Southern Denmark, [10]Sorbonne University Tenon Hospital

# AWARDS:

## BEST REVIEWER AWARDS (LAST 5 YEARS):

| | | 2019 | 2021 | 2022 | 2023 | 2024 |
|---|---|---|---|---|---|---|
| George | Aninwene II | | | | ☼ | |
| Tareq | Aro | ☼ | | | | |
| Jeffrey | Cadeddu | | | ☼ | | |
| Ralph | Clayman | | | | ☼ | ☼ |
| John | Denstedt | | | | | ☼ |
| Oscar | Fugita | | | | | ☼ |
| Petrisor | Geavlete | | ☼ | | | ☼ |
| Bogdan | Geavlete | ☼ | | ☼ | | |
| Philippe | Grange | | | | ☼ | |
| Dylan | Isaacson | ☼ | ☼ | | | |
| Louis | Kavoussi | ☼ | | | | |
| Jaime | Landman | | | ☼ | | ☼ |
| Thomas | Lawson | | | ☼ | | |
| Salvatore | Micali | | ☼ | | | |
| Cristian | Mirvald | | | ☼ | | |
| Steven | Monda | ☼ | | | ☼ | |
| Razvan | Multescu | | | | | ☼ |
| Naren | Nimmagadda | | ☼ | | | |
| Christian | Pavlovich | | | ☼ | | |
| Roxana | Ramos | | | | | ☼ |
| Koon Ho | Rha | ☼ | | | | |
| Abhishek | Singh | | | ☼ | | |
| Nicolas | Soputro | | ☼ | | | |
| Renea | Sturm | | | | | ☼ |

# AWARDS:

## REVIEWERS:

We gratefully acknowledge the contribution of the following reviewers to the success of the meeting and thank them for taking the time to promote the best science.

Omer Anis
Michael Bailey
Ben H Chew
Ralph Clayman
Brandon Cowan
Andrei Cumpanas
John Denstedt
Connor Forbes
Oscar Fugita
Petrisor Geavlete
Akram Gholami
Samir Hernandez
Kyo Chul Koo
Wayne Kreider
Jaime Landman
Thomas Lawson
Wai Lee
Salvatore Micali
Razvan Multescu
Meghana Noonavath
Sahil Parikh
Thomas Polascik
Roxana Ramos
Koon Ho Rha
William Roberts
Juan Sebastian Rodriguez-Alvarez
Saif Sayed
Nicolas Soputro
Karen Stern
Dan Stoianovici
Kazumi Taguchi

# THANKS:


Dr. George Nagamatsu founded the Engineering and Urology Society 1985.

Dr. Jack Vitenson was the first Society Treasurer in 1985.

Special thanks to Dr. Thomas Lawson for his help in formatting this program.

We thank Michelle Paoli and Debra Caridi for organizing this Annual Meeting.

# ACCME ACCREDITATION:

**Engineering Urology Society Meeting at the AUA2024**
**Accreditation Information**

**Accreditation**: The American Urological Association (AUA) is accredited by the Accreditation Council for Continuing Medical Education (ACCME) to provide continuing medical education for physicians.
**Credit Designation**: The American Urological Association designates this live activity for a maximum of 2.0 AMA PRA Category 1 Credits™. Physicians should claim only the credit commensurate with the extent of their participation in the activity.

**Focal Therapy Society Meeting at the AUA2024**
**Accreditation Information**

**Accreditation**: The American Urological Association (AUA) is accredited by the Accreditation Council for Continuing Medical Education (ACCME) to provide continuing medical education for physicians.
**Credit Designation**: The American Urological Association designates this live activity for a maximum of 2.0 AMA PRA Category 1 Credits™. Physicians should claim only the credit commensurate with the extent of their participation in the activity.

**Society of Urologic Robotic Surgeons Meeting at the AUA2024**
**Accreditation Information**

**Accreditation**: The American Urological Association (AUA) is accredited by the Accreditation Council for Continuing Medical Education (ACCME) to provide continuing medical education for physicians.
**Credit Designation**: The American Urological Association designates this live activity for a maximum of 4.25 AMA PRA Category 1 Credits™. Physicians should claim only the credit commensurate with the extent of their participation in the activity.